

Technical Report Documentation Page

TR0003 (REV. 10/98)

1. REPORT NUMBER CA 13-2180	2. GOVERNMENT ASSOCIATION NUMBER	3. RECIPIENT'S CATALOG NUMBER
4. TITLE AND SUBTITLE Post-Earthquake Bridge Damage Mitigation - Post-Earthquake Damage Repair of Various Reinforced Concrete Bridge Components		5. REPORT DATE June, 2013
		6. PERFORMING ORGANIZATION CODE UNR/
7. AUTHOR(S) Amarjeet Saini and M. Saiid Saiidi		8. PERFORMING ORGANIZATION REPORT NO. UNR/CA13-0371
9. PERFORMING ORGANIZATION NAME AND ADDRESS Department of Civil and Environmental Engineering University of Nevada, Reno Reno, Nevada 89557-0152		10. WORK UNIT NUMBER
		11. CONTRACT OR GRANT NUMBER 65A0371
12. SPONSORING AGENCY AND ADDRESS California Department of Transportation Engineering Service Center 1801 30 th Street, MS 9-2/5i Sacramento, California 95816		13. TYPE OF REPORT AND PERIOD COVERED Final Report 9/9/2010 – 6/30/2012
California Department of Transportation Division of Research and Innovation, MS-83 1227 O Street Sacramento CA 95814		14. SPONSORING AGENCY CODE 913
15. SUPPLEMENTAL NOTES Prepared in cooperation with the State of California Department of Transportation.		
16. ABSTRACT Highway bridges are an important component of the transportation system. It is essential to restore the bridge after earthquake damage by means of repair, reconstruction, or replacement. Replacing the entire damaged bridge is cumbersome, time consuming, and expensive. Therefore, appropriate bridge repair needs to be carried out to restore the bridge. The main objective of the present study was to develop repair methods using carbon fiber reinforced polymer (CFRP) for various reinforced concrete (RC) bridge components. This study consisted of three parts. In the first part, a detailed review of damage and repair in past earthquakes was conducted and the data were compiled in tables and gaps in available repair methods were identified. In the second part simple, practical methods were developed to assess the condition of an earthquake damaged bridge structural components in terms of apparent damage states (DS's). For this approach to be successful, internal earthquake damage was quantified and correlated to a series of visible DS's. Because seismic performance objective varies among different bridge components, earthquake damage can vary greatly and not all DS's are applicable to every component. Because, generally bridge columns are designed to be the primary source of energy dissipation through nonlinear action, they undergo a wide range of apparent damage. DS's defined for bridge columns were used as the framework for other components. In the third part repair design recommendations and design examples were developed to aid bridge engineers in quickly designing the number of CFRP layers based on the apparent DS. Repair methods to repair bridge components such as abutments, shear keys, girders, and cap beam-column joints were developed. Repair of bridge columns is addressed elsewhere and is not included in this report. To simplify repair, a new equation was developed to calculate the effective strain in the CFRP for side bonded CFRP configuration. In cases where the extent of damage precludes an economically feasible repair, reconstruction of damaged bridge component is recommended. Because the available data base for components other than columns is limited, many simplifying and conservative assumptions were made about the residual capacity of damaged components.		
17. KEY WORDS Mitigation, bridge, earthquake damage, shear keys, girders, abutments, joints	18. DISTRIBUTION STATEMENT No restrictions. This document is available to the public through the National Technical Information Service, Springfield, VA 22161	
19. SECURITY CLASSIFICATION (of this report) Unclassified	20. NUMBER OF PAGES 172	21. PRICE

Reproduction of completed page authorized

Disclaimer Statement

This document is disseminated in the interest of information exchange. The contents of this report reflect the views of the authors who are responsible for the facts and accuracy of the data presented herein. The contents do not necessarily reflect the official views or policies of the State of California or the Federal Highway Administration. This publication does not constitute a standard, specification or regulation. This report does not constitute an endorsement by the Department of any product described herein.

For individuals with sensory disabilities, this document is available in Braille, large print, audiocassette, or compact disk. To obtain a copy of this document in one of these alternate formats, please contact: the Division of Research and Innovation, MS-83, California Department of Transportation, P.O. Box 942873, Sacramento, CA 94273-0001.

Post-Earthquake Damage Repair of Various Reinforced Concrete Bridge Components

by

Amarjeet Saini
and
M. Saiid Saiidi

Department of Civil and Environmental Engineering
University of Nevada, Reno
Reno, NV 89557

June 2013

Draft Final Report No. CA 13-2180

Final Report Submitted to the California Department of Transportation (Caltrans) under
Contract No. 65A0371

Acknowledgements

The research presented herein was sponsored by California Department of Transportation (Caltrans) under Grant No. 65A0371. However, conclusions and recommendations are made by the authors and do not necessarily present the views of the sponsor.

The comments of Dr. Ashkan Vosooghi, a former post-doctoral fellow at UNR, on some of the chapters are much appreciated. Gratitude also expressed to Prof. K. Kawashima of the Tokyo Institute of Technology for providing information about bridge damage repair in Japan. The authors would like to express their appreciation to Dr. Amir Malek, Dr. Allaoua Kartoum, Dr. Charles Sikorsky, Dr. Jim Gutierrez, Mr. Kyoung Lee, Dr. Mark Mahan, and Mr. Pete Whitfield of Caltrans for their feedback and interest in different aspects of the project. Special thanks due to Mr. Peter Lee, the Caltrans Research Program manager, for his support and advice. .

Table of contents

Technical Report Documentation Page	i
Disclaimer Statement	ii
Acknowledgements	iii
Table of contents	iv
List of Tables	vii
List of Figures	ix
Chapter 1. Introduction	1
1.1 Introduction.....	1
1.2 Summary of Previous Research	3
1.3 Objective and Scope	13
Chapter 2. Past Earthquake Damaged Bridge Repair Practice	15
2.1 Introduction.....	15
2.2 Review of damage and repair in past earthquakes	15
2.3 Analysis of Database.....	18
2.4 Gaps in Knowledge on Past Earthquake Damage Repair of Bridge Components.....	19
Chapter 3. Repair of Earthquake Damaged Abutment Exterior Shear Keys	22
3.1 Introduction.....	22
3.2 Damage States.....	23
3.2.1. Damage State 2	24
3.2.2. Damage State 5	24
3.2.3. Damage State 6	25
3.3 Shear Key Capacity.....	25
3.4 Case Study	26
3.5 Shear Key Repair	27
3.6 Repair Design.....	28
3.6.1. Damage State 2	28
3.6.2. Damage State 5	31
3.6.3. Damage State 6	31
Chapter 4. Repair of Earthquake Damaged Prestressed Girder	34
4.1 Introduction.....	34

4.2	Damage States.....	35
4.2.1.	Damage State 1	36
4.2.2.	Damage State 2	36
4.2.3.	Damage State 3	36
4.2.4.	Damage State 4	36
4.2.5.	Damage State 6	36
4.3	Assumptions and Simplifications.....	37
4.4	Moment-Curvature Analysis.....	37
4.5	P/S Girder Repair.....	38
4.6	Repair Design to Restore Flexural Strength.....	38
4.6.1.	Damage State 1	39
4.6.2.	Damage State 2 and 3.....	39
4.6.3.	Damage State 4	44
Chapter 5.	Repair of Earthquake Damaged RC Bridge Abutments.....	46
5.1	Introduction.....	46
5.2	Damage States.....	47
5.2.1.	Damage State 2	48
5.2.2.	Damage State 3	48
5.2.3.	Damage State 4	48
5.2.4.	Damage State 6	48
5.3	Assumptions and Simplifications.....	48
5.4	Abutment Stem Wall Capacity	49
5.5	Repair Design.....	50
5.5.1.	Damage State 2	51
5.5.2.	Damage State 3 and 4.....	51
5.5.3.	Damage State 6	52
Chapter 6.	Repair of Earthquake Damaged RC Beam-Column Bridge Joints.....	54
6.1	Introduction.....	54
6.2	Damage States.....	56
6.2.1.	Damage State 1	56
6.2.2.	Damage State 2	56
6.2.3.	Damage State 3	57

List of Tables

Tables – Chapter 1 to 6

Table 2-1. Bridge damage and repair of San Fernando Earthquake (1971).....	74
Table 2-2. Bridge damage and repair of Loma Prieta Earthquake (1989).....	79
Table 2-3. Bridge damage and repair of Northridge Earthquake (1994).	83
Table 2-4. Bridge damage and repair of Whittier Earthquake (1987).	85
Table 2-5. Bridge damage and repair of Petrolia Earthquake (1992)	85
Table 2-6. Bridge damage and repair of The Landers and Big Bear Earthquake (1992).....	86
Table 2-7. General damage levels in bridge components (WFEO 2010)	86
Table 2-8. Damage levels in RC pier subjected to flexural failure at base (WFEO 2010).....	87
Table 2-9. Damage levels in RC pier subjected to damage at mid-height cut-off section of longitudinal rebars (WFEO 2010)	88
Table 2-10. Damage levels in RC pier subjected to shear failure (WFEO 2010).....	89
Table 2-11. Repair methods for RC pier (WFEO 2010).....	90
Table 2-12. Repair methods for RC girder (WFEO 2010).....	91
Table 2-13. Repair and retrofit of bridges damaged by Chile Earthquake.	92
Table 2-14. Summary of level of repair detail discussed in Table 2.1 to 2.6 for various bridge components	93
Table 2-15. Summary of repair methods in bridge books for bridge components.....	94
Table 3-1. CFRP material properties (Tyfo [®] SCH-41 composite using Tyfo [®] S epoxy)	95
Table 4-1. Prototype girder geometric and material properties.	95
Table 4-2. Prestressing steel properties.....	95
Table 5-1. Prototype abutment geometric and material properties.	96

Tables – Appendix A

Table A- 1. Effective strain in CFRP calculated by Eq. 3.4 and ACI 440.2R-08, $E_f = 10000$ ksi.	115
Table A- 2. Effective strain in CFRP calculated by Eq. 3.4 and ACI 440.2R-08, $E_f = 11000$ ksi.	116
Table A- 3. Effective strain in CFRP calculated by Eq. 3.4 and ACI 440.2R-08, $E_f = 12000$ ksi.	117
Table A- 4. Effective strain in CFRP calculated by Eq. 3.4 and ACI 440.2R-08, $E_f = 13000$ ksi.	118
Table A- 5. Effective strain in CFRP calculated by Eq. 3.4 and ACI 440.2R-08, $E_f = 14000$ ksi.	119
Table A- 6. Effective strain in CFRP calculated by Eq. 3.4 and ACI 440.2R-08, $E_f = 15000$ ksi.	120
Table A- 7. Required CFRP thickness calculated by ACI 440.2R-08 and proposed method for shear keys under DS2.....	121
Table A- 8. Required CFRP thickness calculated by ACI 440.2R-08 and proposed method for shear keys under DS5.....	122

Tables – Appendix B1 to B4

Table B1- 1. CFRP layer thickness for DS2 and DS5	133
Table B1- 2. Comparison of CFRP-repair design using different approaches	133
Table B2- 1. CFRP repair design summary	148
Table B3- 1. CFRP layer thickness for DS3, DS4, and DS6	151
Table B4- 1. CFRP layer thickness for T joints under DS2, DS3, and DS4.....	155
Table B4- 2. CFRP layer thickness for knee joints under DS2, DS3, and DS4.....	155

6.2.4. Damage State 4	57
6.2.5. Damage State 5	57
6.2.6. Damage State 6	57
6.3 Assumptions and Simplifications.....	57
6.4 Joint Capacity.....	59
6.5 Repair Design.....	60
6.5.1. Damage State 1	61
6.5.2. Damage State 2	61
6.5.3. Damage State 3 and 4.....	62
Chapter 7. Summary and Conclusions.....	63
7.1 Summary	63
7.2 Recommendations and Conclusions	65
References	69
Appendix A. Development of Simple Equation to Estimate CFRP Thickness	110
A-1 - ACI 440.2R-08 Procedure to Determine Shear Contribution of FRP.....	110
A-2 - Simple Equation to Determine Effective Strain in CFRP	112
Appendix B1. Shear Key Repair Design Examples	131
B1-1 Repair of shear keys under DS2.....	131
B1-2 Repair of shear keys under DS5.....	131
B1-3 Repair of shear keys under DS6.....	135
Appendix B2. Girder Repair Design Examples	146
B2-1 Repair of P/S girders under DS2 and DS3	146
B2-2 Repair of P/S girders under DS4	146
Appendix B3. Repair of Bridge Abutments Walls	150
B3-1 Repair for DS3/4	150
B3-2 Repair for DS6	150
Appendix B4. Repair Design Examples for Bridge Cap Beam-Column Joints	153
B4-1 Repair for DS2	153
B4-2 Repair for DS3 and DS4	154

List of Figures

Figures - Chapter 1 to 6

Figure 3-1. Elevation view of reinforcement layout of shear key test unit 4A	98
Figure 3-2. Damage state 2	98
Figure 3-3. Damage state 5	99
Figure 3-4. Damage state 6	99
Figure 3-5. 3D view of shear key	100
Figure 3-6. Shear key reinforcement location layout	100
Figure 3-7. Exterior shear keys, strut-and-tie model (Megally et al. 2001)	101
Figure 4-1. Damage state 1	102
Figure 4-2. Damage state 2	102
Figure 4-3. Damage state 3	102
Figure 4-4. Damage state 4	102
Figure 4-5. Prototype I girder cross section	103
Figure 4-6. Prestressing strands detail	103
Figure 4-7. Moment-curvature of I girder section at various damage states	104
Figure 5-1. Damage state 2	105
Figure 5-2. Damage state 3	105
Figure 5-3. Damage state 4	105
Figure 5-4. Damage state 6	105
Figure 5-5. Side view of bridge abutment (seat type)	106
Figure 6-1. Damage state 1	107
Figure 6-2. Damage state 2	107
Figure 6-3. Damage state 3	107
Figure 6-4. Damage state 4	107
Figure 6-5. Damage state 6	108
Figure 6-6. Elevation view of undamaged T joint	108
Figure 6-7. Plan view of undamaged T joint	109
Figure 6-8. Elevation view of undamaged knee joint	109
Figure 6-9. Plan view of undamaged knee joint	109

Figures – Appendix A

Figure A- 1. Effective strain in CFRP vs thickness for tensile modulus of 10000 ksi	123
Figure A- 2. Effective strain in CFRP vs thickness for tensile modulus of 11000 ksi	124
Figure A- 3. Effective strain in CFRP vs thickness for tensile modulus of 12000 ksi	125
Figure A- 4. Effective strain in CFRP vs thickness for tensile modulus of 13000 ksi	126
Figure A- 5. Effective strain in CFRP vs thickness for tensile modulus of 14000 ksi	127
Figure A- 6. Effective strain in CFRP vs thickness for tensile modulus of 15000 ksi	128
Figure A- 7. Required CFRP thickness for shear keys under DS2	129
Figure A- 8. Required CFRP thickness for shear keys under DS5	130

Figures - Appendix B1 to B4

Figure B1- 1. Shear key repair design for DS2 (front view)	134
Figure B1- 2. Side view of repair for DS2	134
Figure B1- 3. Shear keys repair design for DS5 (front view)	135
Figure B1- 4. Shear keys repair design for DS5 (side view)	135

Figure B1- 5. Elevation view of reinforcement layout	138
Figure B1- 6. Side view of shear key reinforcement layout	139
Figure B1- 7. Failure of shear key	139
Figure B1- 8. Removal of shear key transverse and inclined reinforcement	140
Figure B1- 9. Straightened existing stem wall vertical reinforcement.....	140
Figure B1- 10. Cut off existing stem wall vertical reinforcement and terminate at.....	141
Figure B1- 11. Installation of new vertical bars.....	141
Figure B1- 12. Installation of stirrups (front view).....	142
Figure B1- 13. Installation of stirrups (side view)	142
Figure B1- 14. Elevation view of a shear key repair for DS6.....	143
Figure B1- 15. Cross section of repaired shear key for DS6	144
Figure B1- 16. Side view of shear key vertical reinforcement	144
Figure B1- 17. Side view of shear key repair for DS6.....	145
Figure B2- 1. P/S girder repair under DS2 and DS3.....	149
Figure B2- 2. P/S girder repair under DS4.....	149
Figure B3- 1. Repair of abutment wall under DS3 and DS4	152
Figure B3- 2. Repair of abutment wall under DS6	152
Figure B4- 1. Elevation view of T joints repair under DS2	156
Figure B4- 2. Section A-A of T joints repair under DS2	157
Figure B4- 3. Elevation view of T joints repair under DS3 and DS4	157
Figure B4- 4. Section B-B of T joints repair under DS3 and DS4.....	158
Figure B4- 5. Elevation view of knee joints repair under DS2.....	158
Figure B4- 6. Side view of knee joints repair under DS2	159
Figure B4- 7. Plan view of knee joints repair under DS2	159
Figure B4- 8. Elevation view of knee joints repair under DS3 and DS4	160
Figure B4- 9. Side view of knee joint repair under DS3 and DS4.....	160
Figure B4- 10. Plan view of knee Joint repair under DS3 and DS4	161

Chapter 1. Introduction

1.1 Introduction

Highway bridges are an important component of the transportation system. Bridge damage due to an earthquake not only affects the transportation service but also affects the civil life and economic activities around the damaged area. It has been seen that most of the bridges constructed before 1971 were not designed to meet the current seismic design standards. Vulnerability of pre 1971 bridges was particularly evident in San Fernando Earthquake (1971), Loma Prieta Earthquake (1989), and Northridge Earthquake (1994) in California. Bridges designed as per current seismic standards are also expected to sustain damage to their structural components under extreme earthquake events depending on their type and operational functionality. For example ordinary bridges in California subjected to the design seismic hazards (DSH) are expected to remain standing but may suffer significant damage requiring closure to repair or even replace the bridge (Caltrans SDC 2010). Replacing the entire damaged bridge is cumbersome, time consuming, and expensive. Therefore, appropriate bridge repair needs to be carried out to restore the bridge.

Previous earthquake damage reconnaissance reports show that, damage to bridge components varies from minor cracks in cover concrete to bar fracture. Different types and degree of damage to bridge components require different repair methods. The fastest method to assess the post-earthquake condition of bridge components is the visual damage because it does not require specialized tools. For the majority of bridges visual damage is the only feasible mean to assess the condition of the bridge rapidly. A variety

of destructive and non-destructive techniques are available for detailed evaluation of bridge components but their use is warranted only for specific, perhaps critical bridges. It is, therefore, necessary to quantify the earthquake damage in terms of a series of damage states (DS's) indicating the extent of apparent damage and then develop repair methods for each.

To define apparent DS's specific to each bridge structural component, detailed past earthquake damage reports for various earthquakes (San Fernando Valley 1971, Loma Prieta 1989, and Northridge 1994) were obtained from the California Department of Transportation (Caltrans) compiled in bridge books and compact disks (CD's). Also earthquake damage reports were studied from the Chile earthquake of February 2010 as well as earthquakes in Japan, Taiwan, and Turkey. A uniform definition of seismic apparent DS was developed and used for all bridge components. Because seismic performance objective varies among different bridge components, not all DS's are applicable to all components. The number of applicable DS's depends on the typical detailing and behavior of individual bridge components. Therefore, it is important, to first define all the possible DS's and then their relevance to different bridge components should be evaluated. To define all possible apparent DS's, bridge column was selected as an ideal component. Columns are commonly designed as ductile members and they exhibit a wide range of post-earthquake DS's. Six distinct apparent DS's defined previously for standard columns (those meeting current seismic code requirements) (Vosooghi and Saiidi 2010) were considered and their relevance to each bridge component was assessed. Thus, present study discusses the repair methods for earthquake damaged reinforced concrete (RC) bridge components for different type and degree of

damage. This report discusses the repair of earthquake damaged RC bridge shear keys, girders, abutments, and beam-column joints utilizing unidirectional carbon fiber reinforced polymers (CFRP). In cases where the extent of damage precludes an economically feasible repair, reconstruction of damaged bridge component is recommended. Repair of bridge columns are addressed through other studies as discussed in the following section (Vosooghi and Saiidi 2013 and Saiidi et al. 2013)

1.2 Summary of Previous Research

Many studies have been conducted to strengthen or repair reinforced concrete columns, girders, walls, and other elements utilizing different materials and procedures. By far the majority of repair studies have focused on damage due to non-seismic loading. Studies have been conducted on prestressed CFRP to strengthen prestressed and non-prestressed beams (Kim et al. (2010); Czaderski and Motavalli (2007); Czaderski and Motavalli (2011)). There are few studies available on strengthening of masonry and RC walls (Konstantinos et al. (2003); Sayari and Donchev (2012)). Konstantinos, et al. (2003) conducted a study on five low slenderness RC walls that were designed according to modern design code provisions. Original specimens were initially subjected to cyclic loading to failure and were subsequently conventionally repaired and then strengthened using carbon and glass fiber reinforced polymers (CFRP and GFRP). Repair involved replacement of damaged concrete by a high-strength mortar and lap-welding of fractured reinforcement in the plastic hinge region, while strengthening involved wrapping of the walls with GFRP jackets, as well as the addition of CFRP strips at the wall edges, to enhance both flexural and shear capacity.

Many studies have been conducted on repair of RC columns subjected to seismic loading. In general, repair of RC columns includes one or a combination of the following repairs depending on the severity of earthquake damage: epoxy injection into cracks, patching of spalled zones, CFRP jacket, GFRP jacket, RC jacket, and steel jacket. Few recent studies have been conducted on repair of columns with fractured bars as well. In the following paragraphs a detailed review of past research on repair of RC bridge columns subjected to seismic loading is presented.

Priestley et al. (1993) tested a 0.4-scale high shear sub-standard RC bridge column model under reversed cyclic loading to failure. The original column failed at a displacement ductility of three. Thereafter, the column was repaired with a full height GFRP wraps and retested to evaluate the repair procedure. Open diagonal cracks and spalled concrete were reported as apparent damage at failure. The repair measures consisted of removal of all loose concrete, patching of concrete voids with cement and sand mortar, full height GFRP jacketing, and epoxy injection of cracks through the ports through the jacket. The GFRP wraps were designed for column to be able to reach over-strength plastic shear. The test results indicated that the repair was successful in restoring the column initial stiffness. The repaired column reached a displacement ductility of 10 without any capacity degradation.

Saadatmanesh et al. (1997) investigated the flexural behavior of four cantilever 1/5-scale sub-standard earthquake-damaged RC column models repaired with prefabricated FRP hoops. Columns C-1 and C-2 were circular while columns R-1 and R-2 were rectangular. Columns C-1 and R-1 each had starter bars with a lap length equal to

20 times the bar diameter while Columns C-2 and R-2 had continuous reinforcement. All specimens were tested under reversed inelastic cyclic loading to failure. Thereafter, these specimens were repaired with the FRP hoops. At the end of the tests of the original columns, all specimens exhibited significant damage, such as debonding of starter bars, spalling and crushing of concrete in the compression zone, local buckling of longitudinal steel, and the separation of the main bars from the column core concrete. The column specimens to be repaired were pushed back to the original position (i.e., zero lateral displacement) before the repair operation began. The repair procedures consisted of removing loose concrete in the failure zones, filling the gap with fresh concrete, and applying an active retrofit scheme. An active retrofit scheme consists of wrapping the column with slightly oversized prefabricated FRP straps and filling the gap between the column and the composite wrap with pressurized epoxy. It was concluded that the strength of the repaired columns was increased significantly while the initial stiffness was nearly restored. Furthermore, the repaired columns exhibited significant improvement in the hysteresis loops of lateral load versus displacement. Both repaired columns with lap-splice developed stable loops up to a displacement ductility of four, and the repaired circular and rectangular columns without lap-splice reached a displacement ductility of six and five, respectively, without any significant strength degradation.

Li and Sung (2003) conducted an experimental study on the repair and the retrofit of an earthquake-damaged sub-standard bridge column. The bench mark column was a 40% scale RC circular bridge column damaged as a result of shear failure at low displacement ductility under a reversed cyclic loading. The bench mark column had longitudinal steel ratio of 1.88% and shear reinforcement consisted of two C-shaped No.

3 stirrups lap spliced together. The damaged column was then repaired by epoxy injection, non-shrinkage mortar, and CFRP wraps. The CFRP jacket was designed so that the column could resist the over-strength plastic shear. After repair, the column was tested under cyclic loading. The test results showed improved hysteretic response with stable loops up to displacement ductility of nine in the repaired column. . The failure mode of the repaired column changed from shear failure to flexural failure.

Saiidi and Cheng (2004) conducted an experimental study on repair of earthquake damaged flared columns utilizing fiber composites. Two 0.4-scale RC bridge column models with structural flares that had been retrofitted using steel jacket and tested to failure in previous research (Saiidi et al. 2001) were used. The repaired columns were designated PLS and PHS with 1% and 1.8% longitudinal reinforcement, respectively. The objective of the repair was to restore the column capacity. To repair the columns, the steel jackets were removed. Then, the damaged concrete in and around the plastic hinge was removed and the steel bars were straightened. Low shrinkage, high-strength concrete grout was placed in the column afterward. The broken longitudinal bars were not replaced. The CFRP and GFRP fabrics with fibers running in the axial direction of the column were added to provide flexural strength to the columns. In addition, GFRP fabrics with fibers in transverse direction were installed to provide confinement and shear strength. The composites were installed over the full length rather than a partial length to avoid concentration of stress and to provide enough bond length for FRP fabrics. The longitudinal FRP jackets were designed to provide the same tensile strength as the yield force of the ruptured bars divided equally between GFRP and CFRP laminates. Cyclic

tests of the repaired columns indicated that the repair method was effective in restoring the stiffness, strength and displacement ductility capacity to a moderate level.

Lehman et al. (2001) conducted an experimental study to identify the performance of earthquake-damaged standard RC bridge columns repaired by different techniques. The original columns that were reinforced with spirals conforming to modern bridge requirements for regions of high seismic risk were damaged, repaired, and retested. The procedures for testing the columns in the original and repaired states were nominally identical. The columns were tested under constant axial and cyclic lateral loading. The damage levels were classified as either moderate or severe. The test program consisted of four columns tested to cause varying degrees of damage. Three of the test columns were severely damaged while the fourth column was moderately damaged. The severely damaged columns were designated 407S, 415S, and 430S; the last two numbers indicate longitudinal reinforcement ratios of 0.75, 1.5, and 3, respectively, and the letter S indicates severe damage. A fourth column nominally identical to column 415, was tested to a moderate damage level and was designated 415M. Damage suffered by the moderately damaged column included concrete cracking, cover concrete spalling, and longitudinal reinforcement yielding. Damage sustained by the severely damaged columns included those damage states in addition to core concrete crushing, longitudinal bar buckling, and longitudinal and spiral reinforcement fracture. Four different repair techniques were applied, with the details of each depending on the damage level and the details of the original columns. Column 407S was repaired by removing and replacing the damaged concrete, longitudinal reinforcement, and spiral reinforcement so that the repaired region could sustain the flexural plastic hinging demands. To remove the

damaged section the column was severed just above and below the damaged section, and the existing reinforcement and concrete were removed. New longitudinal reinforcing bars were mechanically spliced to the existing bars in the column and the joint. New spiral reinforcement was placed around the new longitudinal reinforcement, and new concrete was cast within the severed bar region. The use of mechanical splices was considered by the authors to be economical for this column because of the relatively small number of bars and low longitudinal reinforcement ratio resulting in low congestion. The repair for Column 415S involved placement of a strong reinforced concrete jacket along the damaged region so that new flexural hinging would be forced to occur above the jacket. Because this column had relatively larger number of longitudinal bars, this approach was considered preferable to using mechanical couplers. Column 430S was repaired by placing a new concrete jacket at the base of the column, with the intent that flexural yielding would occur at the base of the jacket under seismic loading. As with Column 415S, the larger number of longitudinal bars made use of mechanical couplers seem less economical. Column 415M was repaired by injecting epoxy into cracks and patching the spalled cover concrete. The repaired columns were tested under constant axial load and cyclic lateral loading and the performance of the repaired columns was investigated. It was concluded that the stiffness, strength, and the deformation capacities of the severely damaged standard RC columns could be restored by fully replacing the damaged zones with new materials. The strength and the deformation capacities of the moderately damaged standard RC columns could be restored by repairing the spalled zones and injecting epoxy to the cracks; however, the initial stiffness of the column was not restored due to material degradation.

Belarbi et al. (2008) conducted a study on the use of FRP to repair an earthquake damaged RC column subjected to combined axial, shear, flexural, and torsional loads. As part of their study, one standard column was subjected to significant damage level and subsequently repaired with CFRP composites and retested. The aspect ratio of the column used was six, which indicates that the response of the columns was dominated by flexure. The column was severely damaged under combined loading. Seven out of the 12 longitudinal reinforcing bars buckled. The objective of the repair scheme was to restore the original strength. The repair measures consisted of removal of damaged concrete, restoration of the cross-section of the column using a low viscosity grout, application of CFRP sheet in the longitudinal direction to restore some of the column original flexural strength, application of CFRP sheet in the circumferential direction to restore the axial compressive strength, and application of mechanical anchorage to develop the longitudinal CFRP fibers. The repaired column was tested under the combined loading. It was concluded that the flexural, torsional, and axial capacity of the column can be restored and enhanced using the given repair procedure; however, the longitudinally placed CFRP sheets pulled out from the footing base at low load levels.

Vosooghi and Saiidi (2010) conducted a study on post-earthquake evaluation and emergency repair of earthquake damaged RC bridge columns using CFRP. In their study, they proposed a number of possible distinct apparent damage states (DS's). Rapid repair procedures utilizing CFRP were proposed to restore the strength and displacement ductility capacity of earthquake damaged standard RC columns. Two standard single columns, one standard two-column bent, and two sub-standard columns were tested on a shake table, repaired using CFRP fabrics, and retested on the shake table to evaluate the

repair effectiveness. It was concluded that the strength and ductility of the standard columns were successfully restored and those of substandard columns were upgraded to the current seismic standard after the repair. However, the stiffness was not restored completely due to material degradation during the original column tests. A new repair design methods was developed.

Saiidi et al. (2013) have been conducting a research on repair of earthquake damaged bridge columns with fractured bars using a combination of longitudinal bar replacements and resortation of shear capacity and confinement using CFRP fabrics. Three half scale columns with interlocking spirals were tested under cyclic loading to failure. The same transverse and longitudinal reinforcement ratios of 1.23% and 2.13%, respectively, were used for each column. The columns were subjected to cyclic loading causing different moment to torque ratios. The repaired columns were designated R-Calt-1, R-Calt-2, and R-Calt-3. All the buckled longitudinal bars were repaired with steel couplers. Damaged spirals were removed and CFRP wrap was used to compensate the associated loss of shear capacity. CFRP wrap was also used to provide confinement for the concrete. Repaired columns were tested under the same loading procedure applied to the original column. So far test data for R-Calt-1 and R-Calt-2 have been made available. The tests have identified two reliable coupler types that may be used in column plastic hinge region in high seismic zones. Their tests indicated that new bars replacing damaged bars may be connected with undamaged bars using ultimate couplers as defined by Caltrans. The lateral force displacement response of column R-Calt-1 showed that the strength and displacement capacity of the column were successfully restored. On the other hand test results of R-Calt-2 showed that the strength was completely restored but

there was a significant loss in displacement ductility capacity because of the unusually high torsion that led to the failure of the CFRP jacket. There was no damage in the couplers.

He et al. (2013) conducted an experimental study on rapid repair of three half scaled severely damaged RC rectangular columns. Rapid repair of severely damaged columns were developed utilizing externally bonded unidirectional CFRP without any treatment of the damaged reinforcing bars. Both longitudinal and transverse CFRP sheets were used to repair the columns. The longitudinal and transverse reinforcement volumetric ratios were 2.13% and 1.32%, respectively. Column 1 was subjected to cyclic lateral loading and constant axial load. Columns 2 and 3 were subjected to the constant axial load and lateral cyclic loading and torsion, with torque-to-moment ratios (T/M) of 0.2 and 0.4, respectively. Damage to all three columns included concrete cracking, spalling, core crushing, and longitudinal reinforcement yielding and buckling. Two longitudinal reinforcing bars fractured in column 1 near the base of the column. The damage to all three columns was concentrated near the base of the column. The repair of each column was designed to restore the column strength associated with the peak load in the original test. The original column 1, 2, and 3 after repair were designated 1-R, 2-R, and 3-R, respectively. Because, the objective of their study was to develop a rapid repair method, only the plastic hinge zones were repaired. These regions were divided into two parts primary and secondary regions. A primary region was defined as the region where the damage was concentrated, and a secondary region was the region adjacent to the primary region with the same length. Portions of the columns outside these regions exhibited only minor cracks on the concrete surface and were not repaired.

The repair design of column 1-R consisted of three layers of longitudinal CFRP on the north and south faces of the column. The repair design was modified for column 2-R based on the performance of column 1-R and to include the design for torsion ($T/M = 0.2$). Three layers of longitudinal CFRP on the north and south faces and one layer of longitudinal CFRP in east and west faces of the column 2-R were provided. Similarly, the repair design for column 3-R was modified based on the performance of repaired columns 1-R and 2-R and to include the design for torsion ($T/M = 0.4$). Two layers of longitudinal CFRP on the north and south faces and one layer of longitudinal CFRP on east and west faces of the column 3-R were provided. A different number of transverse CFRP wraps was placed in the plastic hinge zone of different columns. Test results of repaired columns confirmed that strength can be restored or even enhanced for the columns without fractured bars. However, the stiffness was not restored completely due to material degradation during the original column tests. The displacement capacity of the repaired columns without fractured bars was restored nearly to that of the original column.

Rutledge et al. (2013) conducted an experimental study on a repair of three large scale circular bridge columns with buckled and ruptured bars. The design philosophy of the repair for the three columns was to relocate the plastic hinge to a higher location in the column, yet still achieve the same displacement capacity and strength as the original undamaged column. The new plastic hinge was relocated to a distance of one plastic hinge length away from the footing interface. Two different repair alternatives were executed utilizing unidirectional carbon fiber sheets in the hoop and longitudinal directions, with the latter anchored into the RC footing with carbon fiber anchors. The

first column, which contained buckled, but not fractured reinforcement, was repaired to increase the flexural strength of the original hinge, while providing additional confinement to the new hinge location. The second column, which also contained only buckled reinforcement and no ruptured bars, was repaired to increase the flexural strength of the original hinge without attempting to increase the ductility of the new hinge. The third column, which contained buckled and ruptured bars, was repaired in the manner similar to the second column. From force-displacement envelopes it was concluded that the repair restored the initial stiffness up to the level of the original column, as well as increased the displacement and force capacities.

Previous research on repair of RC bridge structural components subjected to seismic loading has been limited to columns. Moreover, few repairs that have been done in the field on other bridge components along with columns are rarely documented except for Caltrans bridge books. Bridge damage and repair information from these bridge books are presented and summarized in tables in Chapter 2. In addition an attempt was made to obtain reports from other countries (Japan and Chile) on earthquake damage to bridge components and their repair methodology. The information is also presented in Chapter 2.

1.3 Objective and Scope

The primary purpose of this study was to develop repair methods for various RC bridge structural components that have undergone different type and degree of damage under seismic loading. In the present report methods to repair bridge components such as beam-column joints, abutments, shear keys, and girders were developed. Repair of

bridge columns is presented through other studies (Vosooghi and Saiidi 2013). Because the available data base for components other than columns is limited, many simplifying and conservative assumptions were made about the residual capacity of damaged components. Because generally bridge columns are designed to be the primary source of energy dissipation through nonlinear action, they undergo a wide range of apparent damage. Six general apparent DS's were defined for standard columns and were used as the framework for other components. The repair methods in this study were developed using unidirectional carbon fiber reinforced polymer (CFRP) fabrics. Among different repair materials, CFRP fabrics were selected due to their light weight, high strength and stiffness-to-weight ratios, durability, and ease of installation. The target of repair was to restore the original capacity of earthquake damaged bridge components. The present study consisted of three parts. The first part was to conduct a detailed review of damage and repair in past earthquakes and compile the data in tables to identify gaps in repair. The second part was to develop practical methods to assess the condition of an earthquake damaged bridge structural components in terms of apparent DS's. In the third part repair design recommendations and design examples were developed to aid bridge engineers in quickly designing the number of CFRP layers based on the apparent DS.

Chapter 2. Past Earthquake Damaged Bridge Repair Practice

2.1 Introduction

California has experienced several moderate to high intensity earthquakes in the last 50 years. Division of Research and Innovation at Caltrans (2008) documented a report on visual inspection and capacity assessment of earthquake damaged RC bridge elements by developing a “visual bridge catalog”. This report documents damage from laboratory experiments and historic earthquakes and classifies the performance in relation to damage level of bridge components and sub-assemblages. However, the Office of Structures Maintenance and Investigations at Caltrans does not have a standard repair procedure/manual to repair earthquake damaged RC bridge components at different damage levels. Therefore, in order to categorize damage, identify repair gaps, and develop a standard repair manual, the bridge damage and their corresponding repair information from historic earthquakes were reviewed and compiled in tables as discussed in the following sections.

2.2 Review of damage and repair in past earthquakes

To develop a standard repair manual for RC bridge components at different damage levels, it is vital to identify the damage and failure modes of each component subjected to earthquake loading. An attempt was made to obtain records of post-earthquake bridge damage repair for recent earthquakes around the world with essentially no success except for California earthquakes for which Caltrans has documented and compiled a summary of the repair work in a methodical fashion. In other countries post-earthquake damage repair methods and repair objectives are not generally documented.

The lack of documentation is due to several reasons: (1) the rush to restore the bridge to service leaves little time to keep records, (2) in the absence of standard repair procedures, engineers, maintenance staff, and contractors tend to devise repair procedures that are highly variable depending on the bridge, and (3) repair objectives are not well defined even within the same agency. Even though repair methods and records could not be obtained from other countries, the bridge earthquake damage records were reviewed in this section.

The Caltrans maintenance records were the only data that could be used. To collect information about earthquake damage, failure modes, and repair of bridge components, several meetings with Structures and Maintenance Department at Caltrans were held. Past earthquake damage reports developed by the Caltrans Post Earthquake Investigating Team (PEQIT) for various significant earthquakes (San Fernando Valley 1971, Whittier 1987, Loma Prieta 1989, the Landers and Big Bear, Petrolia, and Northridge 1994) were reviewed. Utilizing PEQIT reports the bridges that suffered moderate to significant damage were identified, and the bridge books of these bridges in the paper and electronic forms were obtained from Caltrans. Bridge books are also known as bridge inspection records information system (BIRIS). These books compile the record of individual bridge damage (seismic and non-seismic) and the corresponding repairs that have been done through the life of the bridge. To identify the gaps in past earthquake damage bridge repair practices a detailed review of bridge books was conducted. To organize the data from past bridge damage and repair, the bridge damage and repair information was extracted from these bridge books and compiled in various tables. Table 2-1 to Table 2-6 present bridge number, component name, damage

description, and repair. Because the focus of the present study was on developing repair methods only for bridge structural components, non-structural components damage and repairs were not listed in these tables.

To study post-earthquake evaluation practice in Japan, a report on “Post Earthquake Measures of Transportation Facility in Japan” developed by World Federation of Engineering Organization (WFEO) was reviewed. In this report, damage to bridge components was categorized in five different damage levels. These five damage levels defined in alphabetical order (A’s, A, B, C, and D) are presented in Table 2-7. Damage degree A’s and D represents near collapse and no damage, respectively. Damage evaluation of RC piers was performed based on the location of damage and the type of failure. Distinct types of failure and damage level in piers were categorized based on bending damage at bottom of pier (Table 2-8), damage at mid-height section (Table 2-9), and shear damage (Table 2-10). In Table 2-8, P represents longitudinal rebar ratio. Proposed repair methods for these different types of failure, damage degree, and location are presented in Table 2-11. In Table 2-11, numbers 1 to 7 are associated with different damage levels (A’s to C) as shown in Table 2-8 to Table 2-10. The same damage evaluation and repair methods proposed for piers were applied to abutment walls. Report obtained from Japan does not include repair methods for other bridge components subjected to different damage levels. But the typical repair practice in Japan for RC girders and footings are presented in Table 2-12.

Similarly, a detailed review of bridge damage and repair of Chile earthquake was conducted. The repair and the reconstruction of the damaged bridges during Chile earthquake

were made according to the new seismic design standard for the design of bridges in Chile (Unjoh 2012). Post-earthquake bridge repairs of Chile earthquake were summarized and presented in Table 2.13. Basic concept of the repair and retrofit measures are to increase the integrity of girders by adding the end lateral beams and to restrain the lateral displacement by providing end diaphragms and extending support width to prevent unseating. Because, damage to bridges due to soil liquefaction is beyond the scope of the present research, such kind of damage is not discussed in this report.

2.3 Analysis of Database

The level of repair detail provided in Caltrans bridge books vary from general to specific. Therefore, to categorize a level of repair detail, four levels from 1 to 4 were defined. Level 1, 2, 3, and 4 corresponds to general/minimal, moderately detailed, detailed, and detailed step by step, respectively. Table 2-14 represents the summary of total numbers of cases studied for each bridge component using bridge books and their level of repair detail. From Table 2-14, it was concluded that majority of repair information falls under category 1 and 2 and therefore, there is a lack of comprehensive repair detail for bridge components. To identify Caltrans past seismic damage bridge repair practice, the repair methods presented in bridge books were summarized and presented in Table 2-15. The documented repairs in bridge books are described in very general terms. While books provide abundance of information about conducting bridge repairs, the specific efficacy of these repairs was not mentioned.

Besides Caltrans bridge books, bridge repair practice of other countries (Chile and Japan) was also reviewed. The bridge damage and repair report obtained from Japan

mainly discusses the repair of bridge column/pier subjected to different damage level (Table 2-11). Repair methods for other bridge components are described in very general terms. There is a lack of information about when the recommended repairs are the most appropriate.

The objective of post-earthquake repair measures of Chile's earthquake was to increase the integrity of girders by adding the end lateral beams and to restrain the lateral displacement by providing diaphragms and extending the seats (Table 2-13). During this earthquake, most of damage was due to superstructure collapse and therefore, there was a lack of detailed repair information at a component level.

Although some useful general information may be extracted from the repair methods described in the documents from Japan and Chile, the information is of limited use in the step-by-step repair methods discussed in subsequent chapters due to a lack of details.

2.4 Gaps in Knowledge on Past Earthquake Damage Repair of Bridge Components

The records of seismic damage repair conducted by Caltrans help provide an insight on repair practice. Nevertheless, these records address only the cases that were encountered in the field. Therefore, they do not necessarily address all damage states for various bridge components. As a result, there are gaps in the repair methods that need to be identified and addressed. To identify the gaps in past seismic damage bridge repair practice a detailed review of bridge books and the data from Chile and Japan was

conducted. Based on the analysis of database discussed in section 2.3 the following repair gaps are identified:

- While bridge books provide an abundance of information on conducting bridge repairs, the documented repairs are described in very general terms, and the specific efficacy of these repairs are not mentioned.
- There is a lack of information on step-by-step repair detail of bridge components. Moreover, the information about damage and repairs are scattered in various bridge books and extracting information from them is very difficult and time consuming.
- While a repair documented in the Japanese report is very informative for considering column repairs, repair methods for other bridge components are described in very general terms. Additionally, there is a lack of repair information about shear key, abutment wall, piles, diaphragm, and joints, etc.
- No considerations or assumptions are made about the residual capacity of bridge components at a given damage level to guide repair design.

From the above discussion, it was concluded that there is no complete repair guide is ready for use to repair bridge components subjected to different damage levels. While there is an abundance of information available on column/pier repair, the repair information about other bridge components is very limited. Very limited information is available on the behavior of structural components, particularly on the effectiveness of repairs and the relationship between repair technique and damage intensity. As a result, there are gaps in the repair methods that need to be identified and addressed. The goal of

this project is to fill the substantial gaps in knowledge noted above. Thus, present study discusses the repair methods for earthquake damaged RC bridge components for different type and degree of damage. The term “damage,” when used in this document, refers to the bridge damage suffered by an earthquake in its existing condition immediately after the earthquake. Prior affects of environmental deterioration, service conditions, and previous earthquakes are presumed to be pre-existing conditions and not part of the damage to be evaluated. The repair of different bridge components such as shear keys, girders, abutment walls, and joints are discussed in the following chapters.

Chapter 3. Repair of Earthquake Damaged Abutment Exterior Shear Keys

3.1 Introduction

Shear keys are designed to provide transverse support to the superstructure during service load and moderate earthquakes, but are designed as sacrificial elements under strong earthquakes to prevent damage to substructures. Another consideration in treating shear keys as sacrificial elements is that they are accessible, inspectable, and repairable. Based current Caltrans SDC 2010 for shear keys in “ordinary” bridges, the maximum transverse shear capacity of the shear keys is limited to prevent transferring large lateral forces from the superstructure to the substructure. Determining the earthquake force demand on the shear keys is difficult. Therefore, to limit the shear key capacity, Caltrans SDC 2010 has defined a range based on shear capacity of the abutment piles and dead load vertical reaction of the superstructure at the abutment to prevent significant damage to the substructure components. According to the Caltrans SDC 2010, the capacity of the shear key should be the smallest of 50 to 100 % of the dead load vertical reaction at the abutment and 50 to 100% of the 75% of the shear capacity of the piles plus shear capacity of one wing wall.

This report discusses the repair of earthquake damaged RC bridge superstructure shear keys. The study of shear keys is part of a more extensive research project aimed at developing repair methods for different bridge components damaged by earthquakes. The main objectives of this report are to define apparent earthquake damage states for shear keys and to describe a repair method for each damage state.

The shear key dimensions and detailing used in this report are the same as shear key unit 4A tested at University of California, San Diego (Bozorgzadeh et al. 2006), which was the typical Caltrans detailing requirement for the shear keys up to 2006. Therefore, the detailing of test unit 4A is assumed to be the typical detailing of the shear keys in existing bridges in California designed on or before year 2006 and the failure mode of which is the diagonal shear failure. The test unit 4A is shown in Figure 3-1.

3.2 Damage States

To define apparent damage states specific to shear keys, past-earthquake damage reports (Caltrans) and experimental research test data were reviewed. Past-earthquake damage reports of various earthquakes (San Fernando Valley 1971, Loma Prieta 1989, and Northridge 1994) were obtained from Caltrans compiled in bridge books and compact disks (CD's).

In this study, it was decided to use uniform definition of seismic apparent damage states for all bridge components. The apparent damage states represent the level of earthquake damage seen in a bridge component without any evaluation tools (destructive or non-destructive). Six distinct apparent damage states defined previously for standard columns (those meeting current seismic code requirements) (Vosooghi and Saiidi 2010) were considered and their relevance to shear keys was assessed. The column damage states are as follows:

DS-1: Flexural cracks

DS-2: First spalling and minor shear cracks

DS-3: Extensive shear cracks and/or extensive spalling

DS-4: Visible lateral and/or longitudinal bars

DS-5: Start of core concrete failure (imminent failure) but no fractured bars.

DS-6: Failure/fractured bars

Post-earthquake damage reports as well as past experimental research conducted on performance of exterior shear keys at UCSD (Bozorgzadeh et al. 2006) reveal that damage in shear keys is associated with diagonal cracks that become wider and more pronounced as the shear key approaches failure (Figure 3-2 and Figure 3-3). Three apparent damage states are applicable to shear keys: DS2, DS5 and DS6. DS2, DS5 and DS6 correspond to the minor diagonal shear cracking, major diagonal shear cracking (imminent failure), and failure, respectively. Other column damage states are not applicable because, unlike columns, shear keys are shear critical and brittle.

3.2.1. Damage State 2

In this damage state, minor horizontal cracks at the intersection of inclined side of the shear key and abutment stem wall are seen along with some minor diagonal shear cracks propagating towards abutment stem wall. Figure 3-2 shows a few examples of DS2.

3.2.2. Damage State 5

When a major, relatively wide diagonal shear crack propagates from the shear key-stem wall interface to the abutment stem wall the shear key is in damage state 5.

Tests have shown that with major shear cracks, the shear key is on the verge of failure. Hence this damage state is considered to be “imminent failure” or DS5. Figure 3-3 shows an example of DS5 observed after the San-Fernando Earthquake in 1971.

3.2.3. Damage State 6

This damage state is considered to be failure and includes combination of extensive spalling, fractured bars, and wide shear cracks in the abutment stem wall. Under this damage stage, the residual capacity of the shear key is negligible. Figure 3-4 shows a few examples of damage state 6.

3.3 Shear Key Capacity

The strut and tie model to calculate shear key capacity developed by Megally et al (2001) was used in this study. The capacity of exterior abutment shear keys can be calculated using Eq. 3-1.

$$V_n = V_c + V_s \text{ kips} \quad (3-1)$$

$$V_c = 0.03162 \times 2.4 \times \sqrt{f'_{ce}} bd \text{ kips} \quad (3-2)$$

$$V_s = \left[A_{vf} f_y \frac{d}{2} + A_{s,1} f_{y,1} h + A_{s,2} f_{y,2} d + n_h A_{s,s} f_{y,s} \frac{h^2}{2s} + n_v A_{s,s} f_{y,s} \frac{d^2}{2s} \right] \left(\frac{1}{h+a} \right) \text{ kips} \quad (3-3)$$

Where V_n is the nominal shear capacity of shear key (kips); V_c , V_s = concrete and reinforcing steel contribution to shear key capacity (kips), respectively; f_{ce} is the expected compressive strength of concrete; f_y , $f_{y,1}$, $f_{y,2}$, $f_{y,s}$ = specified yield strength of steel (ksi); V , b , d , a_1 , h = shear force demand, width of shear key (in), depth of shear key (in), height of the shear force from top of the abutment stem wall (in), and height of stem wall

(in), respectively, as shown in Figure 3-5 ; $A_{s,1}$, $A_{s,2}$, $A_{s,s}$, $A_{v,f}$ = total area of hanger bars (in^2), total area of shear key reinforcement of row 1 crossing shear key-abutment stem-wall interface (in^2), area of single horizontal or vertical reinforcement (in^2), and total vertical reinforcement that connects the shear key to the stem wall (in^2), respectively (Figure 3-6); n_h , n_v = number of side faces with horizontal and vertical reinforcement of abutment stem wall, respectively. In test unit 4A (Figure 3-1), the shear strength of concrete and steel is 86.7 kips [385.66 kN] and 248.2 kips [1104.05 kN], respectively.

3.4 Case Study

To develop repair procedure for shear keys, test unit 4A studied by Bozorgzadeh et al. (2006) was used as benchmark (Figure 3-1). Bozorgzadeh et al. conducted a study on capacity evaluation of exterior shear keys. In test unit 4A, the shear key was built monolithically with abutment stem wall. Vertical reinforcement was continued from the abutment stem wall and was anchored in the shear key. Experiments conducted on seismic performance of exterior shear key designed according to Caltrans SDC 2006 indicated that under lateral loads on shear keys diagonal shear failure occurs in the abutment stem wall and therefore, the shear key does not act as a fuse (Bozorgzadeh et al. 2006). The experiment also indicated that, the actual strength of the shear keys is significantly higher than the design value

The expected compressive and yield strength of steel was assumed to be 5 ksi [34.47 MPa] and 68 ksi [468.84 Mpa], respectively. The height of the abutment stem wall was 30.5 in. The width and depth of the shear key was 16.75 and 24 in, respectively. The area of reinforcement $A_{v,f}$, $A_{s,1}$, $A_{s,2}$, and $A_{s,s}$ were 2.64, 1.6, 0.44, and

0.11 in², respectively. Figure 3-6 shows these reinforcements. The shear capacity of the original shear key was calculated by Eq. 3-1. The steel contribution to the capacity of the shear key (V_s) was obtained from the equilibrium of forces along the critical diagonal crack BA as shown in Figure 3-7 resulting in Eq. 3-3.

In Figure 3-7, V = shear demand (kips); $T_1 = A_{s,1}f_{y,1}$ is the force developed by the tie at level 1; $T_2 = A_{s,2}f_{y,2}$ is the force developed in the first row of reinforcing bars crossing the shear key interface; T_{ih} and $T_{iv} = A_{s,s}f_{y,s}$ are the tensile forces in a single horizontal and vertical bar placed on the side faces of the abutment stem wall crossing the inclined crack, respectively; s = spacing between horizontal/vertical bars; a_1 as defined in Figure 3-5; and $C_{c,1}$ is the compression strut.

3.5 Shear Key Repair

Most of past research has been on the repair of columns, girders, etc. No research has been reported on the repair of shear keys. To develop repair method, the repair objective was first defined. Shear keys are shear dominated and are generally brittle. Therefore, the repair objective of shear keys is only to restore the shear strength without any explicit concern for ductility. It is hence necessary, to determine the capacity of an undamaged shear key and establish the residual capacity depending on damage state. The residual capacity of a shear key is the summation of the residual concrete and steel shear strength at a given damage state.

Vosooghi and Saiidi 2010 conducted research on repair of high shear columns at the University of Nevada, Reno. They defined five distinct apparent damage states for high shear columns, DS1 to DS5. DS1 to DS5 represents the progression in earthquake

damage to the high shear columns up to failure. The residual concrete shear capacity under DS2 and DS5 in high shear columns was recommended to be 80% and 20% of the undamaged capacity, respectively (Vosooghi and Saiidi 2010). Therefore, in designing repair of shear keys, it was assumed that the residual concrete contribution to shear in shear keys at DS2 and DS5 is 80% and 20%, respectively, while assuming full contribution of steel.

3.6 Repair Design

Using the proposed contribution ratios for concrete and steel to the shear strength of shear keys, a repair design methodology was developed based on apparent DSs. The repair design for each damage state is discussed in the following sections. An example illustrating repair design for each damage state is presented in Appendix B1. Shear Key Repair Design Examples

3.6.1. Damage State 2

The shear strength of the concrete and steel in a shear key at DS2 is 80% and 100% of those in the undamaged shear key, respectively. Consequently, repair is designed only to restore the 20% loss in concrete shear strength. The diagonal shear crack angle is assumed to be 45 degree. Unidirectional CFRP fabrics are applied with fibers in the horizontal direction to repair the crack. Unidirectional CFRP fabrics produced by the FYFE Co. SCH41/Tyfo S, with fibers in the horizontal or vertical direction are used. The material properties of CFRP fabrics used are shown in Table 3-1. To prevent substructure failure, the repair is designed so that the shear key is not over

strengthened. It is recommended to limit over strengthening of repaired shear keys to 10% of the total capacity.

In case of fully wrapped members, the effective strain in the CFRP can be used as 0.4% (Priestley et al. 1996). But in the case of side bonded CFRP wrapping, the effective strain in CFRP is a function of concrete compressive strength, CFRP thickness, CFRP tensile modulus and effective bond length (ACI 440.2R-08). Consequently, an iterative process is required to design the thickness of side bonded CFRP (ACI 440.2R-08). This procedure was found to be complicated for practical design. Therefore, a new equation to calculate directly the effective strain in side bonded CFRP was developed (Eq. 3-4). This equation was developed using a parametric study conducted on a wide range of compressive strength of concrete, CFRP thickness, and tensile modulus of CFRP based on ACI 440.2R-08. Appendix A. Development of Simple Equation to Estimate CFRP Thickness presents the study that led to the development of Eq. 3-4.

The simple equation gives the required CFRP thickness directly for a given required shear strength at a given damage state, (Eq.3-8). To determine the required CFRP thickness at a given damage state, the following step-by-step procedure is proposed:

Step 1. Determine the effective strain in CFRP:

$$\varepsilon_{fe} = 0.015 \times (t_f)^{-0.5} E_f^{-0.36} \left(\frac{f'_{ce}}{5} \right)^{0.67} \quad (3-4)$$

Where, ε_{fe} is the effective strain in CFRP; t_f is the total thickness of CFRP layer (in); E_f is the CFRP tensile modulus (ksi) and f'_{ce} is the expected compressive strength of concrete (ksi).

Step 2. Determine CFRP design shear force:

$$(V_f)_{Required} = \frac{1}{\psi} (V_n - (R_c V_c + V_s)) \text{ kips} \quad (3-5)$$

Where V_f is the shear strength provided by CFRP (Kips); ψ is the additional reduction factor of 0.85 recommended by ACI 440.2R-08, and R_c is the contribution ratio of concrete at a given damage state (0.80 and 0.20 for DS2 and DS5, respectively).

Step 3. Determine the CFRP required thickness. The contribution of the CFRP system to the shear strength of a member is based on the fiber orientation and an assumed crack pattern of 45° (Khalifa et al. 1998). The shear strength provided by the CFRP fabrics is determined by calculating the force resulting from the tensile stresses in the CFRP across the assumed crack as:

$$V_f = \varepsilon_{fe} \cdot t_f \cdot E_f \cdot d_{fv} (\sin \alpha + \cos \alpha) \quad (3-6)$$

$$V_f = \varepsilon_{fe} \cdot t_f \cdot E_f \cdot d_{fv}, \text{ for horizontal CFRP wrapping } (\alpha = 0^\circ) \quad (3-7)$$

Where, d_{fv} , α = total depth (in) and orientation angle (degree) of CFRP, respectively. Other parameters were defined previously in Eq. 3-4. Substituting Eq. 3-4 in Eq. 3-7, the following expression for the total CFRP required thickness is obtained:

$$t_f = \left(\frac{66.67 V_f}{E_f^{0.64} d_{vf}} \right)^2 \left(\frac{5}{f'_{ce}} \right)^{1.34} \text{ inch} \quad (3.8)$$

The bond capacity of FRP is developed over a critical length, l_{df} . To develop the effective FRP stress at a section, the available anchorage length of FRP should exceed the value given by Eq. 3-9 (ACI 440.2R-08). The inch-pound units are to be used in Eq. 3-9.

$$l_{df} = 0.057 \cdot \sqrt{\frac{E_f t_f}{f'_{ce}}} \text{ inch} \quad (3-9)$$

The following steps are recommended to repair shear keys in DS2:

Step 1. Remove any loose concrete.

Step 2. Fill the crack with epoxy injection.

Step 3. Install layers of CFRP with fibers in the horizontal direction to cover the entire crack height and extend beyond the cracks by the larger of l_{df} (Eq. 3-9) and 8 inches to provide sufficient bond.

3.6.2. Damage State 5

The shear strength of concrete and steel in shear keys at DS5 is 20% and 100% of the original strengths, respectively. Consequently, for DS5, repair is designed to restore the 80% loss in concrete shear strength. Unidirectional CFRP fibers are used in the horizontal direction to repair the diagonal shear crack at DS2 and 5. A similar repair procedure as that of DS2 is recommended for DS5.

3.6.3. Damage State 6

Under this damage stage, the residual shear capacity of shear key is negligible and consequently complete replacement is needed. The objective of repair of shear keys at DS6 is to restore the shear capacity and to change the mode of failure from diagonal

shear failure to sliding shear friction failure. Based on the experimental testing of shear keys, Bozorgzadeh et al. 2006 indicated that the previous detailing of Caltrans SDC 2006 of shear keys results in a diagonal shear failure. This is an undesirable mode of failure because it leads to an extensive damage to the abutment stem wall. To achieve the repair objectives of shear keys at DS6, the following step-by-step procedure is recommended.

Step 1. Remove the concrete from the earthquake damaged shear key and expose the steel bars.

Step 2. Remove the existing shear key transverse and inclined reinforcement but keep the abutment stem wall vertical reinforcement. Cut all the vertical reinforcement crossing the shear key-abutment stem wall interface above 45 degree failure plane. The reinforcement labels and layout are shown in Figure B1- 5. Elevation view of reinforcement layout

Step 3. Straighten the vertical reinforcement of abutment stem wall crossing the shear key-stem wall interface and then cut these bars at the shear key-stem wall interface level. Remove all the reinforcement connecting the shear key to the abutment back-wall, if any.

Step 4. Calculate the required shear key vertical reinforcement according to Caltrans SDC 2010 (Eq. 3-10). Provide sufficient development length for these bars (Eq. 3-12).

$$A_{sk} = \frac{F_{sk}}{1.8 \times f_{ye}} \text{ in}^2 \quad (3-10)$$

$$A_{sk,min} = \frac{0.05 \times A_{cv}}{f_{ye}} \text{ in}^2 \quad (3-11)$$

Where, A_{sk} is the required area of shear key vertical reinforcement (in^2); F_{sk} is the Shear key force (kips); A_{cv} is the area of concrete considered to be engaged in

interface shear transfer (in^2) and f_{ye} is the expected yield strength of steel (ksi). The area of shear key vertical reinforcement calculated using Eq. 3-10 should be greater than or equal to the minimum (Eq. 3-11) recommended by Caltrans SDC 2010.

$$l_{dh} = 24 d_b \text{ in} \quad (3-12)$$

Where, l_{dh} and d_b is the development length and diameter of shear key vertical bars.

Step 5. Drill holes in the abutment stem wall and install the shear key vertical reinforcement near the center line of the shear key in the direction parallel to shear force. Fill the drilled holes with epoxy.

Step 6. In the absence of Caltrans detailing guidelines for pre-2006 shear keys, use the ACI provisions (ACI 318-11, section 11.7.4.1 and 11.7.4.2) for minimum stirrups to provide confinement to the shear key. The spacing shall not exceed the smaller of $d/5$ or 12 in. The area of stirrups perpendicular to the flexural tension reinforcement, A_v , shall not be less than $0.0025bs$. Where s is the spacing of stirrups in the vertical direction parallel to the flexural reinforcement (in); b is the width of the section (in) as shown in Figure 3-5. 3D view of shear key. The area of stirrups parallel to the flexural tension reinforcement, A_v , shall not be less than $0.0015bs_2$. Where, s_2 is the spacing of the stirrups in the direction perpendicular to the flexural reinforcement.

Step 7. Provide a smooth construction joint at shear key-abutment stem wall interface to develop a weak plane so a shear friction coefficient of 0.4 can be used.

Chapter 4. Repair of Earthquake Damaged Prestressed Girder

4.1 Introduction

Prestressed (P/S) girders are typically designed as flexural members. Over the past few years numerous repair methods have been proposed by several industrial and academic institutions in order to restore flexural and shear capacity of corrosion and/or an impact damaged P/S girders. However, these repair methods are proposed for non-seismic damage. There is a lack of research on repair of P/S bridge girders damaged due to seismic loads. Therefore, repair methods for non-seismic damage were adapted. In this document, repair methods and repair design examples are presented in order to restore flexural capacity of seismically damaged P/S girders. The focus is on flexure, because girders with significant shear damage need to be replaced rather than repaired due to the brittle nature of shear failure. Also, due to a lack of sufficient data on correlating apparent damage to prestress loss, this report does not address possible prestress loss caused by the earthquake damage. To compensate the prestress loss in steel, prestressed CFRP may be used. Studies have been done on prestressed CFRP to strengthen the prestressed and non-prestressed beams (Kim et al. (PCI journal 2010); Czaderski and Motavalli 2007; Czaderski and Motavalli 2011).

The main objectives of this document are to define apparent earthquake DS's for P/S bridge girders and to describe a repair method for each damage state. In order to define DS's, several earthquake damage reports covering earthquake damage in California and Chile were reviewed. Review of bridge damage reports did not reveal information about seismic damage to girders.

Five (DS1, DS2, DS3, DS4, and DS6) out of six general apparent DS's defined in a previous study at the University of Nevada Reno for standard columns were found to be applicable to P/S bridge girders. Externally bonded unidirectional CFRP fabrics were used to repair P/S girders under DS2, DS3, and DS4 while reconstruction was recommended under DS6. DS1 corresponds to a minor flexure cracks and has no direct impact on the structural capacity of a girder, therefore, repair recommended in DS1 is a non-structural repair and only recommended for aesthetic or preventive measures using epoxy injection. Detailed repair design methodology is presented and discussed along with repair design examples in the following sections. The P/S girder dimensions and prestressing steel properties used in this report are the same as used in the report by Harries and Kasan at University of Pittsburgh, Pennsylvania (June 2009).

4.2 Damage States

To define apparent DS's specific to P/S bridge girders, detailed past-earthquake damage reports of various earthquakes (San Fernando Valley 1971, Loma Prieta 1989, and Northridge 1994) were obtained from Caltrans compiled in bridge books and compact disks (CD's). Also past-earthquake damage reports were studied from Chile earthquake of February 2010. Uniform definition of seismic apparent DS's was used for all bridge components. Six distinct apparent DS's defined in section 3.2 were considered and their relevance to P/S girders was assessed. Past earthquake damage reports reveal that five apparent DS's are applicable to P/S bridge girders: DS1, DS2, DS3, DS4, and DS6. Confined core damage is more common in columns instead of beams because

columns are designed for higher ductility and have higher confinement compared to girders; therefore, DS5 is excluded in P/S bridge girders

4.2.1. Damage State 1

In this damage state minor flexural/shear cracks are seen on the P/S girders soffit and/or sides of a girder and no other damage observed after an earthquake. Figure 4-1 shows an example of DS1.

4.2.2. Damage State 2

This damage state corresponds to minor spalling of the cover concrete and/or relatively wide flexural cracks. Figure 4-2 shows an example of DS2.

4.2.3. Damage State 3

P/S girders under DS3 exhibit extensive spalling of cover concrete. Figure 4-3 shows an example of P/S girder under DS3.

4.2.4. Damage State 4

This damage state consists of extensive spalling of cover concrete and visible longitudinal bars. Figure 4-4 shows an example of P/S girders under DS4.

4.2.5. Damage State 6

This damage state corresponds to a failure of P/S girders. P/S girders under damage state DS6 exhibit tendon fracture.

4.3 Assumptions and Simplifications

In order to conduct analysis and develop a repair method some assumptions and simplifications were made to present a more generalized approach to design seismic repair of P/S girders. All repair methods and design examples presented in this document consider girders that are not integrally attached to barrier walls. Inclusion of barrier walls complicates the analysis and diminishes the issue relevant to present work.

The damage to a P/S girder was modeled by removing strands from the section to mimic earthquake damage. Of course in reality tendons are not fractured in DS1, DS2 DS3, and DS4, but it was considered for sake of simplification of modeling a loss in moment capacity. Loss in moment capacity of a girder under given damage state was tied to a loss in strands effectiveness to provide moment capacity at that damage state

The CFRP repair design presented in this report accounts for the initial strain level of the concrete substrate. The existing strain is calculated assuming the beam is uncracked and the only loads acting on the beam at the time of the FRP installation are dead loads.

4.4 Moment-Curvature Analysis

To develop a repair method, a prototype P/S I-girder section was used in this study. Girder cross section details are shown in Figure 4-5 and Figure 4-6. Section geometric and material properties are presented in Table 4-1. Prototype girder geometric and material properties. Prestressing steel material properties are compiled in Table 4-2. For ease of developing a repair design it was assumed that, the given girder is a simply

supported interior girder. To determine the nominal moment capacity of I-girder, program Xtract was used to obtain the moment-curvature relationship. Effective yield moment was used as a nominal moment capacity of the section. Figure 4-7 shows the moment-curvature plot of the girder section at various DS's.

4.5 P/S Girder Repair

Most of past research has been on the repair of P/S girders subjected to corrosion and/or impact damage. No research has been reported on repair of earthquake damaged P/S girders. To develop a repair method, the repair objective was first defined. P/S girders are designed as flexural members. Therefore, the repair objective of P/S girder is to restore the ultimate flexural capacity of an earthquake damaged girders. It is hence necessary, to determine the capacity of an undamaged girder and establish the residual capacity depending on damage state. The residual capacity of the girder was established by correlating prestressed tendon contribution to moment capacity at each damage state. Therefore, in designing repair of P/S girders, it was assumed that tendon contribution to flexural capacity is 100% and 80% at DS1 and DS4, respectively, while considering 90% tendon contribution in DS2 and DS3. Initially it was decided to consider 5% and 10% loss in flexural strength at DS2 and DS3, respectively. However, it was felt that 5% loss is not significant. Therefore, it was decided to lump DS2 and DS3 and assume 10% capacity loss for both.

4.6 Repair Design to Restore Flexural Strength

Using the proposed contribution ratios for steel to the flexural capacity, a repair design methodology was developed based on apparent DSs. The following assumptions

are made in calculating the flexural resistance of a section strengthened with an externally applied FRP system (ACI 440.2R-08):

- The strains in the steel reinforcement and concrete are directly proportional to the distance from the neutral axis. That is, a plane section before loading remains plane after loading;
- There is no relative slip between external FRP reinforcement and the concrete;
- The shear deformation within the adhesive layer is neglected because the adhesive layer is very thin with slight variations in its thickness;
- The maximum usable compressive strain in the concrete is 0.003;
- The tensile strength of concrete is neglected; and
- The FRP reinforcement has a linear elastic stress-strain relationship to failure.

4.6.1. Damage State 1

This damage state exhibits minor flexural cracks on cover concrete. Damage at this level does not affect member capacity. Therefore flexural strength provided by prestressing steel at DS 1 is 100% of those in the undamaged P/S girder. Minor repair (epoxy injections) is recommended to fill these cracks. The repair recommended in DS1 is a non-structural repair and is only recommended for aesthetic or preventive measures.

4.6.2. Damage State 2 and 3

The moment capacity provided by strands under DS2 and DS3 is 90% of those in the undamaged P/S girder. Consequently, repair is designed to restore 10% loss in the

moment capacity. Unidirectional CFRP fabrics are applied at girder soffit with fibers in the longitudinal direction of the girder for repair.

The following steps are recommended in designing CFRP repair to restore flexural capacity of P/S girders. All equations shown in the repair design procedure are from ACI 440.2R-08 unless noted otherwise.

Step 1 Calculate the FRP system design material properties.

$$f_{fu} = C_E f_{fu}^* \text{ ksi} \quad (4-1)$$

$$\varepsilon_{fu} = C_E \varepsilon_{fu}^* \text{ in/in} \quad (4-2)$$

Where, C_E is the environmental reduction factor, f_{fu}^* is the ultimate tensile strength, ε_{fu}^* is the rupture strain, f_{fu} is the design ultimate tensile strength, and ε_{fu} is the design rupture strain.

Step 2 Preliminary Calculations:

- Modulus of elasticity of concrete, $E_c = 57000\sqrt{f'_{ce}}$ psi.
- Area of FRP layer $A_f = nt_f w_f \text{ in}^2$.

In which n is the number of CFRP layers, t_f is the total CFRP thickness, and w_f is the width of CFRP.

- Radius of gyration, $r = \sqrt{\frac{I_g}{A_g}}$ in.

Where, I_g is the gross moment of inertia and A_g is the gross area of cross section.

- Effective prestressing strain, $\varepsilon_{pe} = \frac{f_{pe}}{E_p}$ in./in.

In which f_{pe} is the effective prestress and E_p is the tensile modulus of prestressing steel.

- Effective prestressing force, $P_e = A_{ps}f_{pe}$ ksi.

Where, A_{ps} = total area of prestressing steel.

- Eccentricity of prestressing steel, $e = d_p - y_t$ in.

In which d_p is the depth of prestressing steel and y_t is the depth of neutral axis from top compression fiber.

Step 3 Determine the existing state of strain on the soffit: The existing state of strain is calculated assuming the beam is uncracked and the only loads acting on the beam at the time of installation are dead loads. Initial strain in the beam soffit is given by:

$$\varepsilon_{bi} = \frac{-P_e}{E_c A_g} \left(1 + \frac{e y_b}{r^2} \right) + \frac{M_{DL} y_b}{E_c I_g} \quad (4-3)$$

In which M_{DL} is the moment due to dead load and y_b is the distance of neutral axis from extreme tension fiber. Other parameters were defined in step 2.

Step 4 Estimate the depth to the neutral axis: Assume initial $c = 0.25h$

Where, c is the depth of the neutral axis from top compression fiber and h is the total depth of the section.

Step 5 Determine the design strain of the FRP system and use as the limiting strain in the FRP. The maximum strain that can be achieved in the FRP reinforcement is governed by the strain limitations due to either concrete crushing, FRP debonding, FRP rupture, or prestressing steel rupture.

- The failure controlled by FRP debonding can be calculated by:

$$\varepsilon_{fd} = 0.083 \sqrt{\frac{f'_c}{nE_f t_f}} \leq 0.9\varepsilon_{fu} \text{ in in.-lb} \quad (4-4)$$

In which f'_c is the compressive strength of concrete, ε_{fd} is the FRP debonding strain, and E_f is the tensile modulus of FRP.

- The effective design strain for FRP reinforcement at the ultimate limit state for failure controlled by concrete crushing can be calculated by:

$$\varepsilon_{fe} = \frac{\varepsilon_{cu}(d_p - c)}{c} - \varepsilon_{bi} \leq \varepsilon_{fd} \quad (4-5)$$

Where, ε_{cu} is the concrete ultimate strain.

- The failure strain controlled by prestressing steel rupture can be calculated by:

$$\varepsilon_{fe} = \frac{(\varepsilon_{pu} - \varepsilon_{pi})(d_p - c)}{(d_p - c)} - \varepsilon_{bi} \leq \varepsilon_{fd} \quad (4-6)$$

$$\text{Where, } \varepsilon_{pi} = \frac{P_e}{E_p A_{ps}} + \frac{P_e}{E_c A_g} \left(1 + \frac{e^2}{r^2}\right) \quad (4-7)$$

Step 6 Calculate the strain in the existing prestressing steel.

$$\varepsilon_{ps} = \varepsilon_{pe} + \frac{P_e}{E_c A_g} \left(1 + \frac{e^2}{r^2}\right) + \varepsilon_{pnet} \leq 0.035 \quad (4-8)$$

ε_{pnet} , can be calculated based on concrete crushing (Eq. 4-9) or FRP rupture or debonding (Eq. 4-10). The value of ε_{pnet} used in Eq. 4-8 is based on the failure mode of the system.

$$\varepsilon_{pnet} = 0.003 \frac{(d_p - c)}{c} \quad (4-9)$$

$$\varepsilon_{pnet} = (\varepsilon_{fe} + \varepsilon_{bi}) \frac{(d_p - c)}{(d_f - c)} \quad (4-10)$$

Where, ε_{pnet} is the net tensile strain in the prestressing steel beyond decompression, at the nominal strength.

Step 7 Calculate the stress level in the prestressing steel and FRP.

$$f_{ps} = \left(\begin{array}{ll} 28500 \varepsilon_{ps} & \text{for } \varepsilon_{ps} \leq 0.0076 \\ 250 - \frac{0.04}{\varepsilon_{ps} - 0.0064} & \text{for } \varepsilon_{ps} \geq 0.0076 \end{array} \right) \text{ ksi} \quad (4-11)$$

$$f_{fe} = E_f \times \varepsilon_{fe} \text{ ksi} \quad (4-12)$$

Where, f_{fe} is the effective stress in the FRP reinforcement and ε_{fe} is the effective strain in the FRP reinforcement.

Step 8 Calculate the equivalent concrete stress block parameters: The strain in concrete can be calculated from strain compatibility as follows:

$$\varepsilon_c = (\varepsilon_{fe} + \varepsilon_{bi}) \left(\frac{c}{d_f - c} \right) \quad (4-13)$$

The strain ε'_c corresponding to f'_{ce} is calculated as:

$$\varepsilon'_c = \frac{1.7f'_{ce}}{E_c} \quad (4-14)$$

Approximate stress block factors may be calculated from the parabolic stress-strain relationship and is expressed as follow

$$\beta_1 = \frac{4\varepsilon'_c - \varepsilon_c}{6\varepsilon'_c - 2\varepsilon_c} \quad (4-15)$$

$$\alpha_1 = \frac{3\varepsilon'_c \varepsilon_c - \varepsilon_c^2}{3\beta_1 \varepsilon'^2_c} \quad (4-16)$$

Where, α_1 and β_1 are the equivalent concrete stress block factors.

Step 9 Calculate the internal force resultant and check if equilibrium is satisfied. Force equilibrium should be verified by checking with initial estimate of c (Step 4).

$$c = \frac{A_p f_{ps} + A_f f_{fe}}{\alpha_1 f'_{ce} \beta_1 b} \text{ in} \quad (4-17)$$

Step 10 Repeat Steps 4 through 9 with different values of c until c is converged, indicating that equilibrium is achieved.

Step 11 Calculate flexural strength components:

The design flexural strength is calculated using Eq. 4-20. An additional reduction factor, $\Psi_f = 0.85$, is applied to the contribution of the FRP system.

Prestressing steel contribution to bending:

$$M_{np} = R_c A_p f_{ps} \left(d_p - \frac{\beta_1 c}{2} \right) \text{ kip-in.} \quad (4-18)$$

In which R_c is the contribution ratio of steel at DS2, DS3 and DS4 (0.90 for DS2 and DS3 and 0.80 for DS4).

FRP contribution to bending:

$$M_{nf} = A_f f_{fe} \left(d_f - \frac{\beta_1 c}{2} \right) \text{ kip-in.} \quad (4-19)$$

Design flexural strength of the section can be calculated as:

$$M_n = [M_{np} + \Psi_f M_{nf}] \text{ kip-in.} \quad (4-20)$$

4.6.3. Damage State 4

The moment capacity provided by strands under DS4 is 80% of those in the undamaged P/S girder. Consequently, repair is designed to restore the 20% loss in strands capacity. Unidirectional CFRP fibers are used in the longitudinal direction of the girder to restore flexural capacity of P/S girder under DS4. The same repair procedure as that of DS2 and DS3 is recommended for DS4 except that in Step 2, the number of CFRP

layers, area of prestressing steel, and eccentricity value should be adjusted and in Step 11 (Eq. 4-18), $R_c = 0.80$ should be used. A numerical example illustrating the proposed repair design for DS2, DS3, and DS4 is presented in Appendix B2. Girder Repair Design Examples

Chapter 5. Repair of Earthquake Damaged RC Bridge Abutments

5.1 Introduction

Abutments are earth retaining structures that provide resistance against deformation and earthquake induced internal forces from bridge superstructure. As a component of a bridge, the abutment provides the vertical support to the bridge superstructure at the bridge ends and also connects the bridge with the approach roadway. Because abutment shears keys are designed to shear off under major earthquakes, the abutment foundation and piles are intended to be capacity protected member although some damage might be expected in the abutment itself. There are few studies available on strengthening of masonry and reinforced concrete walls (Konstantinos et al 1999; Sayari and Donchev 2012), the results of which might be of use for bridge abutment walls. Konstantinos, Thomas, and Andreas (2003) conducted a study on low slenderness reinforced concrete walls. In their study, the walls were designed according to modern design code provisions, initially subjected to cyclic loading to failure and subsequently, repaired using fiber reinforced polymer (FRP) jacket. There is no research data reported specifically on repair of earthquake-damaged bridge abutments with different damage levels. This report discusses the repair of earthquake damaged reinforced concrete bridge abutments utilizing unidirectional carbon fiber reinforced polymer (CFRP). Based on review of past earthquake damage on abutment walls, shear capacity appears to be the most critical abutment resisting force that is affected by earthquake damage. Therefore, the repair was designed to restore the shear capacity of abutment stem wall. The study of bridge abutments is part of a more extensive research project aimed at developing repair

methods for different bridge components damaged by earthquakes. The main objectives of this report are to define apparent earthquake damage states for bridge abutments and to describe a repair method for each damage state. To define apparent damage states specific to bridge abutments, detailed past-earthquake damage reports of various earthquakes were reviewed. Shear key damage repair was presented in a separate report. Furthermore, abutment back wall are expected to be sacrificial and replaced after strong earthquakes. Therefore, the focus of this report is on repair of abutment stem walls.

5.2 Damage States

To define apparent damage states specific to bridge abutments, detailed past earthquake damage reports for various earthquakes (San Fernando Valley 1971, Loma Prieta 1989, and Northridge 1994) were obtained from Caltrans compiled in bridge books and compact disks (CD's). Also earthquake damage reports were studied from Chile earthquake of February 2010. Six distinct apparent damage states defined previously in section 3.2 were considered and their relevance to abutments was assessed.

Past earthquake damage reports reveal that four apparent damage states are applicable to bridge abutments: DS2, DS3, DS4, and DS6. Abutments are typically massive components and effects of minor cracks may be neglected. Therefore, DS1 was excluded in abutments. Also confined core damage is more common in columns instead of abutments because columns are designed for high ductility and have higher confinements compared to abutments; therefore, DS5 was also excluded in abutments.

5.2.1. Damage State 2

This damage state corresponds to minor spalling of the cover concrete. Figure 5-1 shows an example of DS2.

5.2.2. Damage State 3

Abutments under DS3 exhibit extensive spalling of cover concrete. Figure 5-2 shows an example of abutments under DS3.

5.2.3. Damage State 4

This damage state consists of extensive spalling of cover concrete and visible reinforcing bars. Figure 5-3 shows an example of abutments under DS4.

5.2.4. Damage State 6

This damage state corresponds to fractured bars and failure of abutments. Figure 5-4 shows abutments under damage state DS6.

5.3 Assumptions and Simplifications

In order to design repair for abutments some assumptions were made to simplify the repair. Abutments are commonly over designed to carry vertical loads induced by superstructure and soil pressure. It was assumed that the repair for DS2 to DS4 would include replacing any damaged concrete, and, hence, there is no loss in the vertical load and flexural capacity of abutments for these damage states. Furthermore, it was assumed that an abutment with fractured bars (DS6) could be repaired by replacing the fractured or buckled bars and/or utilizing CFRP.

Replacing concrete and epoxy injection of cracks in an abutment under DS2 were also assumed to be sufficient to restore the in-plane shear capacity. However, under DS3 and DS4, it was assumed that shear capacity is reduced by 50% and CFRP fabrics are used to restore the capacity. Also because abutments are lightly reinforced, the contribution of steel to shear capacity under DS3, DS4, and DS6 was ignored. Another assumption was to use the same repair method for DS3 and DS4. This assumption was made due to a lack of data on internal stress distribution in abutments with different damage states. This repair design would be conservative for DS3.

For abutments under DS6, it was assumed that shear capacity of abutment is reduced by 80% in and near the damaged area. To develop a repair method for abutments under DS6 two assumptions were made: out of plane movement is negligible and there is no significant reduction in the wall height due to failure.

Finally, in the absence of research data on repair of earthquake-damaged bridge abutments, repair methods for non-seismic damage were adopted. To develop repair methods, 45-degree diagonal crack pattern was assumed. Therefore it was assumed that unidirectional CFRP fabrics placed with fibers in the horizontal or vertical fibers are equally effective in resisting shear in stem wall. Consequently, 50% of the lost shear strength is restored by CFRP horizontal fibers and 50% is restored by CFRP vertical fibers.

5.4 Abutment Stem Wall Capacity

To demonstrate the repair design, the shear capacity at bottom of the stem wall was calculated. In bridge abutments, only minimum shear reinforcement is placed to

prevent cracking. Therefore, concrete shear strength (V_C) is the main part of the total nominal shear capacity. Eq. 5-1 (ACI 318-11) was utilized to estimate the in-plane nominal shear capacity of stem wall. Where A_{cv} , α_c , f'_{ce} , and f_{ye} , are the gross area of concrete section bounded by web thickness and length of section in the direction of shear force, the coefficient defining the relative contribution of concrete strength to nominal wall shear strength, the expected compressive strength of concrete, and the expected yield strength of reinforcement, respectively. The coefficient α_c varies linearly between 3.0 and 2.0 for $\frac{h_w}{l_w}$ between 1.5 and 2.0 (ACI 318-11). Where h_w and l_w are the height and length of abutment stem wall. In this report α_c equal to 3 was used for typical abutments. Term ρ_t is the ratio of area of distributed transverse reinforcement to gross concrete area perpendicular to that reinforcement. Because abutments are lightly reinforced, the contribution of steel to shear capacity was assumed equal to zero ($\rho_t f_{ye} = 0$). In calculating A_{cv} , the entire l_w may be conservatively used. If damage is localized, the designer may use a shorter length not to be less than $1.5 \times h_w$.

$$V_n = A_{cv} (0.03162 \alpha_c \sqrt{f'_{ce}} + \rho_t f_{ye}) \text{ kips} \quad (5-1)$$

or

$$V_n = V_c = 0.03162 A_{cv} (3 \sqrt{f'_{ce}}) \text{ kips}$$

5.5 Repair Design

Assuming no loss in the shear capacity for DS2, 50% loss in shear capacity for DS3 and DS4, and 80% loss in shear capacity for DS6, a repair design methodology was developed based on apparent DSs. The repair design for each damage state is discussed

in the following sections. A numerical example illustrating the proposed repair design for DS3, DS4, and DS6 is presented in Appendix B3. Repair of Bridge Abutments Walls

5.5.1. Damage State 2

This damage state exhibits minor spalling of cover concrete. Damage at this level does not affect member capacity. Therefore, shear strength provided by concrete at DS2 is 100% of that in the undamaged abutment. Epoxy injections and concrete patching is recommended to fill cracks and minor spall in concrete. The repair recommended in DS2 is a non-structural repair and its purpose is to protect reinforcement against corrosion and for aesthetic reasons.

5.5.2. Damage State 3 and 4

As discussed in Section 5.3, the same repair method is recommended for DS3 and DS4. The shear strength of the concrete in a bridge abutment at DS3 and DS4 is assumed to be 50% of that in the undamaged abutment. Consequently, repair is designed only to restore 50% loss in the concrete shear strength. The diagonal shear crack angle is assumed to be 45 degree. Unidirectional CFRP fabrics bonded on the wall surface are applied in the horizontal and vertical direction. Eq. 3-8 was used to determine the thickness for a given required shear strength at a given damage state. To determine the required CFRP thickness at a given damage state, the following step-by-step procedure is proposed:

Step 1. Determine CFRP design shear force:

$$(V_f)_{Required} = \frac{1}{\psi} (V_n - (R_c V_c)) \text{ kips} \quad (5-2)$$

Where V_f is the shear strength provided by CFRP (Kips); Ψ is the additional reduction factor of 0.85 recommended by ACI 440.2R-08; and R_c is the contribution ratio of concrete at a given damage state.

Step 2. Determine the CFRP required thickness using Eq. 3-8. Term d_{fv} was taken equal to the length of the wall.

The bond capacity of FRP is developed over a critical length, l_{df} . To develop the effective FRP stress at a section, the available anchorage length of FRP should be at least the value given by Eq. 3-9.

The following steps are recommended to repair abutments in DS3/DS4:

Step 1. Remove any loose concrete.

Step 2. Fill the crack with epoxy injection.

Step 3. Install layers of CFRP with fibers in the horizontal and vertical direction to cover the entire crack height and extend beyond the cracks by at least l_{df} (Eq. 3-9) to provide sufficient bond. It is assumed that horizontal and vertical fibers have equal contribution to the shear strength because the crack angle is 45 degrees.

5.5.3. Damage State 6

Walls with fractured and/or buckled reinforcing bars may be repaired by replacing the damaged bars. If there is a significant permanent rotation associated with out of plane bending or reduction in the wall height due to the loss of vertical load resistance, the wall would have to be replaced.

Recent tests of reinforced columns under cyclic loading have identified several reliable coupler types that may be used in plastic hinges (Caltrans and UNR 2010; Saiidi et al 2013). New bars replacing damaged bars may be connected with undamaged bars using service couplers as defined by Caltrans. In this case the repair steps would consist of removing loose concrete and damaged bars, epoxy injecting the cracks, placing new bars, and casting new concrete. Alternatively, CFRP fabrics with horizontal and vertical fibers may be used to provide tensile strength that matches that of damaged bars. In this case, the damage bars will not be replaced, and may left in place. The recommended repair method when CFRP is used is as follows:

Step 1. Remove all loose concrete from the earthquake damaged stem wall and expose the steel bars.

Step 2. Fill cracks by injecting epoxy.

Step 3. Straighten the reinforcement in the damaged portion of abutment stem wall.

Step 4. Cast new concrete in the damaged portion of the stem wall.

Step 5. Assuming 80% loss in shear strength ($R_c = 0.20$), design CFRP repair utilizing Eq. 5-2 and 3-8.

Step 6. Place the unidirectional CFRP fabrics in horizontal and vertical direction to cover the entire crack height and extend beyond the cracks by at least l_{df} (Eq. 3-9) to provide sufficient bond. It is assumed that horizontal and vertical fibers have equal contribution to the shear strength because the crack angle is 45 degrees.

Chapter 6. Repair of Earthquake Damaged RC Beam-Column Bridge Joints

6.1 Introduction

Beam-column joints are critical elements of reinforced concrete (RC) bridge structures under earthquake loading. According to Caltrans bridge design specification (BDA 2008), beam-column joints designed before early 1990's are categorized as weak, moderate, and intermediate joints whereas the joints designed subsequently are categorized as strong, capacity-protected joints. Categorization of these joints is based on the amount of transverse reinforcement, ductility, and post cracking moment resisting capability. Therefore, in existing bridges there is a blend of weak, moderate, and strong joints depending on their design year. Consequently, joints in existing bridges could be vulnerable to damage.

In the past few years an extensive and detailed research has been done on repair of earthquake-damaged beam-column joints in buildings utilizing various methods. For example; epoxy injections, local replacement of damaged concrete and steel, RC jacket, CFRP, GFRP, and steel plates, etc. (French et al. 1990; Adin et al. 1993; Tsonos and Konstantinos 2003; Engindeniz 2008; Li and Pan 2011; Al-Salloum et al. 2011; and Sezen 2012). These seismic repairs were developed for beam-column joints that are typical in buildings. There is a lack of research on seismic repair of beam-column joints in bridges. It is generally doubtful that repairs developed for joints in buildings will be effective for bridge joints. In comparison with building construction, existing bridge joints are likely to involve larger member cross sections, larger reinforcing bar diameters, different joints geometries, and yielding in columns instead of beams. A limited number

of studies have been conducted on retrofit of existing beam-column joints in bridges (Pantelides and Gergely 1999; Lowes and Moehle 1999; and Silva et al. 2007). While retrofit methods may be used as a general guide for possible adaptation for repair, they are not generally applicable to repair of standard joints because: (1) “retrofit” is normally done for undamaged substandard joints to make up for the lack of proper design and detailing, and (2) “repair” has to address loss of capacity due to damage. Another consideration is that a comprehensive document on seismic damage repair has to address repair for different damage states. There are no available studies to develop and experimentally verify the performance of repair methods for joints with different damage states. An additional possible source to seek past work on repair of earthquake damaged joints is the records of repair after earthquakes. Indeed Caltrans has repaired a few bridge joints in the field but the extent of documentation for these repairs is not sufficient to readily adopt those methods for a systematic repair process.

Bridge joints are designed as shear critical elements. In general, joints suffer shear failure if the joint shear stresses (principal tensile and compression) exceed the joint capacity (Priestley et al. 1996). Because, standard joints are less likely to undergo vertical splitting and/or reinforcing bar anchorage failure, the main objective of this study was to restore loss in the shear strength. In the present report, repair methods were developed to restore the shear strength loss of seismically damaged knee and tee (T) joints of RC bridges subjected to different levels of earthquake damage. The visual seismic damage data of joints from historic earthquakes as well as data from experimental tests revealed that all six general apparent damage states (DS's) discussed in Chapter 3 are applicable to beam-column joints. Based on the earthquake damage

level, the repair was designed for each damage state, and in cases where the extent of damage precludes an economically feasible repair, reconstruction of joints is recommended. DS1 corresponds to a minor flexure cracks and has no direct impact on the joint structural capacity. Therefore, repair recommended for DS1 is a non-structural repair for aesthetic reasons using epoxy injection. Externally bonded unidirectional CFRP fabrics were used to repair RC beam-column joints under DS2, DS3, and DS4, while joint replacement is recommended for DS5 and DS6. Repair design examples are presented in Appendix B4.

6.2 Damage States

To define apparent DS's specific to joints, detailed review of past-earthquake damage reports of various earthquakes was conducted as previously discussed in Chapter 2. Uniform definition of seismic apparent DS's was used for all bridge components. Six distinct apparent DS's defined previously in section 3.2 were considered, and their relevance to joints was assessed. Past earthquake damage reports and test data on bridge joints reveal that all six apparent DS's are applicable to the joints.

6.2.1. Damage State 1

This DS corresponds to minor flexural cracks at column-joint and/or beam-joint interface. Figure 6-1 shows an example of DS1.

6.2.2. Damage State 2

This DS corresponds to shear cracking and/or minor spalling of the cover concrete. Figure 6-2 shows an example of DS2.

6.2.3. Damage State 3

Joints under DS3 exhibit extensive spalling of cover concrete. Figure 6-3 shows an example of joints under DS3.

6.2.4. Damage State 4

This DS consists of extensive spalling of cover concrete and visible bars. Figure 6-4 shows an example of joints under DS4.

6.2.5. Damage State 5

DS5 corresponds to start of crushing of joint core concrete.

6.2.6. Damage State 6

This DS corresponds to the core concrete crushing and/or bar fracture. Figure 6-5 shows an example of joints under DS6.

6.3 Assumptions and Simplifications

In order to develop a repair method for joints, the following simplifying assumptions were made:

- a) Epoxy injection of cracks under DS1 was assumed to be sufficient to restore the lost shear strength.
- b) Under DS2, it was assumed that the shear strength is reduced by 30% while considering a 60% loss under DS3 and DS4. CFRP fabrics are used to restore the capacity. Another assumption was to use the same repair method for DS3 and DS4. This

assumption was made due to a lack of data on internal stress distribution in joints with different DS's. This repair design would be conservative for joints under DS3.

c) Joints under DS5 and DS6 have substantially lost their strength and stiffness due to damage in the core concrete and /or reinforcing bars. Consequently, replacement of joints is recommended under DS5 and DS6.

d) Caltrans SDC 2010 provides recommendations for T-joint shear design including principal tensile and compressive stress limits, minimum joint shear reinforcement, and detailing of column main reinforcement extending into the cap-beam. However, there are no provisions for design levels of joint shear stress applicable to knee joints. Caltrans considers knee joints as nonstandard elements. The response of knee joint varies with the direction of the moment (opening or closing) applied. In the absence of Caltrans design stress limits for knee joints, and to be consistent, ACI provisions (ACI-ASCE 352R-02) were used for both T and knee joints.

e) To develop repair methods, a 45-degree crack angle was assumed. Unidirectional CFRP fabrics with horizontal or vertical fibers were utilized to resist joint shear. To restore lost shear strength, CFRP was provided on both sides of the cap-beam. Therefore, the total required CFRP thickness in each direction on each side was designed to restore 25% of total loss in the shear strength.

f) Finally, the same percentage of loss in shear strength and the same repair method were used for T joints and knee joints under a given DS.

Experimental evidence indicates that diagonal cracking is initiated in the joint region when the principal diagonal tension stress is approximately $3.5 \sqrt{f'_c}$ psi (Priestley et al. 1996). This stress level is nearly 29% of the total allowable shear stress of $12 \sqrt{f'_c}$

psi for T-joints. Therefore, an assumption of 30% strength loss for T-joints under DS2 was considered to be reasonable.

Except for columns, there is a lack of research on bridge components to correlate visual damage to the residual capacity. Therefore, under DS3 and DS4 the loss of joint shear strength was tied to a shear strength loss in columns under DS4. As defined in a previous study conducted by Vosooghi and Saiidi (2010), loss in concrete contribution to shear strength at DS4 is 60%. Consequently, 60% loss in shear strength was considered for T and knee joints under DS3 and DS4. It is to be noted that the assumed reductions are intended to be conservative.

6.4 Joint Capacity

To demonstrate a repair design, rectangular beam-column configuration was used as a benchmark. The joints shown in Figure 6-6 to Figure 6-9 were used to determine the shear strength of T and knee joint. The nominal joint shear strength (V_{jn}) was calculated using Eq. 6-1 (ACI 352 R-02).

$$V_{jn} = 0.03162 \gamma \sqrt{f'_{ce}} b_j h_c \text{ kips} \quad (6-1)$$

Where f'_{ce} is the expected compressive strength of concrete. Term γ is equal to 12 and 8 for T and knee joints, respectively. Terms b_j and h_c are the effective joint width and depth of the column, respectively, in the direction of joint shear being considered. As per ACI-ASCE 352 R-02 the effective joint width should not exceed the smallest of 6-2 (a), (b), and (c).

$$\frac{b_b + b_c}{2} \quad 6-2 \text{ (a)}$$

$$b_b + \sum \frac{mh_c}{2} \quad 6-2 \text{ (b)}$$

$$b_c \quad 6-2 \text{ (c)}$$

Terms b_b and b_c are the width of the longitudinal beam and the width of the column, respectively. Term m is the slope to define the effective joint width transverse to the direction of the shear. For joints where the eccentricity between the beam centerline and the column centroid exceeds $\frac{b_c}{8}$, m is 0.3 and for all other cases m is 0.5 (ACI-ASCE 352 R-02).

6.5 Repair Design

Assuming no loss in the shear strength for DS1, 30% loss in shear strength for DS2, and 60% loss in shear strength for DS3 and DS4, a repair design methodology was developed based on apparent DSs. Unlike knee joints the presence of bearing pads over cap beam was considered for T-joints. Therefore, the repair was conservatively designed for side bonded CFRP configuration for both T and knee joints. The simple equation developed for shear keys (Eq. 3-8) was used to determine the required CFRP thickness for joints under a given DS. For knee joints, it is recommended to use U wraps to provide better confinement and integrity to the joint.

The width of CFRP fabrics with vertical fibers was taken equal to the depth of a cap-beam to cover entire crack width and enhance joint integrity. To provide development length for CFRP fabrics with vertical fibers, it is recommended to bend the

fibers at the bottom of a cap beam and extend up to the outer face of the column. The repair design for each DS is discussed in the following sections. A numerical example illustrating the proposed repair design for DS2, DS3, and DS4 is presented in Appendix B4. Repair Design Examples for Bridge Cap Beam-Column Joints

6.5.1. Damage State 1

This DS exhibits minor flexural cracks in the cover concrete of the beam or column adjacent to the joint. Damage at this level does not affect joint capacity. Therefore, shear strength at DS1 is 100% of that in the undamaged joint. Epoxy injection is recommended to fill cracks in concrete. The repair recommended in DS1 is a non-structural repair and its purpose is to protect reinforcement against corrosion and for aesthetic reasons.

6.5.2. Damage State 2

Shear strength of a joint at DS2 is 70% of that in the undamaged joint. Consequently, repair is designed only to restore the 30% loss in the shear strength. The diagonal shear crack angle is assumed to be 45 degree. Unidirectional CFRP fabrics bonded on the joint surface are applied in the horizontal and vertical direction on both sides of the joint. To determine the required CFRP thickness at a given DS, the following step-by-step procedure is proposed:

Step 1. Determine CFRP design shear force:

$$(V_f)_{Required} = \frac{1}{\psi} (V_{jn} - (RV_{jn})) \text{ kips} \quad 6-3$$

Where R is the percentage of original shear strength left at a given DS, R is equal to 0.70 for DS2 and 0.4 for DS3 and DS4.

Step 2. Determine the required CFRP thickness using Eq. 3-8. In Eq. 3-8, d_{fv} was taken equal to the depth of a cap beam.

The following steps are recommended to repair joints in DS2:

Step 1. Remove any loose concrete.

Step 2. Inject epoxy in the cracks.

Step 3. Install layers of CFRP with fibers in the horizontal direction to cover the entire crack height and extend beyond the cracks by at least l_{df} (Eq. 3-9) to provide sufficient bond.

Step 4. Install layers of CFRP with fibers in the vertical direction to cover the entire crack width and then, bend the fibers at the bottom of a cap beam to extend up to the outer face of the column. It is assumed that horizontal and vertical fibers have equal contribution to the shear strength because the crack angle is 45 degrees.

6.5.3. Damage State 3 and 4

The same repair method used for DS2 is recommended for DS3 and DS4. The joint shear strength at DS3 and DS4 is assumed to be 40% of that in the undamaged joint. Consequently, repair is designed only to restore 60% loss in the shear strength. The diagonal shear crack angle is assumed to be 45 degree. Unidirectional CFRP fabrics bonded on the wall surface are applied in the horizontal and vertical direction on both sides of the joint.

Chapter 7. Summary and Conclusions

7.1 Summary

Highway bridges need to be restored after earthquake damage. Based on post-earthquake inspection of bridge elements, engineers have to decide whether the bridge/component is repairable within a reasonable cost and time frame, or if it needs to be replaced. In this study repair methods to repair bridge components such as abutments, shear keys, girders, and cap beam-column joints were developed. Repair of columns is presented through other studies (Vosooghi and Saiidi 2013 and Saiidi et al. 2013). In parallel with the previous research on repair of bridge columns, repair methods using CFRP materials were developed for other earthquake damaged RC bridge components with distinct damage levels. Repair methods developed were based on the visual damage evaluation with no non-destructive testing involved to expedite decision making. To develop repair methods the present study was conducted in three different phases: (1) conduct a detailed review of damage and repair in past earthquakes to identify repair methods that can be readily adopted and to determine gaps in repair methodologies, (2) develop practical methods to assess the condition of earthquake damaged bridge structural components in terms of apparent damage states (DS's), and (3) develop repair design recommendations and design examples to aid bridge engineers in quickly designing the number of CFRP layers based on the apparent DS.

In the first phase of the study, detailed review of past earthquake damage and repair practice was conducted. There was a relatively large amount of information

available for repair of bridge columns compared to other bridge components. In addition to columns, an attempt was made to obtain records of post-earthquake damage repair for other bridge components around the world. The past bridge repair work documented by Caltrans in various bridge books was found to be the most comprehensive. In other countries post-earthquake damage repair methods and repair objectives were not generally documented. Even though repair methods and records could not be obtained from other countries, the bridge earthquake damage records and their evaluation methods were reviewed. Finally, all past earthquake damage and repair data that were reviewed presented in various tables to categorize and rate the extent by which they can be used in development of a general repair guideline and to identify gaps in repair methods.

In the second phase of this study practical methods were developed to access the condition of earthquake damaged bridge structural components in terms of apparent DS's. Earthquake damage was quantified and correlated to a series of visible DS's. Upon consultation with Caltrans engineers, a uniform definition of apparent DS's that had been developed for bridge columns in a previous study at UNR (Vosooghi and Saiidi 2010) was used as the framework for other bridge components, with the understanding that not all DS's are applicable to all components.

The third phase of this study consisted of developing repair design recommendations and design examples to aid bridge engineers in quickly designing the number of CFRP layers and the necessary bond transfer length based on the apparent DS. Unidirectional CFRP fabrics were used to develop repair methods. Because ACI 440.2R-08 method of calculating the effective strain in CFRP for sided boned FRP

configuration was iterative and found to be time consuming, a new simple equation was developed to calculate the effective strain in the CFRP. The equation was extensively evaluated for a wide range of parameters. The results showed a good agreement with ACI 440.2R-08 results. Hence the proposed simple method was adopted in the repair design recommendations. In cases where the extent of damage precludes an economically feasible repair, reconstruction of damaged bridge component was recommended. Because of limited data base for bridge components other than columns, many simplifying and conservative assumptions were made about the residual capacity of damaged components.

7.2 Recommendations and Conclusions

The following conclusions were drawn based on the study presented in this document:

- While Caltrans bridge books provide many cases of post-earthquake bridge damage repair, the documented repairs are described in very general terms, and the specific efficacy of these repairs are not mentioned. Repair data collected from Japan was informative with respect to column repairs. However, there was a lack of systematic step-by-step repair procedures for other bridge components. In general, repair methods described in the Caltrans bridge books and reports from other countries do not take into account nor discuss the residual capacity of bridge components at a given damage level to guide repair design.
- Because, generally bridge columns undergo a wide range of apparent damage, uniform definition of damage states that had been developed for columns were adopted and their applicability to other bridge components was assessed.

- The proposed simple equation to determine the effective strain in CFRP provides results that were very close to those from the ACI 440 2R-08. The proposed equation was preferred because it is non-iterative.
- The repair for shear keys under DS2 and DS5 was developed to restore the shear strength loss of 20% and 80% of concrete, respectively, without changing the mode of failure. However, A shear key under DS6 needs to be replaced with a new shear key with a different design. The repair design for DS6 was presented to achieve two objectives: one to restore the shear capacity of the shear key and the second to change the mode of failure from diagonal shear failure extended into the abutment wall to sliding shear friction failure with the purpose of limiting shear demand on the superstructure.
- The repair recommended for prestressed girders under DS1 was epoxy injections. Because damage at this level does not affect member capacity, repair recommended for DS1 was a non-structural repair and was recommended only for aesthetic reasons.
- In prestressed girder repair, the proposed repair design was simple and effective in restoring the original flexural capacity of girders under DS2, DS3, and DS4. The repair for DS2 and DS3 was developed to restore an assumed flexural strength loss of 10% of prestress steel and 20% for DS4 without restoring the prestress loss in steel. To compensate the prestress loss in steel, prestressed CFRP may be considered.
- Replacement was recommended for girders under DS6. From the results, it was concluded that, once the loss in strand contribution to flexural strength is more than 20%, it is not possible to restore the original capacity of the girders and hence, girder replacement is a more appropriate option.

- Repair methods were recommended for abutment stem walls in damage states associated with minor spalling (DS2), major spalling (DS3), exposed reinforcement (DS4), and fractured or buckled bars (DS6). Walls with minor cracking (DS1) may be left unrepaired. Damage state 5 (start of core damage) was believed not to be applicable to walls because the amount of confinement in walls is typically too small to distinguish between core damage and unconfined concrete damage.
- The repair recommended for abutment walls under DS2 was epoxy injections of the cracks and patching of concrete. Because damage at this level does not affect member capacity, repair recommended for DS2 was a non-structural repair and only recommended for aesthetic reasons.
- In abutment wall repair, the same repair method was recommended for DS3 and DS4. Unidirectional CFRP fabrics placed with fibers running in horizontal or vertical directions were recommended to restore an assumed shear capacity loss of 50% in walls with DS3 and DS4.
- Unless there is significant reduction in the abutment wall height due to failure or significant permanent rotation due to out of plane bending, walls with fractured bars (DS6) may be repaired by replacing fractured or buckled portion of the bars using new bars and service couplers as defined by Caltrans and using information that has become available recently from cyclic load studies of reinforced concrete columns with couplers in plastic hinges. A simpler alternative is to use CFRP fabrics in lieu of the damaged bars. CFRP fabrics with fibers in horizontal or vertical directions are recommended to be used to restore an assumed shear capacity loss of 80% in walls with DS6.

- The repair recommended for joints under DS1 was epoxy injections. The repair recommended in DS1 is a non-structural repair and only recommended for aesthetic reasons.
- In joints, the repair for DS2 was developed to restore the shear strength loss of 30% while considering the same percentage loss of 60% strength loss in DS3 and DS4. Joints under DS6 were recommended to be replaced.

References

- AASHTO (2007). *LRFD Bridge Design Specifications*, 4th Edition, American Association of State Highway and Transportation Officials, Washington, DC.
- ACI Committee 440.2R. (2008), “Guide for the Design and Construction of Externally Bonded FRP Systems for Strengthening Concrete Structures,” American Concrete Institute.
- ACI Committee 318. (2008), “Building Code Requirement for Structural Concrete,” American Concrete Institute.
- ACI Committee 318. (2011), “Building Code Requirement for Structural Concrete,” American Concrete Institute.
- ACI Committee 352R-02 (2002), “Recommendations for Design of Beam-Column Connections in Monolithic Reinforced Concrete Structures,” Reported by Joint ACI-ASCE Committee 352.
- Adin, M.A., Yankelevsky, D.Z., and Farhey, D.N. (1993), “Cyclic Behavior of Epoxy-Repaired Reinforced Concrete Beam-Column Joints,” *ACI Structural Journal*, March-April, pp. 170-179.
- Al-Solloum, Y.A., Almusallam, T.H., Alsayed, S.H., and Siddiqui, N.A. (2011), “Seismic Behavior of As-Built, ACI-Complying, and CFRP-Repaired Exterior RC Beam-Column Joints,” *Journal of Composites for Construction ASCE*, July/August, pp. 522-534.
- Bozorgzadeh, A., Megally, S., and Restrepo, J. (2003), “Seismic Response of Sacrificial Exterior Shear Keys in Bridge Abutments: Recommended Design and Construction Details.” Rep. to Caltrans, Contract No. 59A0337, Dept. of Structural Engineering, UC San Diego, San Diego.
- Bozorgzadeh, A., Megally, S., and Restrepo, J., and Ashford, S. A. (2006), “Capacity Evaluation of Exterior Sacrificial Shear Keys of Bridge Abutments.” *J. Bridge Eng.* 11(5), 555-565.
- Bousselham, A., and Chaallal, O., (2006), “Behavior of Reinforced Concrete T beams strengthened in Shear with Carbon Fiber-Reinforced Polymer-An Experimental Study,” *ACI Structural Journal*, Title No. 103-S35, pp. 339-347.
- Caltrans (1994), “The Northridge Earthquake,” California Department of Transportation, Post Earthquake Investigation Report, Division of Structures.
- Caltrans (1971), “The San Fernando Earthquake,” California Department of Transportation, Post Earthquake Investigation Report, Division of Structures.
- Caltrans (1989), “Loma Prieta Earthquake,” California Department of Transportation, Post Earthquake Investigation Report, Division of Structures.
- Caltrans (1994), “The Northridge Earthquake,” California Department of Transportation, Post Earthquake Investigation Report, Division of Structures.

- Caltrans (2006), "Seismic Design Criteria (SDC)," version 1.4, California Department of Transportation, Sacramento, CA.
- Caltrans LRFD (2008), "Bridge Design Aid," California Department of Transportation, Sacramento, CA.
- Caltrans (2010), "Seismic Design Criteria (SDC)," version 1.6, California Department of Transportation, Sacramento, CA.
- Caltrans and UNR (2012), "Seismic Performance of Next Generation Bridge (NGB) Components for Accelerated Bridge Construction (ABC)," <http://wolfweb.unr.edu/homepage/saiidi/caltrans/NextGen/PDFs/ResearchNotes.pdf>
- Czaderski, C., Motavalli, M. and Pfyl-Lang, K.(2011), "Prestressed CFRP for Strengthening of Reinforced Concrete Structures: Recent Developments at Empa, Switzerland," ASCE, Journal of Composites for Construction.
- Engindeniz, M., Kahn, L.F, and Zureick, A. H. (2005), "Repair and Strengthening of Reinforced Concrete Beam-Column Joints: State of the Art," ACI Structural Journal, March-April, pp. 1-14.
- Engindeniz, M. (2008), "Repair and Strengthening of Pre-1970 Reinforced Concrete Corner Beam-Column Joints Using CFRP Composites," Georgia Institute of Technology, School of Civil and Environmental Engineering, August, pp. 1-397.
- French, C.W., Thorp, G.A., and Tsai, W.J. (1990), "Epoxy Repair of Techniques for Moderate Earthquake Damage," ACI Structural Journal, July-August, pp. 416-424.
- Harries, K.A., Kasan, J.L. and Aktas, J. (2009), "Repair Methods for Prestressed Girder Bridges," Pennsylvania Department of Transportation.
- Khalifa, A., T. Alkhrdaji, A. Nanni, and S. Lansburg. (1999), "Anchorage of Surface Mounted FRP Reinforcement," Concrete International: Design and Construction, Vol. 21, No. 10, October, pp. 49-54.
- Kim, Y. J., M. F. Green and Wight R. G. (2010), "Effect of prestress levels in prestressed CFRP Laminates for strengthening prestressed concrete beams: A numerical Parametric Study," PCI Journal spring 2010.
- Konstantinos, K., Antoniadis, Thomas, N., Salonikios, and Andreas, J., Kappos, (2003). "Cyclic Tests on Seismically Damaged Reinforced Concrete Walls Strengthened using fiber-reinforced polymer reinforcement," ACI Structural Journal, Title No. 100-S54, pp. 510-518.
- Lowes, L.N., and Moehle, J.P. (1999), "Evaluation and Retrofit of Beam-Column T-Joints in Older Reinforced Concrete Bridge Structures, ACI Structural Journal, July-August, pp. 519-533.
- Li, B., and Pan, T.C. (2011), "Recent Tests on Seismically Damaged Reinforced Concrete Beam-Column Joints Repaired Using Fiber-Reinforced Polymers," Proceedings

of the Ninth Pacific Conference on Earthquake Engineering, April, Auckland, New Zealand, pp. 1-7.

Mofidi, A., and Chaallal, O., (2011), "Shear Strengthening of RC Beams with EB FRP: Influencing Factors and Conceptual Debonding Model," *Journal of Composites for Construction*, ASCE, pp. 62-74.

Nuebauer, U., and Rostasy, F.S. (1997). "Design Aspects of Concrete Structures Strengthened with Externally Bonded CFRP Plates," ECS Publications, Edinburgh, 109-118.

Pantelides, C.P., and Gergely, J. (1999), "Seismic Retrofit of Reinforced Concrete Beam-Column T-Joints in Bridge Piers with FRP Composite Jackets," *ACI Structural Journal*, SP 258-1, pp. 1-18.

Priestley, M.J.N., Seible, F., and Calvi, G.M. (1996), "Seismic Design and Retrofit of Bridges," John Wiley & Sons, Inc. New York.

Saiidi, M., and Voosoghi, A., (2010). "Seismic Damage States and Response Parameters for Bridge Columns," *ACI Structural Journal*, SP 271-02, pp. 29-46.

Saiidi, M., Sneed, L., and Belarbi, D.J. (2013). "Repair of Earthquake Damaged Bridge Columns with Fractured Bars," Funded by Caltrans, Tested at Missouri University of Science and Technology, <http://wolfweb.unr.edu/homepage/saiidi/caltrans/fractured.html>

Sayari, A., and Donchev, T., (2012). "Comparison of Different Configurations for FRP Strengthening of Masonry Walls," APFIS, Hokkaido University, Japan.

Sezen, H. (2012), "Repair and Strengthening of Reinforced Concrete Beam-Column Joints with Fiber-Reinforced Polymer Composites," *ASCE Journal of Composites for Construction*, September-October, pp. 499-506.

Shattarat N. K., and McLean, D.I. (2007), "Seismic Behavior and Retrofit of Outrigger Knee Joints," *Journal of Bridge Engineering ASCE*, September/October, pp. 591-599.

Silva, P.F., Ereckson, N.J., and Chen, G.D. (2007), "Seismic Retrofit of Bridge Joints in Central U.S. with Carbon Fiber-Reinforced Polymer Composites," *ACI Structural Journal*, March-April, pp. 207-217.

Triantafillou, T.C., (1998). "Shear strengthening of Reinforced Concrete Beams Using Epoxy-Bonded FRP Composites," *ACI Structural Journal*, 95(2), pp. 107-115.

Tsonos, A.G., and Papanikolaou, K.P. (2003), "Post-Earthquake Repair and Strengthening of Reinforced Concrete Beam-Column Connections (Theoretical&Experimental Investigation)," *Bulletin of the New Zealand Society for Earthquake Engineering*, Vol 36, No. 2, June, pp. 73-93.

Vosooghi, A., and M. Saiidi, "Shake Table Studies of Repaired RC Bridge Columns Using CFRP Fabrics," *American Concrete Institute, ACI Structural Journal*, V. 110, No. 1, January-February 2013, pp. 105-114.

WFEO (2010), "Draft on Current Practice of Pre-Earthquake and Post-Earthquake Measures of Transportation Facility," Vol. 3, Post-Earthquake Measures of Transportation Facility, December, Japan, pp. 1-79.

Wipf, T.J., Klaiber, F.W., Rhodes, J.D. and Kempers, B.J. (2004), "Repair of Impact Damaged Prestressed Concrete Beams with CFRP," Effective Structural Concrete Repair Vol 1 of 3, Iowa Department of Transportation.

Tables

Chapter 2. Tables

Table 2-1. Bridge damage and repair of San Fernando Earthquake (1971).

Bridge Number	Bridge Component	Damage Description	Repair
SF 53-1012	Abutment wall	Minor damage to abutment wall.	The damage was repaired by injecting epoxy in cracks.
	Footing	Minor damage to abutment footing.	The damage was repaired by injecting epoxy in cracks and recasting small sections of broken footing.
SF 53-1896	Column	Columns at bents 4, 5 and 6 were out of plumb.	All support footings were exposed by excavating soil and the columns of bents 4, 5 and 6 were plumbed by pushing the structure by applying 30 kip force by a "grader" against the top of the bent. Bents 2&3 were slightly out of plumb but efforts to plumb them failed since they were shorter and stiffer.
	Footing	Most of the columns and their footings were badly cracked and spalled.	Cracked and spalled concrete were repaired by injecting epoxy and patching with epoxy bonded Portland cement concrete (PCC), respectively.
SF 53-1924 R/L	Wing wall	The wing walls were broken and lost their integrity with the abutment.	Wing walls were removed and re-casted.
	Piles	Piles were damaged due to the movement of superstructure in vertical as well as in transverse direction.	A new foundation consisting of a diaphragm abutment on CIDM piles was casted behind each existing abutment and keyed and doweled to the existing diaphragm.
SF 53-1925	Abutment wall	The abutment walls at abutment 1 and 7 were sheared off.	Re-casted abutment walls.
	Bent	At bents 2, 3, 4 and 6 the columns were spalled at the soffit but sound at the footing. Bent 5 was badly spalled for 3 to 4 feet above the footing with 1 exposed steel bars. Columns at bent 4, 5 and 6 were slightly out of plumb.	The cracked concrete and spall at the columns were repaired by injecting the cracks with epoxy and patching the spalls with epoxy bonded mortar. For Bent 4, 5 and 6, the footings were exposed by excavating soil, and the columns were partially plumbed by applying the controlled force near the top of the columns. The columns were temporarily anchored in the desired position until the superstructure was re-casted. Also the concrete jacket was placed over the damaged portion of the columns.

Table 2-1. (Continued)			
SF 15-1936 RL	Abutment Wall	Abutment had minor spalling, and vertical and diagonal cracks.	All cracks were sealed with epoxy injections. Removed and replaced the unsound concrete.
	Column	Minor cracking and spalling at the top of the column.	Chipped out all spalls and cracked concrete and patched with epoxy bonded mortar.
SF 53-1963	Abutment Wall	The abutment wall was cracked and spalled throughout the width of the bridge. These cracks were extended through to the back face of the abutment. The abutment had one diagonal and one vertical crack. The CIDH piles were cracked and several appear to be cracked at the connection to the abutment wall.	A temporary support was constructed and rebuilt the abutment wall below soffit elevation and also repaired top of piles as necessary. All cracks were epoxy injected.
	Pier	There were heavy diagonal cracks. There was no evidence of damage to the pier beyond the plane of reinforcement except for thin cracks extending into the concrete.	All cracks were epoxy injected, and re-casted the concrete removal area with epoxy bonded mortar.
	Hinge	Most of the hinges experienced concrete spalling at seat width.	A temporary bent was constructed under the hinge to jack up the seated section to allow for repair and restoration of the hinge. Removed the damaged portion of spalled concrete. Rebuilt the seated section of the hinge as necessary. Also installed new hinge restrainer unit.
SF 53-1964	Hinges	Opening in the hinges from ¼ inch to 2-1/4 inch.	Added restrainer units to the hinges.
	Deck	Spalling in the deck.	Repaired all spalls (no information about repair method is provided).
	Column	Cracking in the soffit near pier 3.	All cracks were filled with epoxy.
SF 53-1965	Pier cap	Pier 2, 3 and 4, had vertical hair line cracks along the faces of the pier caps.	No repair information was given.
	Exterior shear key	Complete failure of a shear key at abutments.	The shear key was removed and rebuilt.

Table 2-1. (Continued)			
	Abutment Wall	Diagonal cracks at the abutments.	Removed all unsound concrete at spalls and cracked concrete region and replaced with epoxy bonded PCC.
	Deck	Cracked concrete in the deck.	Removed all unsound concrete at cracked concrete region and replaced with epoxy bonded PCC.
SF 53-1983	Deck	Major cracking in the deck.	Removed and replaced the damaged portion of the deck. All cracks were epoxy injected.
	Abutment wall	Cracking and spalling of the abutment wall.	Removed and replaced loose concrete from damaged sections of abutment wall and re-casted with epoxy bonded mortar. All cracks were epoxy injected.
	Footing	The footing was cracked. The footing steps were cracked at some locations.	Removed and replaced the cracked footing steps. All cracks were filled with epoxy. It was also recommended to remove structure backfill as required to complete repair works.
SF,53-1986	Bent	Bent 2 was damaged at the top. There were numerous cracks in the column.	At bent 2 all cracks were epoxy injected.
		Bent 3 was heavily cracked and spalled on the corners for the bottom 4 feet.	At bent 3 damaged portion of the column was removed and reconstructed but remain existing longitudinal reinforcement.
Bent 4 column was severely cracked and spalled for the bottom 12 feet.		At bent 4 damaged portion of the column was removed and reconstructed but remain existing longitudinal reinforcement.	
		Bent 6 was heavily cracked and spalled for the bottom 6 feet. Top of the column had some cracking.	Bent 6 was jacked up to relieve the load on the column. The bottom 6 feet of bent 6 was removed and the ties were replaced in more quantity than the original amount. The bottom of the column was replaced with collar approximately 2feet larger than the original column dimensions.
	Footing	Bent 5 footing was completely cracked and exposed piles show spalling at the top.	Pier 5: Removed and reconstructed footing.

Table 2-1. (Continued)			
	Abutment Wall	Abutment 1 was heavily damaged by the earthquake. It was tilted out of plumb. The corners and joints where the soffit and abutment meet were completely Pulverized. Grade lines for the bridge and wing-walls no longer matched.	Both abutments 1 and 8 were removed and replaced.
	Hinge	Abutment 8 was tilted out of plumb. Abutment wall showed cracking and spalling. Damage occurred at the hinge where longitudinal and transverse movement took place.	Hinge was repaired by installing restrainers.
SF 53-2166 R/L	Abutment wall	Abutment walls #1L and #2R were severely cracked. Abutment #1L footing moved down station 11 inch on the left side and 6.5 inch on the right. The entire abutment and footing moved to the left by approximately 2 feet.	Abutment walls #1L and #2R were removed from top of footing to soffit line. These walls were removed in 8 feet sections spaced on 16 feet center. Additional reinforcing steel were added. These sections were replaced with the width of wall being increased to 2.5 feet. Expansion paper 1 inch thick was placed on the top of footing to ensure that only 1.25 feet of wall was bearing on center portion of footing. After these replaced sections had reached required strength, the remainder sections were removed and replaced.
	Abutment footing and shear key	The left end abutment #2L was fractured and only hairline cracks were visible on right one half of this wall. Abutment #1L footing shear key was torn off from top of footing.	Only the fractured concrete portion of abutment #2L wall was removed. The left end of wall was removed from top of the footing to soffit line and replaced to same thickness as original wall. The hair line cracks were injected with two component epoxy. The cracked left end of #1L footing and end shear key was removed and the footing was patched. Also additional reinforcing steel was added to the footing.

Table 2-1. (Continued)			
SF 53-2171	Abutment Wall	The ends of abutment walls were severely cracked and spalled. The back face of the abutment wall was also cracked. The cracks were not visible on the front face of the wall.	The cracks and the spall in the abutment walls were patched and then injected with two component epoxy. The epoxy was injected into walls via short pieces of copper tubing ¼ inch in diameter. This tubing was inserted into cracks during patching operations.
	Column	The left column at bent 2 had cracked concrete at top and bottom region. The cracks were 2 feet long and penetrated to the depth of main reinforcing steel. At bent 3 both columns had spalled concrete at the top.	The cracked concrete in the columns was removed and replaced.
	Abutment footing and shear key	The left end shear key and end of abutment footing were torn off.	The left end shear key and the end of the footing were removed and replaced.
SF 53-2200	Bent cap	Bent caps at bents 2, 10 and 11 were severely cracked with ¾ inch wide cracks on both sides.	The bent caps were removed and replaced.
	Footing	The pedestals at bents 2, 10 and 11 were cracked. These cracks were 1/16 inch wide on each side of columns at pedestal top and went downward at 45 degrees toward center line of columns.	The cracks in the pedestal were injected with two component epoxy. The collars were placed around each footing after cracks were epoxy injected.
	Bent	Bent 2 column had flexural cracks.	The cracks in the column were injected with two component epoxy.
	Hinges	The hinges were cracked. Each hinge had two cracks. The cracks were 1/8 inch wide at top.	The hinges were injected with two component epoxy.
	Footing	Abutment 1 footing moved 3 inch to the right and 8 inch up.	Abutment 1 footing was increased in size so that the abutment wall not to be bearing on one edge. The footing reinforcing steel was extended by drilling holes in the footing and epoxy grouted. The space of 3 inch wide in stepped footing was filled with concrete.

Table 2-2. Bridge damage and repair of Loma Prieta Earthquake (1989)

Bridge Number	Bridge Component	Damage Description	Repair
L 28-0171	Pile shafts	The pile shafts at bents 4, 5, 6 and 8 had cracks at the top and these cracks extending 2 feet down from the deck soffit. Bents 2 and 3 had cracks extending from ground up to the soffit level	All cracks were epoxy injected.
L 28-0218	Abutment Wall	Minor Spalling at the abutment.	No repair information was given.
L 33-0061	Bent	Several bents suffered minor to major flexural/shear cracks and spalls. Bent MB 25 had a series of major flexural and shear cracks, and spalling starting at 10 feet above the ground. Also one longitudinal reinforcement bar was buckled.	Removed all loose concrete, patched the spalls and the cracks were epoxy injected. 2 inch of column core was taken out at the cracked portions of the column and it was found that the column core was intact. The concrete was stripped down to the main vertical reinforcing steel all around the column up to 18 feet height. Additional #5 hoops were placed at 5 inch spacing and spliced with OS splice clips in damaged area and then covered with air blown mortar.
	Deck	There were numerous medium to large size cracks and spalls in the deck.	All loose concrete was removed and patched the spalls on the deck.
	Footing	The earthquake movement has left a gap between the supports and adjacent earth at many locations at abutment. The back of the abutment footing had settled more than the front causing abutment rotation	No repair information was given.
	Back wall	The abutment MB 1 back wall was damaged. (Damage detail was not given)	The upper 18 inch of the back wall was rebuilt. #4 stirrups were added along with 2-#4 continuous bars in the top of the wall.
	Restrainer	Several earthquake restrainer cables were damaged.	Replaced the existing earthquake restrainers.

Table 2-2. (continued)			
L 33-0126	Bent	Major cracking and spalling was experienced at Bent JL 27 and 52, at the column bases.	Cracks epoxy injected and spalls dry pack repaired.
	Abutment Wall	Concrete spalling at the abutment wall.	Spalls were repaired with dry pack and #3 stirrups at 6 inch epoxied into holes drilled in abutment.
L 33-0483	Bent	Bent 38: The bridge had sustained major structural damage to this outrigger bent. The movement was such that the major reinforcement at the corners of the outrigger has undergone plastic deformation forming a hinge at the corner.	Damaged concrete was removed and re-casted.
	Bent cap	Multiple shear cracks were experienced at bent 35 and 38.	No repair information was given.
	Deck	At bent 38, crack in the deck were approximately 1/32 inch – 1/16 inch width.	No repair information was given.
	Abutment wall	Spalling at the abutment wall.	Repaired by dry packing with cement.
	Shear keys	Failure of abutment external shear key.	No repair information was given.
L 34-0055	Bent	At most of the bent, there were shear cracks at the top of the column.	After shoring the bridge, earthquake damaged concrete was removed, reinforcing steel was cleaned and it was recommended that new earthquake mitigation measures can be installed if required by design.
	Deck	Spall in the deck.	No repair information was given.
L 34-0077	Bent	Bents 42, 43, 44, 45, 46, and 48 had similar cracking patterns which consisted of mostly heavy and medium shear cracks. Some columns exhibit extensive spalling, loss of concrete and rebar bond.	It was recommended to place false work adjacent to distressed columns. But no repair design information was provided.
	Bent cap	There were vertical and diagonal cracks on the face of the bent cap.	Support was placed under girder. Area of spalled concrete was removed from the bent cap under each bearing plate.

Table 2-2. (continued)			
		These cracks were extended from the bottom to approximately the mid height of the cap.	Sand blasted any rusty steel. Drilled holes and steel bars were hooked into the face of the bent cap and new concrete was re-casted.
L 34-0100	Bent cap	Bent 31: Diagonal cracks in the bent cap. Bent S2-41: There were moderate to severe vertical and diagonal cracks in the outside corner areas of the bent cap. Bent A32: There was 6 inch wide spall on the top right side of the bent cap, which runs diagonally towards the bent cap column corner.	Sealed the cracks with epoxy. Chipped away loose concrete. Applied sand blast to clean the area to seal cracks with epoxy. Removed damaged corners and replaced with new concrete.
	Outrigger Joint	Bent N 35: The top of the outrigger on both sides of the bent #3 was severely damaged.	Removed damaged corners of this outrigger and repaired.
	Restrainer	Hinge A 44: Suffered a longitudinal movement and longitudinal earthquake restrainers were broken in the exterior bays.	Longitudinal restrainers were replaced.
L 36-0018	Exterior Shear key	The shear key was sheared off.	Shear key was replaced.
L 36-0058	Wing wall	The abutment 5 wing wall had a 30 inch portion which was broken off and there was a large spall with exposed reinforcing steel on the exterior side of the wing wall.	No repair information was given
L 37-0007	Back wall	The abutment 5 back wall was badly broken up in an area of 8 to 10 square feet with many horizontal and vertical cracks.	Removed all loose concrete from damaged area and re-casted. All cracks were epoxy-injected.

Table 2-2. (continued)			
L 37-0050	Column	At bent 3 the column had fairly extensive flexural and shear cracks. The column of bent 4 was spalled about 3 feet long and 10 inch deep	All cracks were injected with epoxy and the spall was repaired.
L 37-0059	Abutment	The damage included a rotation of the abutment about its footing, the plumb-ness of the bearing bars, and the large transverse opening was visible in the AC pavement along the paving notches.	Placed the bearing bars to their proper position. Masonry plate was removed and resettled.
	Interior shear key	Extensive shear cracking and spalling of shear key.	No repair information was given
L 37-0120	Shear key	At abutment 4 shear key experienced extensive spalling.	No repair information was given

Table 2-3. Bridge damage and repair of Northridge Earthquake (1994).

Bridge Number	Bridge Component	Damage Description	Repair
N 53-1615	Bent	Bent 2 exhibit minor spalling at top of all four columns.	No repair information was given.
	Abutment Wall	Vertical cracks on the face of the abutment wall.	Cracks in the abutment were filled with epoxy.
N53-1637	Diaphragm	At bent 7, there was a horizontal crack in the diaphragms located at the level of the seismic restrainer. Diaphragm of the span #7 separated from the girders of the span # 7. There were cracks between the girders and the diaphragm.	Removed the unsound concrete along the horizontal hairline crack of the diaphragm in span #7 and the cracks were epoxy injected Removed the diaphragm of the span #7 and broken portion of the exterior girders and the diaphragm was re-casted. Also the additional reinforcements in the diaphragm were provided. Provided #3 spirals with low pitch around the opening provided for the passage of seismic restrainers to give some ductility to this diaphragm and avoid future spalling.
N 53-1917	Exterior Shear key.	Shear keys at the abutment were sheared off.	Shear keys were re-casted.
N 53-1921	Depressed shear key	The depressed transverse shear keys were damaged	Removed and replaced unsound concrete. Repaired the spalled concrete adjacent to the key.
N 53-1984	Shear key	There was a major shear key damage at all locations at all abutments	Replaced all exterior shear keys at all abutments.
	Column	There was a major damage at the top plastic hinge location of various columns.	Chipped out and removed all the unsound concrete at damaged area and the spalls were filled with epoxy bonded mortar and cured with non-pigmented material. Also additional horizontal ties were installed to achieve 3 inch center to center spacing.
	Back wall	There was damage at the end of back walls.	Damaged section of the back walls was removed and re-casted.
	Hinge	There was a minor spalling at the exterior girders at all hinges.	Removed unsound concrete at the locations of concrete spall and reconstructed. Cracks were epoxy injected. Also the holes were drilled and bonded with additional rebar at locations where rebar was missing.

Table 2-3. (continued)			
N 53-1989F	Shear key	At abutment 1 and 9, exterior shear keys failed at both sides.	Exterior keys at both abutments were repaired. Information about repair design was not given.
	Back wall	Abutment back wall was damaged.	No repair information was given.
	Bent 2	Bent 2 experienced large diagonal cracks at the bottom and minor cracks and spalls at column top.	Repaired the cracks/spalls by backfilling the slurry cement.
N 53-2329G	Abutment Wall	There was extensive spalling at the abutment with exposed bars.	Chipped out and removed the loose unsound concrete to expose rebar. Re-casted with concrete mortar, and then cured with non-pigmented curing compound.
	Bent	At bent 2, there was a major shear crack starting at the bottom of the flared section of the bent and ends at the top of CIDH pile.	Removed the broken concrete cover and exposed the main core. Removed the unsound concrete inside of the core located between the flare section and the top of the CIDH pile and then the column was re-casted.
	Hinge	All hinges had vertical offset. This offset occurred at the high end of super-elevation, but not at the low end.	Removed concrete for joint seal anchorage. Removed the existing joint seal.
N 53-2395	Abutment Wall	Abutment had cracked and spalled concrete on the face of abutment.	All loose concrete from the damaged area was removed and all cracks were epoxy injected. Spalls were patched.
	Column	Minor spalling at top of the flared section.	Spalls were repaired. No repair information was given.
N 53-2396	Column	There were Cracks in the columns with exposed reinforcing steel. Cracks appeared to be propagating inside the core. No damage to longitudinal and spiral reinforcement recorded and the column core was intact.	All cracks were epoxy injected. The surface of the columns was sand blasted. Air-blown concrete technique was used to resurface the column faces utilizing regular strength structural concrete.

Table 2-4. Bridge damage and repair of Whittier Earthquake (1987).

Bridge Number	Bridge Component	Damage Description	Repair
53-1660	Bent	At bent #6 major damage was sustained to the five columns. There were many large diagonal shear cracks on the face of all the columns. The most severely damaged column was the center column.	Removed the column concrete to expose longitudinal reinforcement and added new ties and then the columns were re-casted.
	Bent cap	There was large incipient concrete spall in the bent cap at bent #5. Few vertical cracks were present in bent cap at bent #7.	At bent#5, the corner of the bent cap was reconstructed. #5 bars at 12 inch both ways inserted into bent cap corner by drilling holes into it and then these holes were grouted. At bent #7 the cracks in bent were filled with epoxy.

Table 2-5. Bridge damage and repair of Petrolia Earthquake (1992)

Bridge Number	Bridge Component	Damage Description	Repair
4-0017R/L	Column	At bent #10 of span 3 had a large transverse cracks across the full section at the top, and large open spalls that has removed about 40% of the concrete cross section from this column around the perimeter of the column. The main longitudinal reinforcement was completely exposed and had buckled slightly. In addition, the transverse floor-beam had large spalls on both faces above this location, and there was a medium to large vertical crack that extends from the inside of the column/floor-beam connection about halfway up the depth of the floor-beam.	Imminent replacement of this structure was recommended.

Table 2-6. Bridge damage and repair of The Landers and Big Bear Earthquake (1992)

Bridge Number	Bridge Component	Damage Description	Repair
56-0532G	Shear key	The internal shear key at abutment #1 & #5 had crushed.	Chipped out the entire shear key, protected all the existing reinforcement in the key area. Drilled 1 inch diameter holes 6 inch deep into the soffit for additional reinforcing steel dowels. Using dry pack mortar, #5 rebar dowels were placed in the holes. Re-casted the key using six sack air blown mortar.

Table 2-7. General damage levels in bridge components (WFEO 2010)

Damage Degree	Definitions	
	Reinforced Concrete Piers	Reinforced Concrete Girders
A's	Near collapse and large tilting	Near collapse
A	Fracture of rebars and large deformation	Several longitudinal rebars or prestressing cables are fractured as well as failure of bearings
B	Fracture of part of rebars and deformation of rebars, crack and spalling of concrete	Large cracks and spalling of concrete
C	Crack and local spalling of cover concrete	Minor cracks. Crack width less than 2mm
D	Minor cracks	No or slight damage without effect on bearing capacity

Table 2-8. Damage levels in RC pier subjected to flexural failure at base (WFEO 2010)

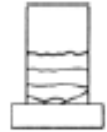
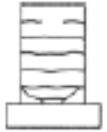
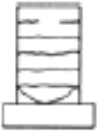
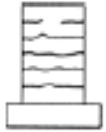
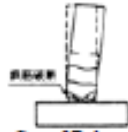
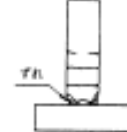
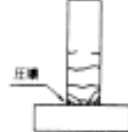
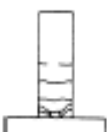
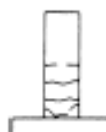
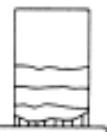
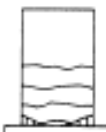
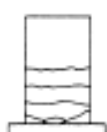
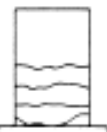
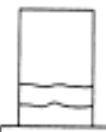
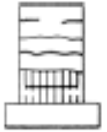
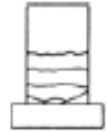
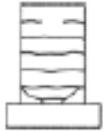
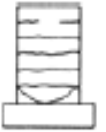
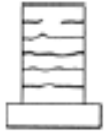
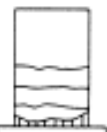
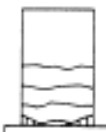
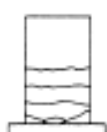
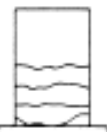
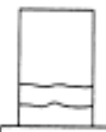
Observed Damage		1. Cut of Rebar and Tilting of Pier	2. Deformation of Rebar	3. Spalling-off of cover concrete	4. Diagonal Cracks (Penetrated)	5. Diagonal Cracks (Not Penetrated)	6. Only Horizontal Cracks	
Damage Situation	General Case	Side View	 Cut of Rebar	 Deformation of Rebar	 Spalling-off			
		Front View						
	Low Longitudinal Rebar Ratio	Side View	 Cut of Rebar	 Displacement	 Crush			
		Front View						
	$p \geq 0.5\%$							
	$p < 0.5\%$							
Damage Degree		A: Critical Damage	B: Medium Damage	B: Medium Damage	C: Slight Damage	C: Slight Damage	C: Slight Damage	

Table 2-9. Damage levels in RC pier subjected to damage at mid-height cut-off section of longitudinal rebars (WFEO 2010)

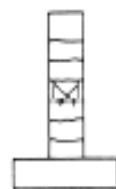
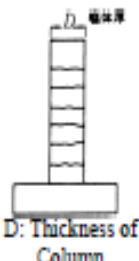
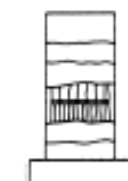
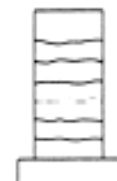
Observed Damage		1. Failure of Rebars Crack of Core Concrete	2. Deformation of Rebar	3. Spalling-off of Cover Concrete	4. Diagonal Cracks Penetrated (Progress of Vertical Cracks)	5. Diagonal Cracks (Greater than $D/2$)	6. Diagonal Cracks (Less than $D/2$)	7. Horizontal Cracks
Damage Situation	Side View		 Deformation of Rebar			 Spalling-off		 D: Thickness of Column
	Front View			 Cut-off of Longitudinal rebar				
Damage Degree		As: Near Collapse	A: Critical Damage	B: Medium Damage	B: Medium Damage	C: Slight Damage	C: Slight Damage	C: Slight Damage

Table 2-10. Damage levels in RC pier subjected to shear failure (WFEO 2010)

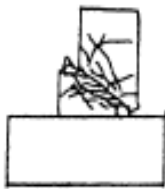
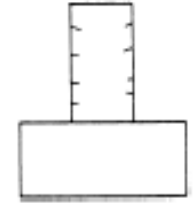
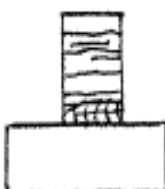
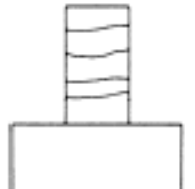
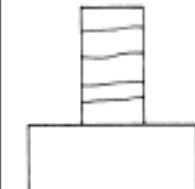
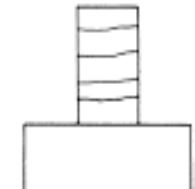
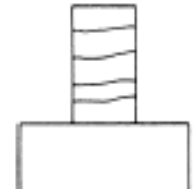
Observed Damage		1. Dislodgement and Settlement at Shear Failure	2. Diagonal Crack Width $W \geq 2\text{mm}$	3. Diagonal Crack Width $0.5\text{mm} \leq W < 2\text{mm}$	4. Diagonal Crack (Penetrated) (Crack Width $W \leq 0.5\text{mm}$)	5. Diagonal Cracks (Not Penetrated)	6. Only Horizontal Cracks
Damage Situation	Side View		 W ≥ 2 mm Spalling-off of Cover Concrete				
	Front View		 Spalling-off				
Damage Degree		A: Near Collapse	A: Critical Damage	B: Medium Damage	B: Medium Damage	B: Medium Damage	C: Slight Damage

Table 2-11. Repair methods for RC pier (WFEO 2010)

Damage Degree		A's: Near Collapse	A: Critical Damage	B: Medium Damage	C, D: Slight Damage	
Damage Location						
Damage at Base of Pier	Damage Shown in Table 2.8	1	2	3	4	5.6.
	Repair Method	* Removal and Reconstruction	* RC Jacketing * Steel Plate Jacketing * Removal and Reconstruction	* RC Jacketing * Steel Plate Jacketing	* RC Jacketing * Steel Plate Jacketing * Fiber Sheet Jacketing	* Resin Injection
Damage at Mid-Height (Cut-off Section of Longitudinal Rebars)	Damage Shown in Table 2.9	1	2	3	4.5.	6.7.
	Repair Method	* Removal and Reconstruction	* RC Jacketing * Steel Plate Jacketing * Removal and Reconstruction	* RC Jacketing * Steel Plate Jacketing	* RC Jacketing * Steel Plate Jacketing * Fiber Sheet Jacketing	* Resin Injection
Damage in Shear	Damage Shown in Table 2.10	1	2	3	4	5.6.
	Repair Method	* Removal and Reconstruction	* RC Jacketing * Steel Plate Jacketing * Installation of Seismic Wall * Removal and Reconstruction	* RC Jacketing * Steel Plate Jacketing * Installation of Seismic Wall	* RC Jacketing * Rebar Anchor * Stressing * Fiber Sheet Jacketing	* No Repair

Table 2-12. Repair methods for RC girder (WFEO 2010)

Bridge Component	Repair Methods
RC Girder	* Crack repair by resin mortar and resin injection * Steel plate attachment on vertical sides of the girder by anchor bolt and epoxy injection
Footing	* Adding piles to the footing * Construction of underground walls and / or beams * Soil improvement * Removal and reconstruction

Table 2-13. Repair and retrofit of bridges damaged by Chile Earthquake.

Bridge Name	Bridge Component	Damage Description	Repair Measures adopted
Mira Flores Overpass and Lo Echeveres Overpass	Superstructure	Collapse of Superstructure	<ul style="list-style-type: none"> * Collapsed superstructure were replaced with new Prestressed Concrete (PC) girders. * Added lateral stopper at abutments. * Added lateral beam and lateral stopper at piers. * Widened the abutment seat width.
Les Mercedes Bridge	Girder	Unseated PC girders at the abutment	<ul style="list-style-type: none"> * End section of concrete girders were repaired and strengthened by adding RC. * Lateral beams to connect adjacent girders were placed. * Widened the abutment seat width. * Added lateral stopper at abutments and piers.
Llacolen Bridge	Column Girder Pier Cap	Flexural cracks Collapsed None	<ul style="list-style-type: none"> * Damaged column was repaired and retrofitted by fiber sheet jacketing. * Collapsed concrete girders were replaced by new steel girders which were connected by lateral beams at both ends. * Pier caps seat support width were increased by adding RC.

Table 2-14. Summary of level of repair detail discussed in Table 2.1 to 2.6 for various bridge components.

Bridge Component	No. of Cases	Level of Repair Detail			
		1	2	3	4
		General/Minimal	Moderately Detailed	Detailed	Detailed Step-by-Step
Abutment wall	16	7	8	1	0
Beam-column joints	1	1	-	-	-
Cap beam/Bent Cap/Pier Cap	6	4	1	1	-
Column/Pier/Bent	22	12	5	3	2
Diaphragm	1	-	-	1	-
Footing/pedestal	9	7	1	1	-
Girder	0	-	-	-	-
Pile	2	1	1	-	-
Restrainer	2	2	-	-	-
Shear key	12	11	-	-	1
Superstructure hinge	6	6	-	-	-
Wing wall	2	2	-	-	-
Back wall	4	3	1	-	-
Deck	6	6	-	-	-

Table 2-15. Summary of repair methods in bridge books for bridge components.

Bridge Component	Caltrans Past Earthquake Damaged Bridge Repair Practice in Field
Column	<ul style="list-style-type: none"> * Epoxy injection * Patching * Reinforced concrete jacket * Removal and reconstruction
Girders	<ul style="list-style-type: none"> * Epoxy injection * Steel Plate * Removal and reconstruction
Abutment Wall	<ul style="list-style-type: none"> * Epoxy injection * Patching * Removal and reconstruction
Shear Key	* Removal and reconstruction
Beam Column Joints	* Patching
Cap beam	* Removal and reconstruction
Footing	<ul style="list-style-type: none"> * Epoxy injection * Patching * Increment in footing size * Removal and reconstruction
Pile	<ul style="list-style-type: none"> * Epoxy injection * Removal and reconstruction
Retrainer	* Replacement
Back wall	<ul style="list-style-type: none"> * Epoxy injection * Patching * Removal and reconstruction
Diaphragm	<ul style="list-style-type: none"> * Epoxy injection * Patching * Installation of restrainers
Wing Wall	* No repair information is provided
Superstructure Hinge	<ul style="list-style-type: none"> * Epoxy injection * Patching * Installation of hinge restrainers * Removal and reconstruction
Deck	<ul style="list-style-type: none"> * Epoxy injection * Patching

Chapter 3. Tables

Table 3-1. CFRP material properties (Tyfo[®] SCH-41 composite using Tyfo[®] S epoxy)

Property	Composite Gross Laminate Properties
Ultimate tensile strength in primary fiber direction, psi	121000 psi [834 Mpa]
Elongation at break	0.85%
Tensile modulus, psi	11.9×10^6 [82 Gpa]
Nominal laminate thickness	0.04 in. [1 mm]

Chapter 4. Tables

Table 4-1. Prototype girder geometric and material properties.

Property	I Girder
Section	P/S concrete I-girder
Prestressing Steel	50-250 ksi 7/16 in. seven-wire strand
Young's modulus of prestressing steel, E_p	28500 ksi [196,500 Mpa]
Young's modulus of deck and girder, E_c	4030 ksi [27,786 Mpa]
Concrete deck and girder expected compressive strength, f'_{ce}	5 ksi [34.47 Mpa]
Girder Length	75.5 ft. [23 m]

Table 4-2. Prestressing steel properties

Property	Prestressing Steel
Effective stress in prestressing steel after all losses, f_{pe}	133.6 ksi [921 Mpa]
Yield stress, f_{py}	212.5 ksi [1465 Mpa]
Ultimate Stress, f_{pu}	250 ksi [1724 Mpa]
Tensile modulus, E_p	28500 ksi [196,500 Mpa]

Chapter 5. Tables

Table 5-1. Prototype abutment geometric and material properties.

Property	Abutment
Abutment stem wall height	7 ft [2134 mm]
Abutment thickness	4 ft [1219 mm]
Abutment length in transverse direction	50ft [15.24 m]
Young's modulus of concrete, E_c	3605 ksi [27,786 Mpa]
Expected concrete compressive strength, f'_{ce}	5 ksi [34.5 Mpa]
Steel Grade, f_{ye}	68 ksi [468.8 Mpa]

Figures

Chapter 3. Figures

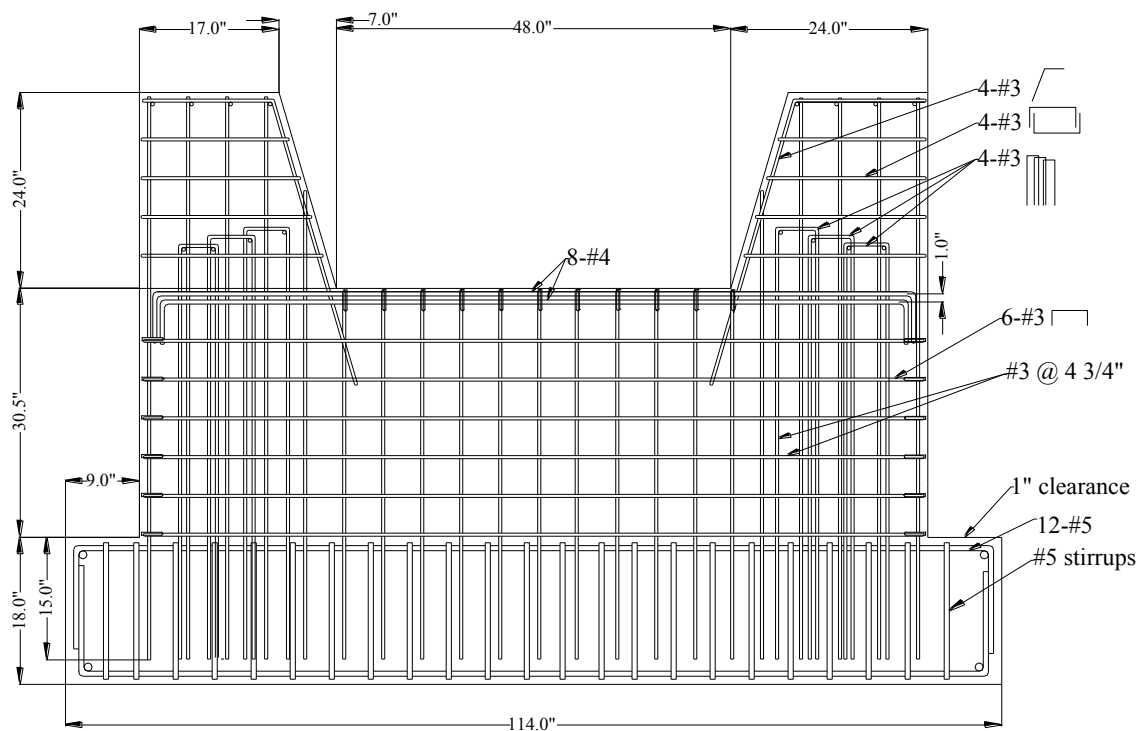


Figure 3-1. Elevation view of reinforcement layout of shear key test unit 4A

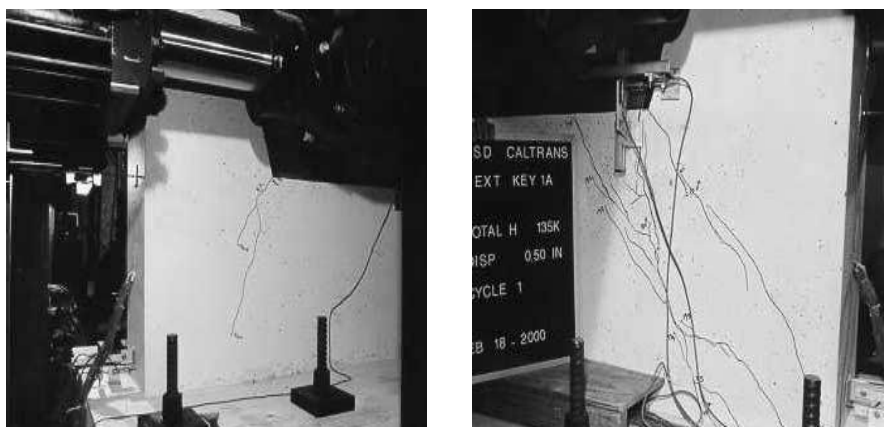


Figure 3-2. Damage state 2



Figure 3-3. Damage state 5

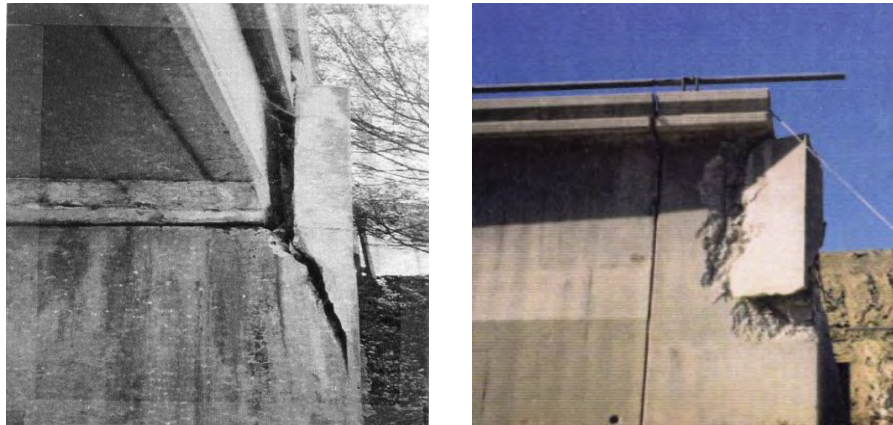


Figure 3-4. Damage state 6

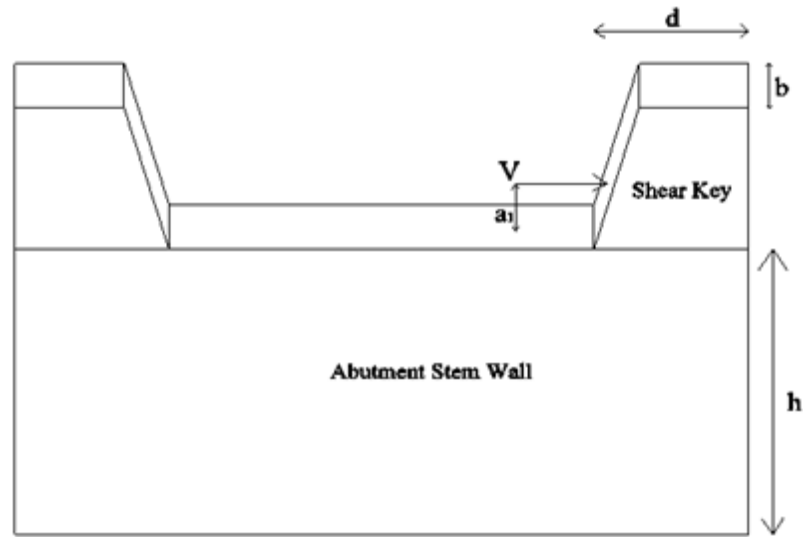


Figure 3-5. 3D view of shear key

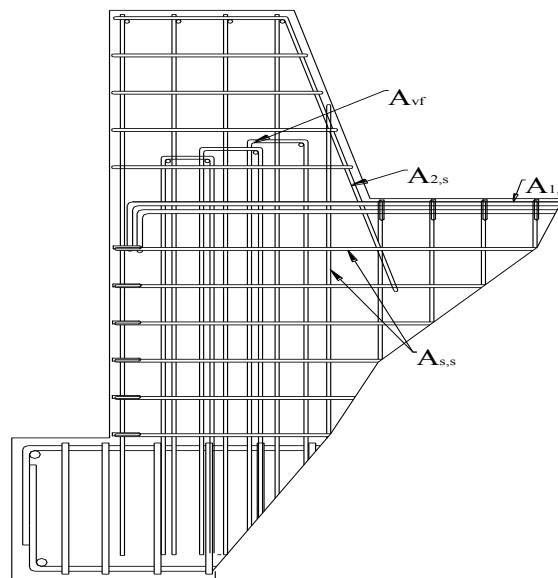


Figure 3-6. Shear key reinforcement location layout

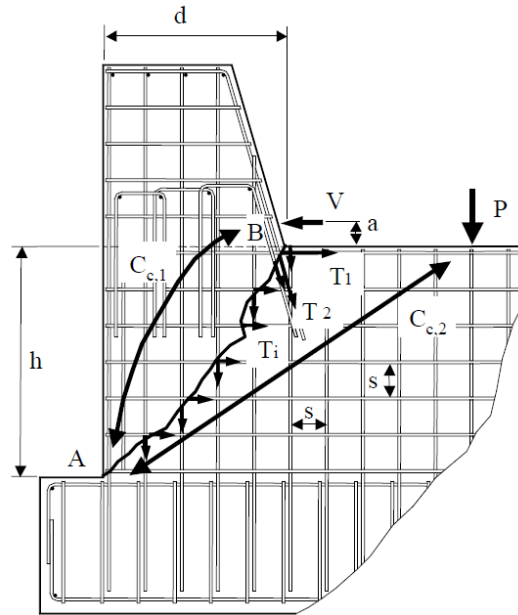


Figure 3-7. Exterior shear keys, strut-and-tie model (Megally et al. 2001)

Chapter 4. Figures



Figure 4-1. Damage state 1

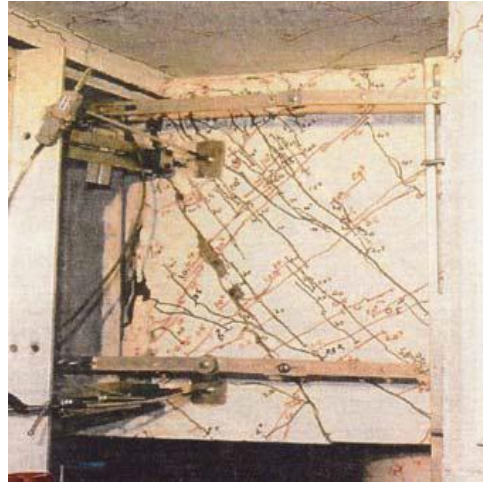


Figure 4-2. Damage state 2

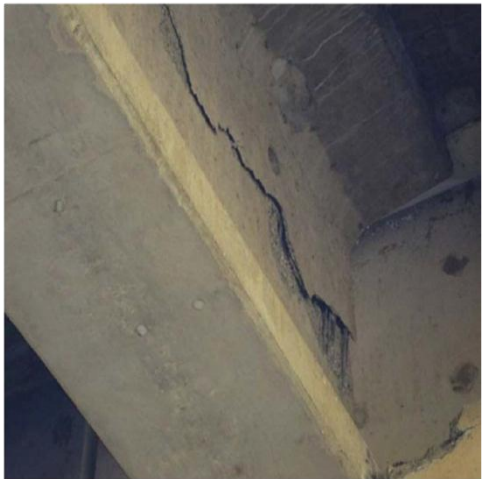


Figure 4-3. Damage state 3



Figure 4-4. Damage state 4

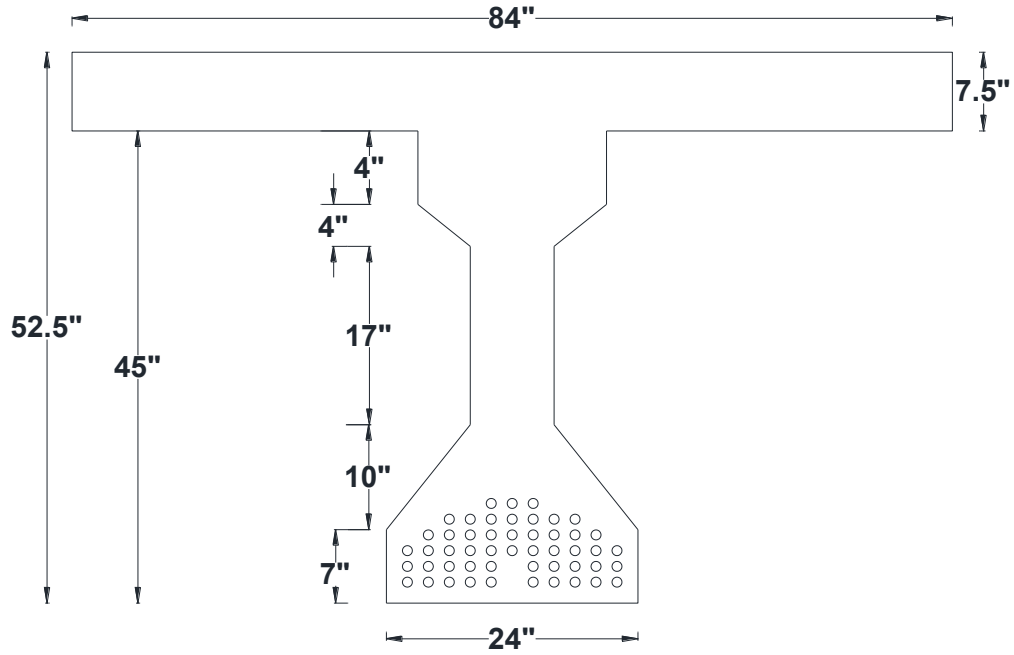


Figure 4-5. Prototype I girder cross section

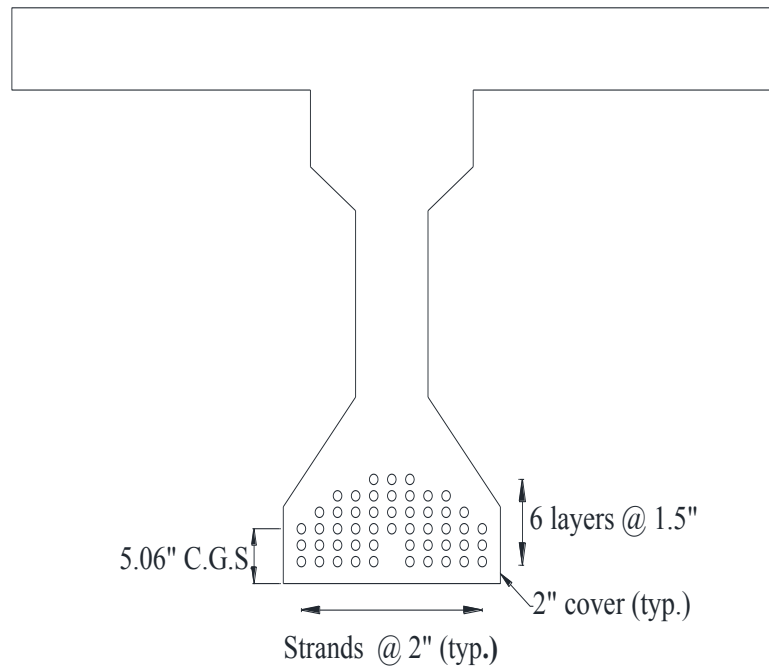


Figure 4-6. Prestressing strands detail

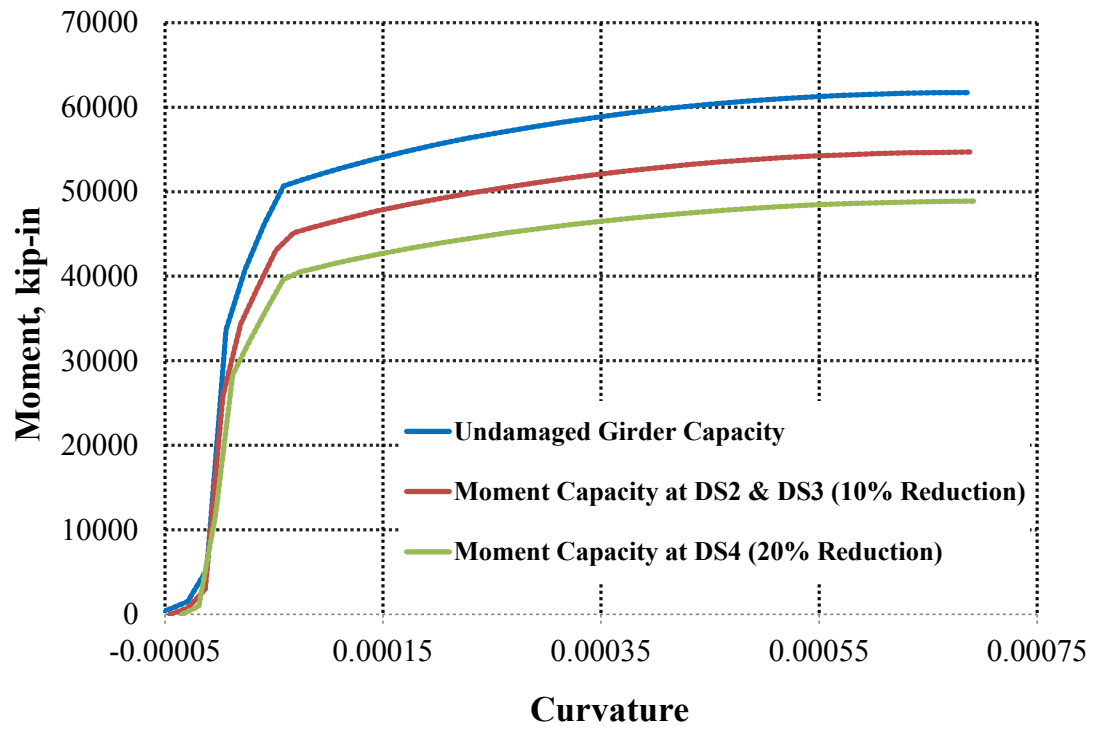


Figure 4-7. Moment-curvature of I girder section at various damage states

Chapter 5. Figures



Figure 5-1. Damage state 2



Figure 5-2. Damage state 3



Figure 5-3. Damage state 4



Figure 5-4. Damage state 6

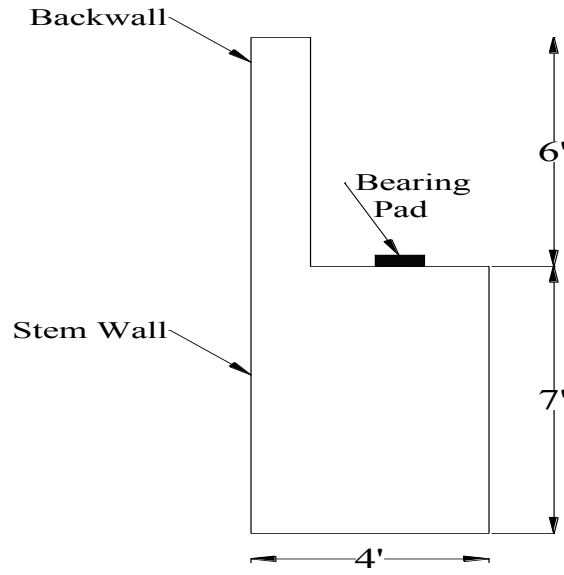


Figure 5-5. Side view of bridge abutment (seat type)

Chapter 6. Figures

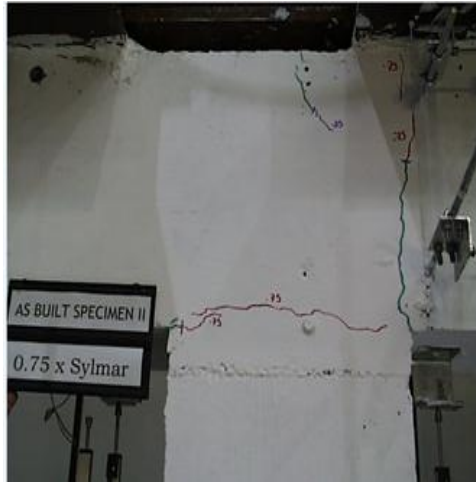


Figure 6-1. Damage state 1

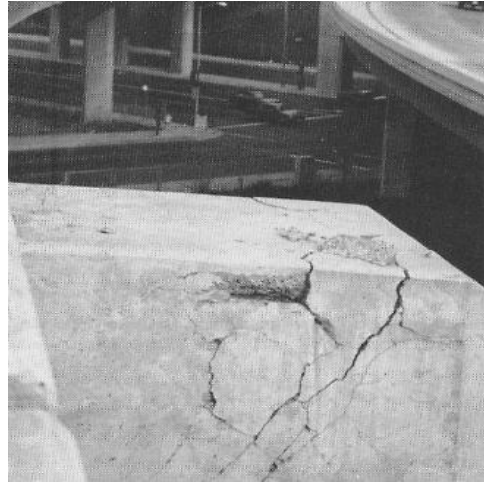


Figure 6-2. Damage state 2

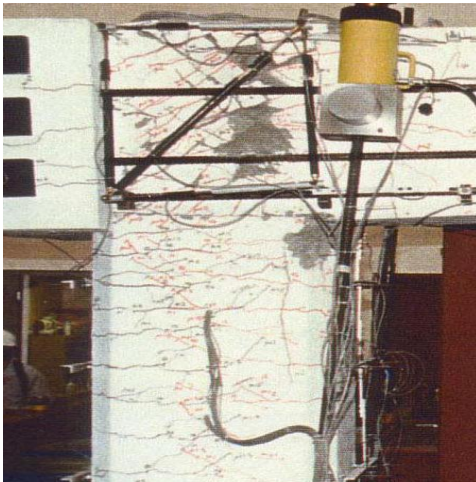


Figure 6-3. Damage state 3



Figure 6-4. Damage state 4



Figure 6-5. Damage state 6

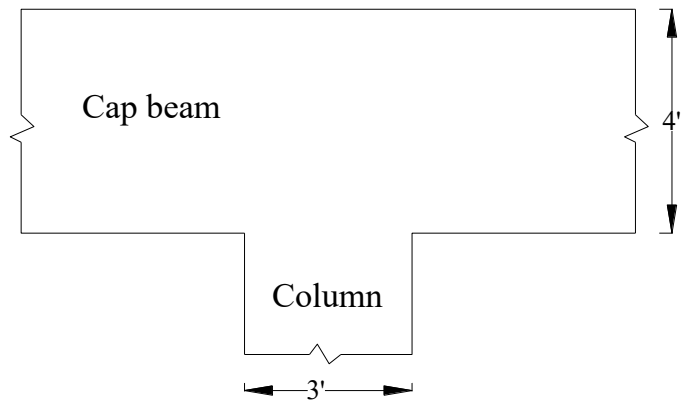


Figure 6-6. Elevation view of undamaged T joint

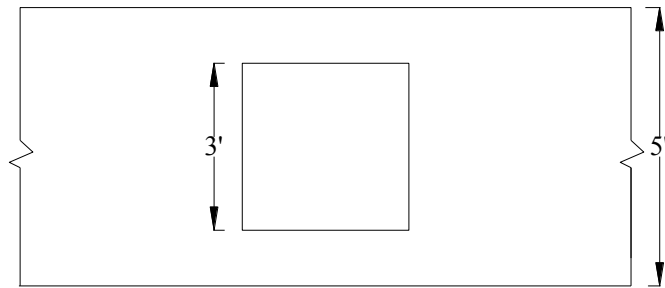


Figure 6-7. Plan view of undamaged T joint

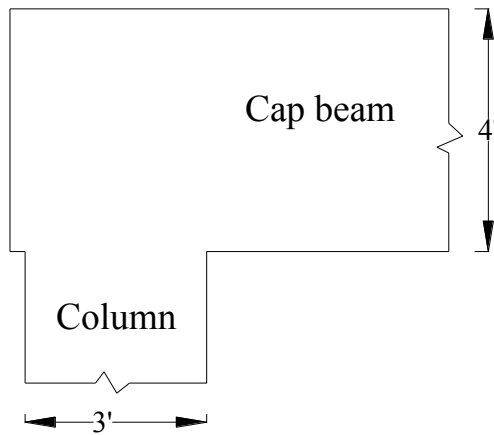


Figure 6-8. Elevation view of undamaged knee Joint

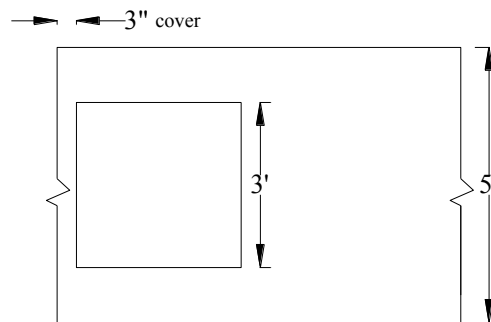


Figure 6-9. Plan view of undamaged knee joint

Appendix A. Development of Simple Equation to Estimate CFRP Thickness

A-1 - ACI 440.2R-08 Procedure to Determine Shear Contribution of FRP

The ACI 440.2R-08 procedure to determine shear contribution of side bonded CFRP to a member is based on the fiber orientation and an assumed fiber angle of 45 degree (Khalifa et al. 1998). The shear contribution of the FRP is given by Eq. A-1.

$$V_f = \frac{\varepsilon_{fe} \cdot t_f \cdot E_f \cdot w_f (\sin \alpha + \cos \alpha) d_{fv}}{s_f} \quad (\text{A-1})$$

Where w_f and s_f are the width and spacing of CFRP strips. The other parameters in Eq. A-1 were defined in section 3.6. When CFRP wrapping is covers the entire height rather than being in the form of strips, the term $\frac{w_f}{s_f}$ is equal to one. Therefore, for continuous side bonded FRP and orientation angle of zero degree (horizontal fibers), Eq. A-1 will reduce down to Eq. A-2.

$$V_f = \varepsilon_{fe} \cdot t_f \cdot E_f \cdot d_{fv} \quad (\text{A-2})$$

The following step by step procedure is recommended by ACI 440.2R-08 to determine the shear contribution of CFRP to a member.

Step 1. Compute the design material properties.

$$\varepsilon_{fu} = C_E \cdot \varepsilon_{fu}^* \quad (\text{A-3})$$

Where ε_{fu} , C_E and ε_{fu}^* are the design ultimate rupture strain of FRP, environmental reduction factor of 0.85, and ultimate rupture strain of FRP, respectively.

Step 2. Calculate the effective strain in the FRP shear reinforcement (Eq. A-4). The effective strain is calculated using the bond reduction coefficient κ_v applicable to shear. The bond reduction coefficient can be computed from Eq. A-5.

$$\varepsilon_{fe} = \kappa_v \cdot \varepsilon_{fu} \leq 0.004 \quad (\text{A-4})$$

$$\kappa_v = \frac{k_1 \cdot k_2 \cdot L_e}{468 \cdot \varepsilon_{fu}} \leq 0.75 \text{ In-lb units} \quad (\text{A-5})$$

Where k_1 and k_2 are the modification factors and L_e is the active bond length over which the majority of the bond stress is maintained (Eq. A-6). The modification factors k_1 and k_2 can be computed using Eq. A-7 and A-8, respectively.

$$L_e = \frac{2500}{(n t_f E_f)^{0.58}} \text{ In-lb units} \quad (\text{A-6})$$

$$k_1 = \left(\frac{f'_{ce}}{4000} \right)^{\frac{2}{3}} \text{ In-lb units} \quad (\text{A-7})$$

$$k_2 = \frac{d_f - 2L_e}{d_f} \text{ In-lb units} \quad (\text{A-8})$$

Step 3. Contribution of the FRP to the shear strength can then be calculated using Eq. A-2.

Step 4. Calculate the shear strength of a member using Eq. A-9. Parameters in Eq. A-9 were defined in section 3.3 and 3.6 of this report.

$$\phi V_n = \phi (V_c + V_s + \Psi_f V_f) \quad (\text{A-9})$$

In the case of fully wrapped members, the effective strain in the CFRP is 0.4% (Priestley et al. 1996) and in the case of side bonded CFRP wrapping, the effective strain in CFRP is a function of concrete compressive strength, CFRP thickness, CFRP tensile modulus and effective bond length (ACI 440.2R-08). Consequently, an iterative process is required to design the thickness of side bonded CFRP based on ACI 440.2R-08.

A-2 - Simple Equation to Determine Effective Strain in CFRP

The ACI 440.2R-08 method requires iteration and is complicated for practical design. Therefore, it was decided to simplify the ACI 400.2R-08 procedure by developing a direct equation for the effective strain of CFRP. The direct equation was developed using an extensive parametric study on a wide range of compressive strength of concrete, CFRP thickness, and tensile modulus of CFRP to learn about the sensitivity of the results to these parameters and to determine if a simple, non-iterative method can be developed. Curve fitting and trial and error method were used to obtain a simple equation (Eq. A-10) to estimate an effective strain in CFRP.

$$\varepsilon_{fe} = 0.015 \times (t_f)^{-0.5} E_f^{-0.36} \left(\frac{f'_{ce}}{5} \right)^{0.67} \quad (\text{A-10})$$

Substituting Eq. A-10 in Eq. A-2, the following expression is obtained for CFRP thickness:

$$t_f = \left(\frac{66.67 V_f}{E_f^{0.64} d_{vf}} \right)^2 \left(\frac{5}{f'_{ce}} \right)^{1.34} \quad (\text{A-11})$$

Equation A-10 and A-11 are the same as Eq. 3-4 and Eq. 3-8, respectively, discussed in section 3.6 of this report.

To compare the results from the proposed equation and the ACI 440 method, a parametric study was conducted covering a wide range for key parameters. The key parameters were: the CFRP thickness, the concrete compressive strength, and CFRP tensile modulus elasticity. Parameter ranges were: 0.04-0.40 inch for CFRP thickness, 3-6 ksi for concrete compressive strength, and 10000-15000 ksi for CFRP tensile modulus.

The objective of choosing such a wide range was to investigate the potential influence of these parameters on the effective strain in CFRP.

Figure A- 1 to Figure A- 6 present graphs for CFRP effective strain vs CFRP layer thickness for various CFRP tensile modulus and compressive strengths of concrete. These Figures show that Eq. 3-4 gives effective strains that are very close to those calculated by ACI 440.2R-08 procedure. The calculated CFRP effective strain using Eq. 3-4 and ACI 440.2R-08 procedure were presented and compared in Table A- 1 to Table A- 6. The results presented in these tables show good agreement between Eq. 3-4 and ACI 440.2R-08 procedure. For a given tensile modulus, the difference in the results is decreasing from lower CFRP thickness to higher CFRP thickness. The range of percentage difference in the results was from 0% to 12% and the average percentage difference in the results was from 1% to 7%.

Figure A- 7 and Figure A- 8 present graphs of CFRP layer thickness vs tensile modulus for various compressive strengths of concrete for DS2 and DS5, respectively. Figure A- 7 shows that Eq. 3-8 gives conservative estimate of required CFRP thickness for concrete compressive strengths of 3, 4, and 5 ksi compared to those calculated by ACI 440. 2R-08. For, concrete compressive strength of 6 ksi, Eq. 3-8 underestimates required CFRP thickness by 5% to 13% compared to those calculated by ACI 440.2R-08. The calculated required CFRP thickness for DS2 using Eq. 3-8 and ACI 440.2R-08 procedure were presented and compared in Table A- 7. Table A- 7 shows that, the CFRP thickness calculated by Eq. 3-8 is conservative by 6% to 26% for concrete compressive strength of 3, 4, and 5.ksi. Figure A- 8 shows that the required CFRP thickness calculated by Eq. 3-8 is very close to those calculated by ACI 440.2R-08 procedure. The calculated required

CFRP thickness for DS5 using Eq. 3-8 and ACI 440.2R-08 procedure were presented and compared in Table A- 8. Table A- 8 shows that, Eq. 3.8 overestimate CFRP thickness by 3 to 8% for compressive strength of 4, 5, and 6 ksi and tensile modulus less than 14000 ksi.

Overall, the results show good agreement between the proposed simplified method and ACI 440.2R-08 procedure. Consequently, the proposed simplified method (Eq. 3-8) can be used in repair design for side bonded CFRP configuration.

Appendix A- Tables

Table A- 1. Effective strain in CFRP calculated by Eq. 3.4 and ACI 440.2R-08, $E_f = 10000$ ksi.

$f'_c = 3$ ksi, $E_f = 10000$ ksi			
t_f	ACI 440 2R-08	Eq. 3.4	% diff
inch	ϵ_{fe}	ϵ_{fe}	
0.04	0.00219	0.00193	12%
0.08	0.00153	0.00137	11%
0.12	0.00123	0.00112	9%
0.16	0.00105	0.00097	8%
0.20	0.00093	0.00086	7%
0.24	0.00084	0.00079	6%
0.28	0.00077	0.00073	5%
0.32	0.00072	0.00068	5%
0.36	0.00067	0.00064	4%
0.40	0.00063	0.00061	3%

$f'_c = 4$ ksi, $E_f = 10000$ ksi			
t_f	ACI 440 2R-08	Eq. 3.4	% diff
inch	ϵ_{fe}	ϵ_{fe}	
0.04	0.00266	0.00234	12%
0.08	0.00186	0.00166	11%
0.12	0.00149	0.00135	9%
0.16	0.00128	0.00117	8%
0.20	0.00113	0.00105	7%
0.24	0.00102	0.00096	6%
0.28	0.00094	0.00089	5%
0.32	0.00087	0.00083	5%
0.36	0.00081	0.00078	4%
0.40	0.00077	0.00074	3%

$f'_c = 5$ ksi, $E_f = 10000$ ksi			
t_f	ACI 440 2R-08	Eq. 3.4	% diff
inch	ϵ_{fe}	ϵ_{fe}	
0.04	0.00308	0.00272	12%
0.08	0.00215	0.00193	11%
0.12	0.00173	0.00157	9%
0.16	0.00148	0.00136	8%
0.20	0.00131	0.00122	7%
0.24	0.00118	0.00111	6%
0.28	0.00109	0.00103	5%
0.32	0.00101	0.00096	5%
0.36	0.00094	0.00091	4%
0.40	0.00089	0.00086	3%

$f'_c = 6$ ksi, $E_f = 10000$ ksi			
t_f	ACI 440 2R-08	Eq. 3.4	% diff
inch	ϵ_{fe}	ϵ_{fe}	
0.04	0.00348	0.00308	12%
0.08	0.00243	0.00218	11%
0.12	0.00196	0.00178	9%
0.16	0.00167	0.00154	8%
0.20	0.00148	0.00138	7%
0.24	0.00134	0.00126	6%
0.28	0.00123	0.00116	5%
0.32	0.00114	0.00109	5%
0.36	0.00107	0.00103	4%
0.40	0.00101	0.00097	3%

Table A- 2. Effective strain in CFRP calculated by Eq. 3.4 and ACI 440.2R-08, $E_f = 11000$ ksi.

$f'_c = 3$ ksi, $E_f = 11000$ ksi			
t_f	ACI 440 2R-08	Eq. 3.4	% diff
inch	ϵ_{fe}	ϵ_{fe}	
0.04	0.00209	0.00187	11%
0.08	0.00146	0.00132	9%
0.12	0.00117	0.00108	8%
0.16	0.00100	0.00093	7%
0.20	0.00088	0.00084	5%
0.24	0.00080	0.00076	4%
0.28	0.00073	0.00071	4%
0.32	0.00068	0.00066	3%
0.36	0.00064	0.00062	2%
0.40	0.00060	0.00059	2%

$f'_c = 4$ ksi, $E_f = 11000$ ksi			
t_f	ACI 440 2R-08	Eq. 3.4	% diff
inch	ϵ_{fe}	ϵ_{fe}	
0.04	0.00253	0.00227	10%
0.08	0.00176	0.00160	9%
0.12	0.00142	0.00131	8%
0.16	0.00121	0.00113	6%
0.20	0.00107	0.00101	5%
0.24	0.00097	0.00093	4%
0.28	0.00089	0.00086	4%
0.32	0.00082	0.00080	3%
0.36	0.00077	0.00076	2%
0.40	0.00073	0.00072	1%

$f'_c = 5$ ksi, $E_f = 11000$ ksi			
t_f	ACI 440 2R-08	Eq. 3.4	% diff
inch	ϵ_{fe}	ϵ_{fe}	
0.04	0.00294	0.00263	10%
0.08	0.00205	0.00186	9%
0.12	0.00164	0.00152	8%
0.16	0.00141	0.00132	6%
0.20	0.00124	0.00118	5%
0.24	0.00112	0.00107	4%
0.28	0.00103	0.00099	4%
0.32	0.00096	0.00093	3%
0.36	0.00090	0.00088	2%
0.40	0.00084	0.00083	1%

$f'_c = 6$ ksi, $E_f = 11000$ ksi			
t_f	ACI 440 2R-08	Eq. 3.4	% diff
inch	ϵ_{fe}	ϵ_{fe}	
0.04	0.00332	0.00297	10%
0.08	0.00231	0.00210	9%
0.12	0.00186	0.00172	8%
0.16	0.00159	0.00149	6%
0.20	0.00140	0.00133	5%
0.24	0.00127	0.00121	4%
0.28	0.00116	0.00112	3%
0.32	0.00108	0.00105	3%
0.36	0.00101	0.00099	2%
0.40	0.00095	0.00094	1%

Table A- 3. Effective strain in CFRP calculated by Eq. 3.4 and ACI 440.2R-08, $E_f = 12000$ ksi.

$f'_c = 3$ ksi, $E_f = 12000$ ksi			
t_f	ACI 440 2R-08	Eq. 3.4	% diff
inch	ϵ_{fe}	ϵ_{fe}	
0.04	0.00200	0.00181	9%
0.08	0.00139	0.00128	8%
0.12	0.00112	0.00105	6%
0.16	0.00095	0.00091	5%
0.20	0.00084	0.00081	4%
0.24	0.00076	0.00074	3%
0.28	0.00070	0.00068	2%
0.32	0.00065	0.00064	1%
0.36	0.00061	0.00060	0%
0.40	0.00057	0.00057	0%

$f'_c = 4$ ksi, $E_f = 12000$ ksi			
t_f	ACI 440 2R-08	Eq. 3.4	% diff
inch	ϵ_{fe}	ϵ_{fe}	
0.04	0.00242	0.00220	9%
0.08	0.00168	0.00155	8%
0.12	0.00135	0.00127	6%
0.16	0.00115	0.00110	5%
0.20	0.00102	0.00098	4%
0.24	0.00092	0.00090	3%
0.28	0.00085	0.00083	2%
0.32	0.00078	0.00078	0%
0.36	0.00073	0.00073	0%
0.40	0.00069	0.00069	0%

$f'_c = 5$ ksi, $E_f = 12000$ ksi			
t_f	ACI 440 2R-08	Eq. 3.4	% diff
inch	ϵ_{fe}	ϵ_{fe}	
0.04	0.00281	0.00255	9%
0.08	0.00195	0.00180	8%
0.12	0.00157	0.00147	6%
0.16	0.00134	0.00128	5%
0.20	0.00118	0.00114	4%
0.24	0.00107	0.00104	3%
0.28	0.00098	0.00096	2%
0.32	0.00091	0.00090	1%
0.36	0.00085	0.00085	0%
0.40	0.00080	0.00081	0%

$f'_c = 6$ ksi, $E_f = 12000$ ksi			
t_f	ACI 440 2R-08	Eq. 3.4	% diff
inch	ϵ_{fe}	ϵ_{fe}	
0.04	0.00317	0.00288	9%
0.08	0.00221	0.00204	8%
0.12	0.00177	0.00166	6%
0.16	0.00151	0.00144	5%
0.20	0.00134	0.00129	4%
0.24	0.00121	0.00118	3%
0.28	0.00111	0.00109	2%
0.32	0.00103	0.00102	1%
0.36	0.00096	0.00096	0%
0.40	0.00091	0.00091	0%

Table A- 4. Effective strain in CFRP calculated by Eq. 3.4 and ACI 440.2R-08, $E_f = 13000$ ksi.

$f'_c = 3$ ksi, $E_f = 13000$ ksi			
t_f	ACI 440 2R-08	Eq. 3.4	% diff
inch	ϵ_{fe}	ϵ_{fe}	
0.04	0.00192	0.00176	8%
0.08	0.00133	0.00124	7%
0.12	0.00107	0.00102	5%
0.16	0.00091	0.00088	3%
0.20	0.00081	0.00079	2%
0.24	0.00073	0.00072	1%
0.28	0.00067	0.00067	0%
0.32	0.00062	0.00062	0%
0.36	0.00058	0.00059	-1%
0.40	0.00055	0.00056	-2%

$f'_c = 4$ ksi, $E_f = 13000$ ksi			
t_f	ACI 440 2R-08	Eq. 3.4	% diff
inch	ϵ_{fe}	ϵ_{fe}	
0.04	0.00232	0.00213	8%
0.08	0.00161	0.00151	6%
0.12	0.00129	0.00123	5%
0.16	0.00110	0.00107	3%
0.20	0.00098	0.00095	2%
0.24	0.00088	0.00087	1%
0.28	0.00081	0.00081	0%
0.32	0.00075	0.00075	0%
0.36	0.00070	0.00071	-1%
0.40	0.00066	0.00067	-2%

$f'_c = 5$ ksi, $E_f = 13000$ ksi			
t_f	ACI 440 2R-08	Eq. 3.4	% diff
inch	ϵ_{fe}	ϵ_{fe}	
0.04	0.00270	0.00248	8%
0.08	0.00187	0.00175	6%
0.12	0.00150	0.00143	5%
0.16	0.00128	0.00124	3%
0.20	0.00113	0.00111	2%
0.24	0.00102	0.00101	1%
0.28	0.00094	0.00094	0%
0.32	0.00087	0.00088	-1%
0.36	0.00082	0.00083	-1%
0.40	0.00077	0.00078	-2%

$f'_c = 6$ ksi, $E_f = 13000$ ksi			
t_f	ACI 440 2R-08	Eq. 3.4	% diff
inch	ϵ_{fe}	ϵ_{fe}	
0.04	0.00305	0.00280	8%
0.08	0.00211	0.00198	6%
0.12	0.00170	0.00162	5%
0.16	0.00145	0.00140	3%
0.20	0.00128	0.00125	2%
0.24	0.00116	0.00114	1%
0.28	0.00106	0.00106	0%
0.32	0.00098	0.00099	-1%
0.36	0.00092	0.00093	-1%
0.40	0.00087	0.00089	-2%

Table A- 5. Effective strain in CFRP calculated by Eq. 3.4 and ACI 440.2R-08, $E_f = 14000$ ksi.

$f'_c = 3$ ksi, $E_f = 14000$ ksi			
t_f	ACI 440 2R-08	Eq. 3.4	% diff
inch	ϵ_{fe}	ϵ_{fe}	
0.04	0.00185	0.00171	7%
0.08	0.00128	0.00121	5%
0.12	0.00103	0.00099	4%
0.16	0.00088	0.00086	2%
0.20	0.00077	0.00077	0%
0.24	0.00070	0.00070	0%
0.28	0.00064	0.00065	-1%
0.32	0.00059	0.00061	-2%
0.36	0.00056	0.00057	-3%
0.40	0.00052	0.00054	-3%

$f'_c = 4$ ksi, $E_f = 14000$ ksi			
t_f	ACI 440 2R-08	Eq. 3.4	% diff
inch	ϵ_{fe}	ϵ_{fe}	
0.04	0.00224	0.00208	7%
0.08	0.00155	0.00147	5%
0.12	0.00124	0.00120	3%
0.16	0.00106	0.00104	2%
0.20	0.00094	0.00093	1%
0.24	0.00085	0.00085	0%
0.28	0.00078	0.00079	-1%
0.32	0.00072	0.00073	-2%
0.36	0.00067	0.00069	-3%
0.40	0.00063	0.00066	-4%

$f'_c = 5$ ksi, $E_f = 14000$ ksi			
t_f	ACI 440 2R-08	Eq. 3.4	% diff
inch	ϵ_{fe}	ϵ_{fe}	
0.04	0.00260	0.00241	7%
0.08	0.00180	0.00171	5%
0.12	0.00144	0.00139	3%
0.16	0.00123	0.00121	2%
0.20	0.00109	0.00108	1%
0.24	0.00098	0.00098	0%
0.28	0.00090	0.00091	-1%
0.32	0.00084	0.00085	-2%
0.36	0.00078	0.00080	-3%
0.40	0.00074	0.00076	-4%

$f'_c = 6$ ksi, $E_f = 14000$ ksi			
t_f	ACI 440 2R-08	Eq. 3.4	% diff
inch	ϵ_{fe}	ϵ_{fe}	
0.04	0.00293	0.00273	7%
0.08	0.00203	0.00193	5%
0.12	0.00163	0.00157	3%
0.16	0.00139	0.00136	2%
0.20	0.00123	0.00122	1%
0.24	0.00111	0.00111	0%
0.28	0.00102	0.00103	-1%
0.32	0.00094	0.00096	-2%
0.36	0.00088	0.00091	-3%
0.40	0.00083	0.00086	-4%

Table A- 6. Effective strain in CFRP calculated by Eq. 3.4 and ACI 440.2R-08, $E_f = 15000$ ksi.

$f'_c = 3$ ksi, $E_f = 15000$ ksi				$f'_c = 4$ ksi, $E_f = 15000$ ksi			
t_f	ACI 440 2R-08	Eq. 3.4	% diff	t_f	ACI 440 2R-08	Eq. 3.4	% diff
inch	ϵ_{fe}	ϵ_{fe}		inch	ϵ_{fe}	ϵ_{fe}	
0.04	0.00178	0.00167	6%	0.04	0.00216	0.00203	6%
0.08	0.00123	0.00118	4%	0.08	0.00149	0.00143	4%
0.12	0.00099	0.00096	2%	0.12	0.00120	0.00117	2%
0.16	0.00084	0.00084	0%	0.16	0.00102	0.00101	1%
0.20	0.00075	0.00075	0%	0.20	0.00090	0.00091	-1%
0.24	0.00067	0.00068	-2%	0.24	0.00081	0.00083	-2%
0.28	0.00062	0.00063	-3%	0.28	0.00075	0.00077	-3%
0.32	0.00057	0.00059	-3%	0.32	0.00069	0.00072	-3%
0.36	0.00053	0.00056	-4%	0.36	0.00065	0.00068	-4%
0.40	0.00050	0.00053	-5%	0.40	0.00061	0.00064	-5%

$f'_c = 5$ ksi, $E_f = 15000$ ksi				$f'_c = 6$ ksi, $E_f = 15000$ ksi			
t_f	ACI 440 2R-08	Eq. 3.4	% diff	t_f	ACI 440 2R-08	Eq. 3.4	% diff
inch	ϵ_{fe}	ϵ_{fe}		inch	ϵ_{fe}	ϵ_{fe}	
0.04	0.00250	0.00235	6%	0.04	0.00283	0.00266	6%
0.08	0.00173	0.00166	4%	0.08	0.00196	0.00188	4%
0.12	0.00139	0.00136	2%	0.12	0.00157	0.00154	2%
0.16	0.00118	0.00118	0%	0.16	0.00134	0.00133	1%
0.20	0.00105	0.00105	0%	0.20	0.00118	0.00119	-1%
0.24	0.00094	0.00096	-2%	0.24	0.00107	0.00109	-2%
0.28	0.00087	0.00089	-3%	0.28	0.00098	0.00101	-3%
0.32	0.00080	0.00083	-4%	0.32	0.00091	0.00094	-4%
0.36	0.00075	0.00078	-4%	0.36	0.00085	0.00089	-4%
0.40	0.00071	0.00074	-5%	0.40	0.00080	0.00084	-5%

Table A- 7. Required CFRP thickness calculated by ACI 440.2R-08 and proposed method for shear keys under DS2.

Damage State 2			
f_c = 3 ksi			
E_r	t_r		% Diff
	ACI 440.2R-08	EQ-3.8	
ksi	inch	inch	
10000	0.023	0.029	26%
11000	0.021	0.026	24%
12000	0.019	0.023	21%
13000	0.018	0.021	17%
14000	0.016	0.019	19%
15000	0.015	0.017	13%

Damage State 2			
f_c = 4 ksi			
E_r	t_r		% Diff
	ACI 440.2R-08	EQ-3.8	
ksi	inch	inch	
10000	0.021	0.026	24%
11000	0.019	0.023	21%
12000	0.018	0.021	17%
13000	0.016	0.019	19%
14000	0.015	0.017	13%
15000	0.014	0.016	14%

Damage State 2			
f_c = 5 ksi			
E_r	t_r		% Diff
	ACI 440.2R-08	EQ-3.8	
ksi	inch	inch	
10000	0.021	0.024	14%
11000	0.019	0.022	16%
12000	0.018	0.019	6%
13000	0.016	0.017	6%
14000	0.015	0.016	7%
15000	0.014	0.014	0%

Damage State 2			
f_c = 6 ksi			
E_r	t_r		% Diff
	ACI 440.2R-08	EQ-3.8	
ksi	inch	inch	
10000	0.023	0.023	0%
11000	0.021	0.020	-5%
12000	0.019	0.018	-5%
13000	0.018	0.016	-11%
14000	0.017	0.015	-12%
15000	0.016	0.014	-13%

Table A- 8. Required CFRP thickness calculated by ACI 440.2R-08 and proposed method for shear keys under DS5.

Damage State 5			
f _c = 3 ksi			
E _f	t _f		% Diff
	ACI 440.2R-08	EQ-3.8	
ksi	inch	inch	
10000	0.44	0.46	5%
11000	0.40	0.41	2%
12000	0.39	0.37	-5%
13000	0.36	0.33	-8%
14000	0.31	0.30	-3%
15000	0.29	0.28	-3%

Damage State 5			
f _c = 4 ksi			
E _f	t _f		% Diff
	ACI 440.2R-08	EQ-3.8	
ksi	inch	inch	
10000	0.39	0.42	8%
11000	0.36	0.37	3%
12000	0.33	0.33	0%
13000	0.30	0.30	0%
14000	0.28	0.27	-4%
15000	0.26	0.25	-4%

Damage State 5			
f _c = 5 ksi			
E _f	t _f		% Diff
	ACI 440.2R-08	EQ-3.8	
ksi	inch	inch	
10000	0.36	0.39	8%
11000	0.33	0.35	6%
12000	0.30	0.31	3%
13000	0.28	0.28	0%
14000	0.26	0.25	-4%
15000	0.24	0.23	-4%

Damage State 5			
f _c = 6 ksi			
E _f	t _f		% Diff
	ACI 440.2R-08	EQ-3.8	
ksi	inch	inch	
10000	0.34	0.37	9%
11000	0.31	0.32	3%
12000	0.28	0.29	4%
13000	0.26	0.26	0%
14000	0.24	0.24	0%
15000	0.22	0.22	0%

Appendix A- Figures

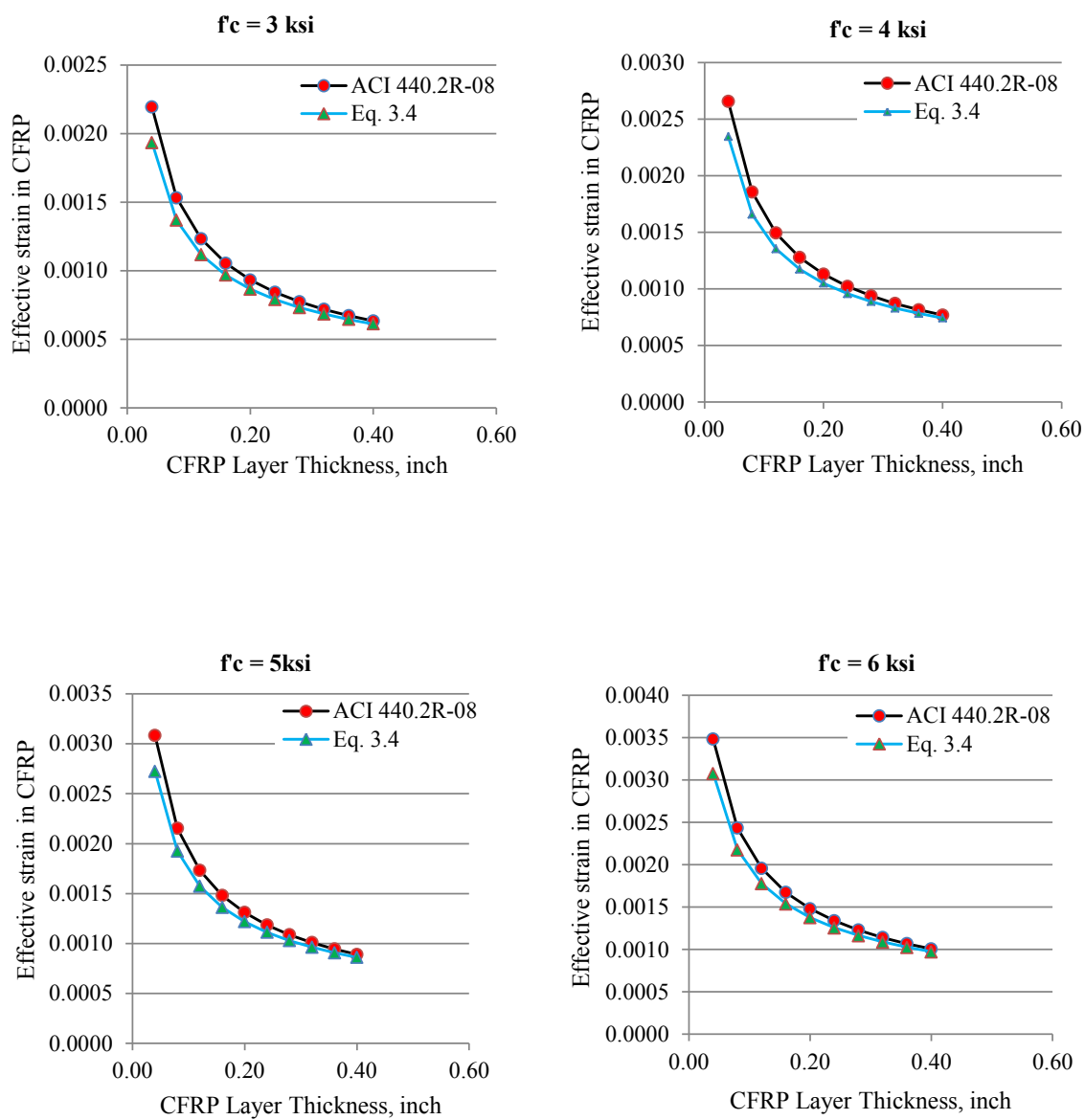


Figure A- 1. Effective strain in CFRP vs thickness for tensile modulus of 10000 ksi

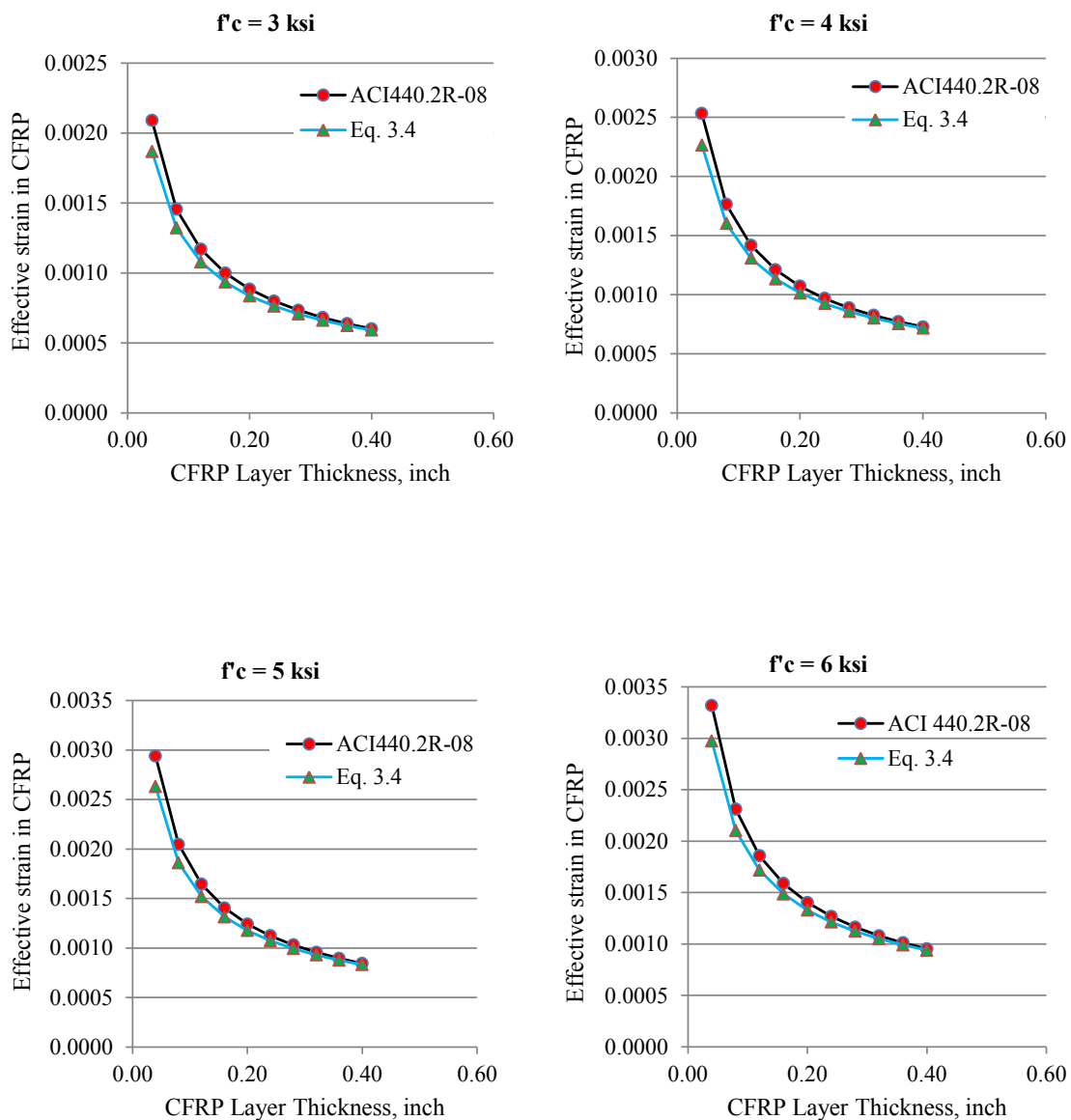


Figure A- 2. Effective strain in CFRP vs thickness for tensile modulus of 11000 ksi

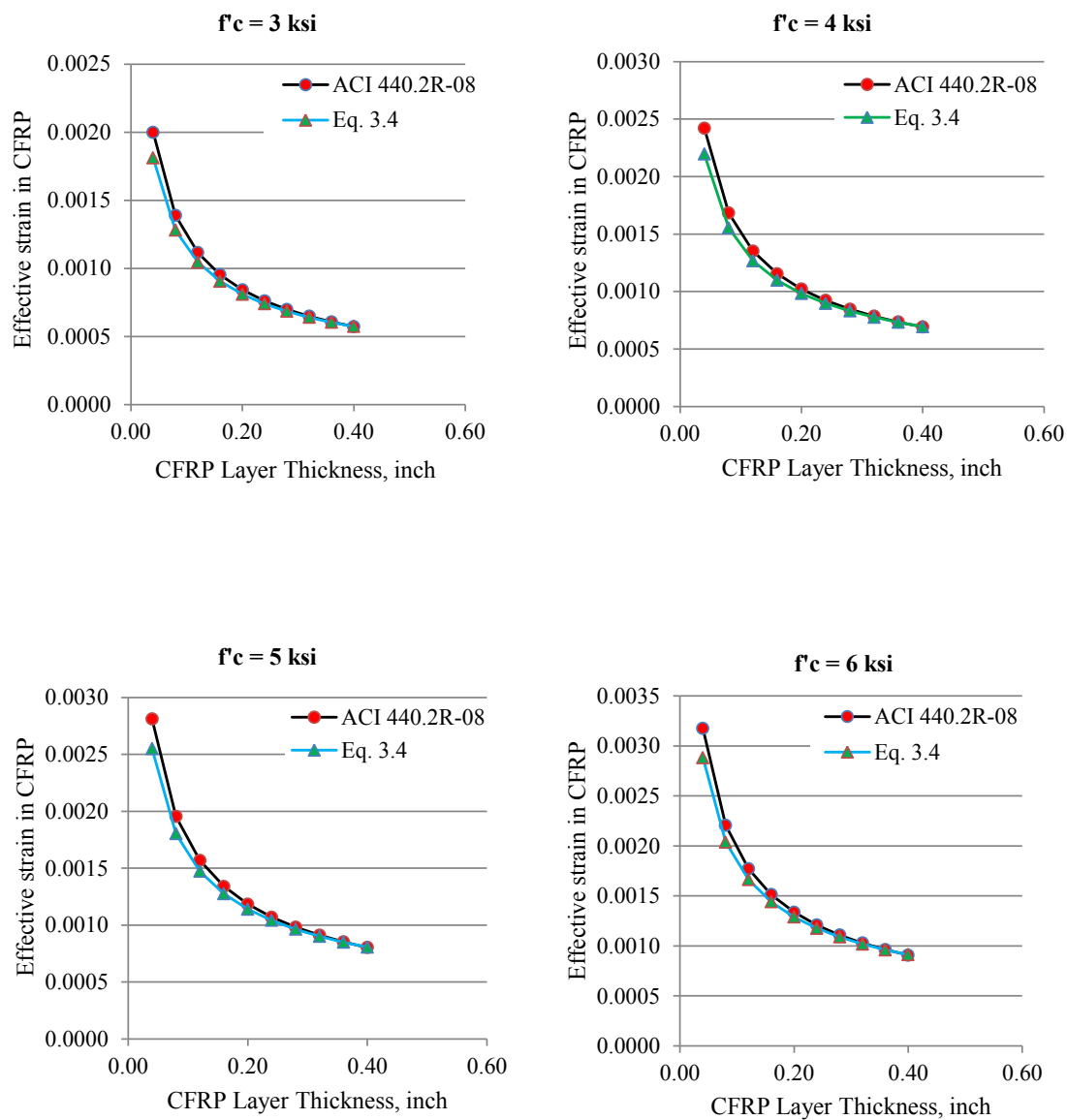


Figure A- 3. Effective strain in CFRP vs thickness for tensile modulus of 12000 ksi

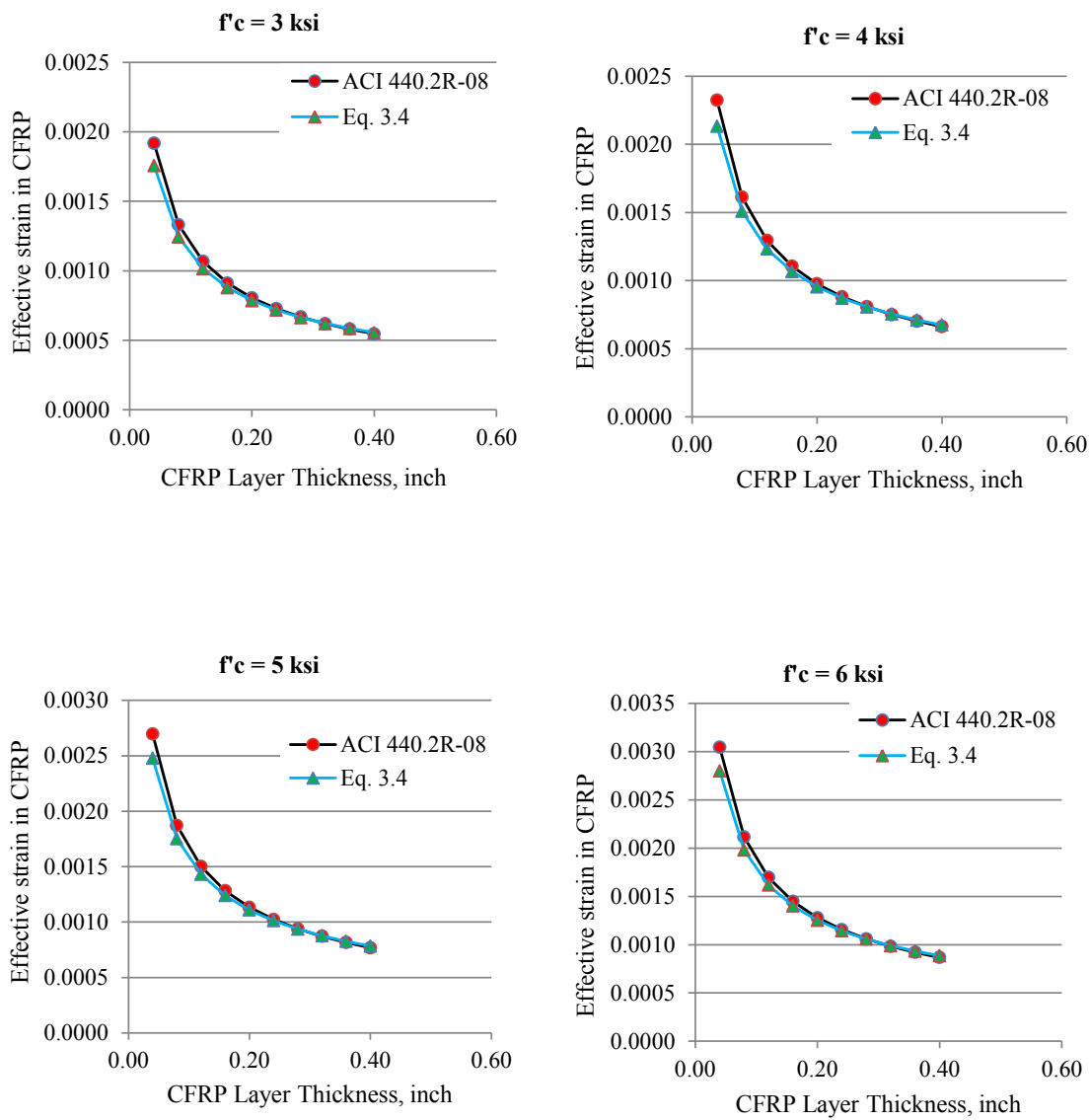


Figure A- 4. Effective strain in CFRP vs thickness for tensile modulus of 13000 ksi

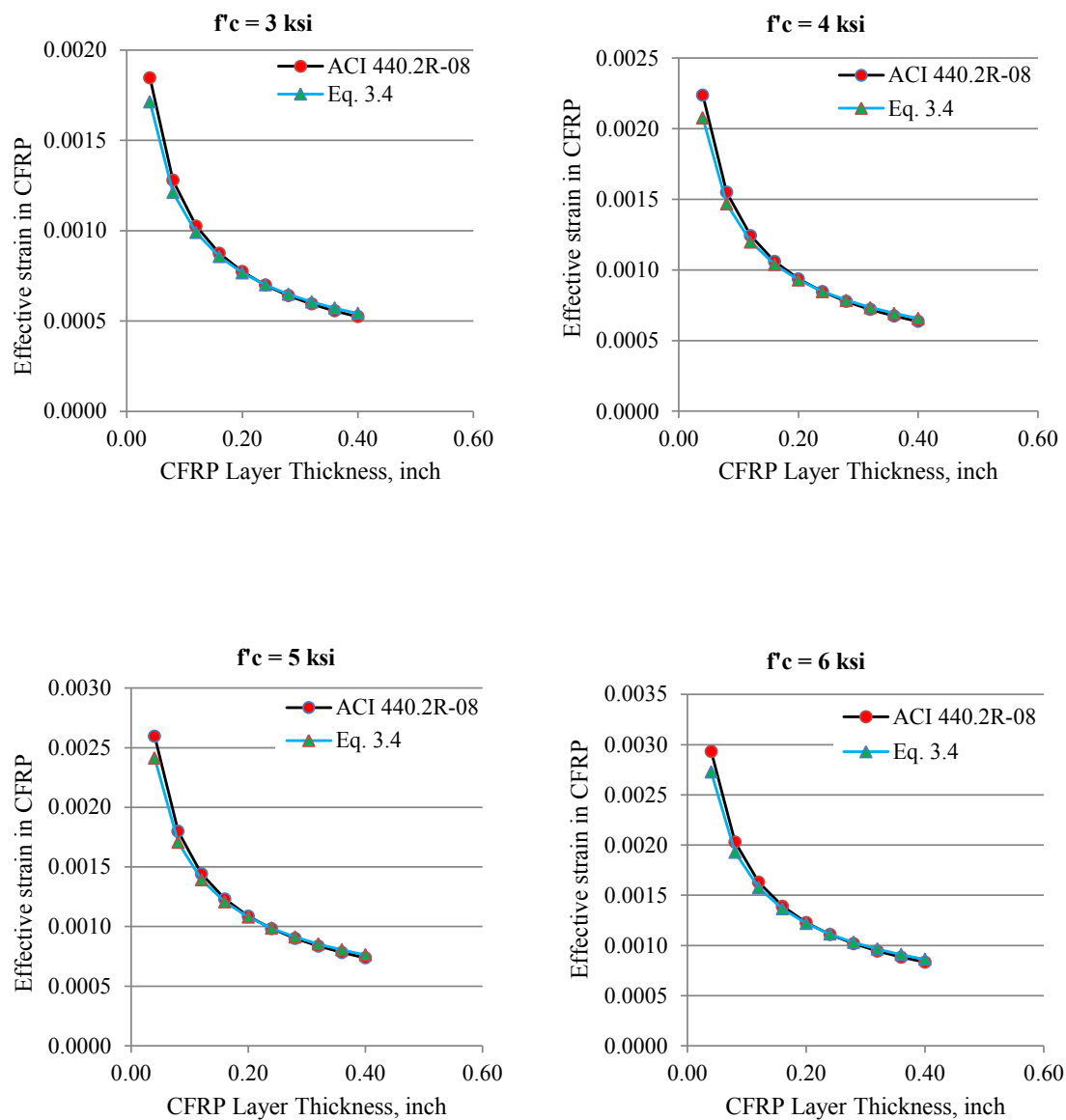


Figure A- 5. Effective strain in CFRP vs thickness for tensile modulus of 14000 ksi

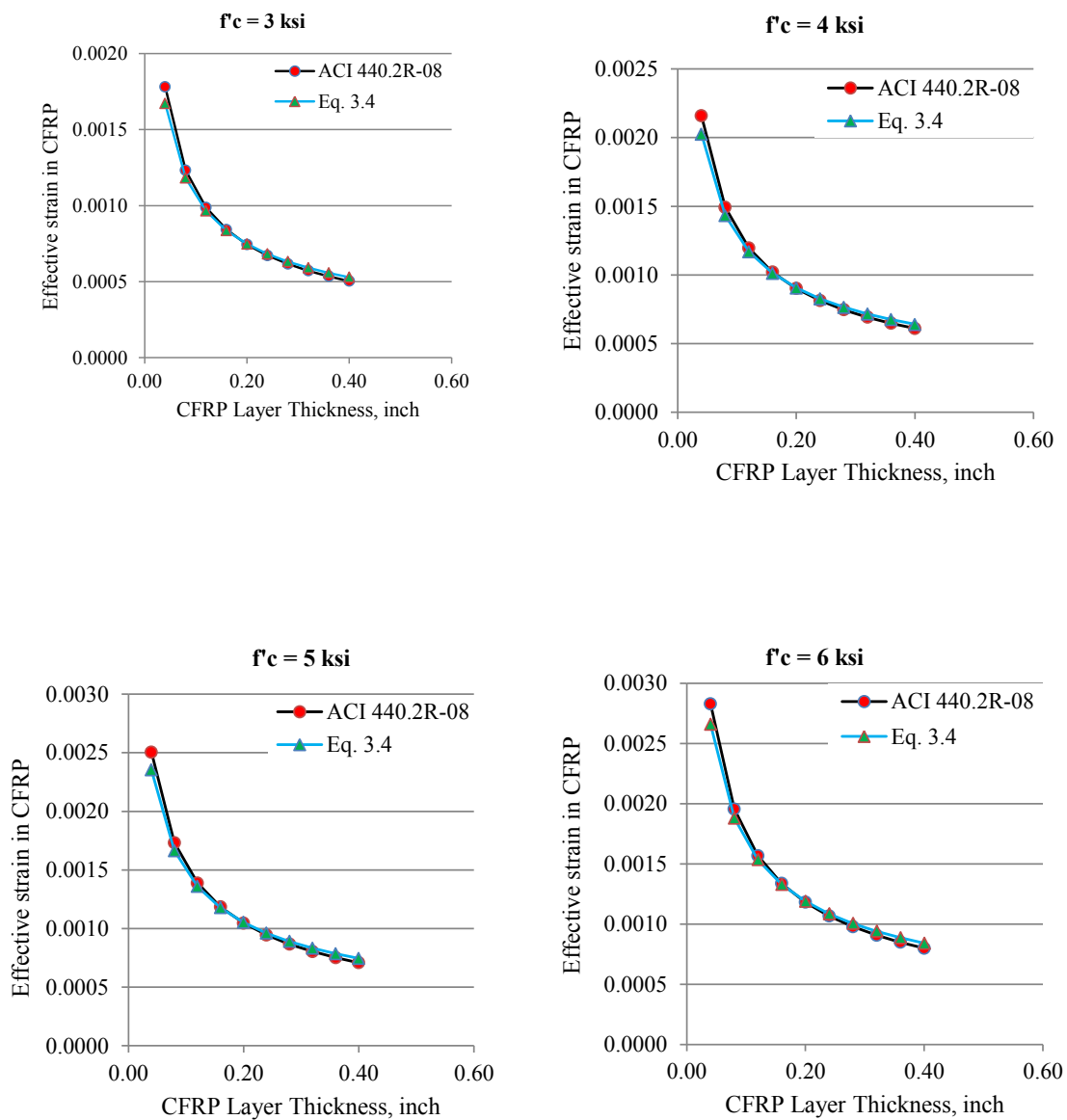


Figure A- 6. Effective strain in CFRP vs thickness for tensile modulus of 15000 ksi

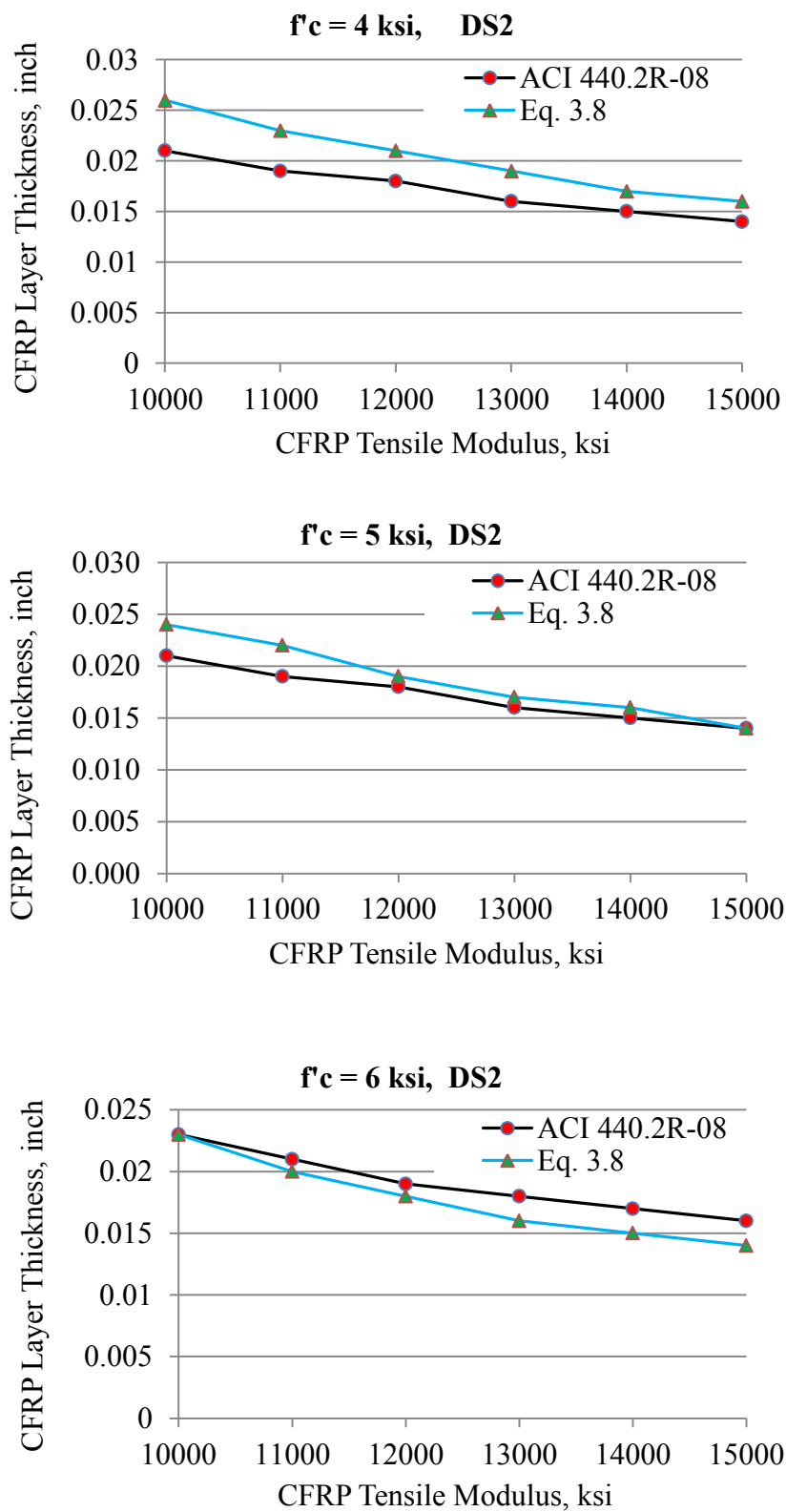


Figure A- 7. Required CFRP thickness for shear keys under DS2.

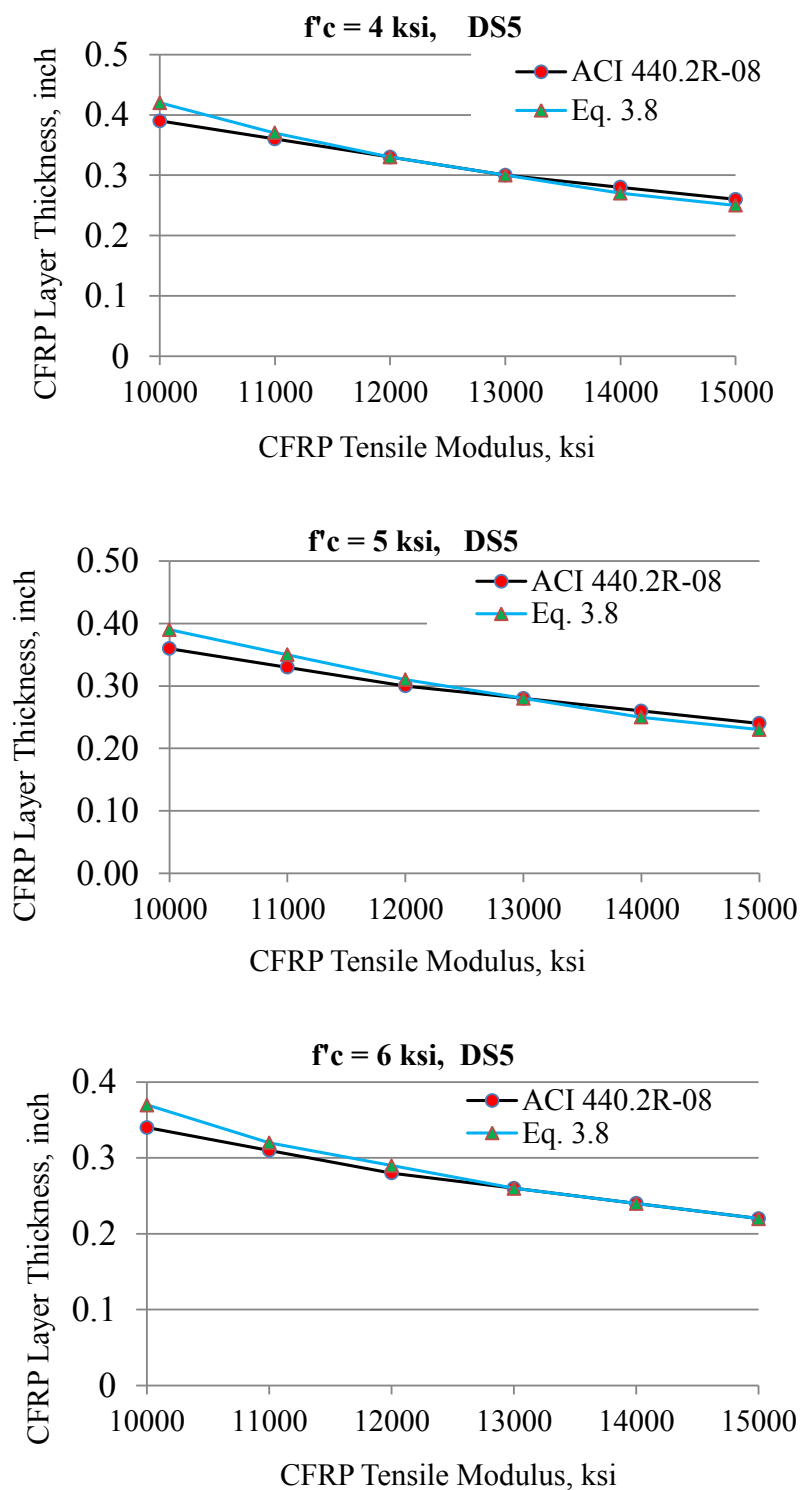


Figure A- 8. Required CFRP thickness for shear keys under DS5.

Appendix B1. Shear Key Repair Design Examples

B1-1 Repair of shear keys under DS2

The repair of shear keys under DS2 is illustrated through an example in this section. The objective of the repair for shear keys under DS2 is to restore shear strength loss of 20% of concrete component without changing the mode of failure. The shear key test unit 4A (Figure 3-1) was used as a benchmark with original shear capacity of 334.9 kips [1489.7 kN]. The material properties were presented in Section 3.4.

The material properties of unidirectional CFRP fabrics used are shown in Table 3-1. The required CFRP thickness to restore strength is calculated using the proposed Eq. 3-8. The concrete shear strength in the original shear key is 86.7 kips [385.66 kN]. The required CFRP thickness to provide 20% of this strength is 0.019 in [0.48 mm], but the minimum thickness that can be provided is 0.04 in [1 mm], which is for one layer. Other parameters are shown in Table B1- 1. The total capacity of the repaired shear key with this design is 344.1 kips [1530.6 kN] compared to the original shear key capacity of 334.9 kips [1489.71 kN]. The over-strength of 9.2 kips [40.9 kN] is less than 10% compared to the total capacity of the original shear key. Figure B1- 1 and Figure B1- 2 show the front and side view of repaired shear key, respectively.

B1-2 Repair of shear keys under DS5

The objective of repair of shear keys under DS5 is to restore shear strength loss of 80% of concrete component without changing the mode of failure. The repair is developed for the shear key test unit 4A used in the previous example.

The CFRP material used in repair of DS5 is the same as that used in DS2.

Unidirectional CFRP fibers were used in the horizontal direction to repair shear keys in DS5. The required CFRP thickness to restore shear strength loss at DS5 is determined by using the proposed simple equation, (Eq. 3-8). The required CFRP thickness calculation presented in Table B1- 1 are based on the assumption that shear strength loss in concrete component of shear keys is 80%, which is 69.4 kips [308.71 kN], while utilizing 100% contribution of steel to shear strength. The required CFRP thickness was determined as 0.312 in [7.92 mm] and provided is 0.315 in [8 mm]. The shear strength provided with this design is 70.23 kips [312.4 kN] compared to the target strength of 69.4 kips [308.71 kN]. Figure B1- 3 and Figure B1- 4 show the front and side view of shear keys repair design for DS5, respectively.

The required CFRP thicknesses for DS2 and DS5 using the proposed Eq.3-8 were compared with those calculated by ACI440.2R-08 design procedure (Table B1- 2). The results show good agreement between the simplified and ACI 440.2R-08 procedure. Consequently, the proposed simplified method (Eq.3-8) can be used effectively in repair design of shear keys.

Table B1- 1. CFRP layer thickness for DS2 and DS5

Damage state	Shear capacity of undamaged shear key $V_c + V_s$	CFRP required shear strength $(V_f)_{required}$	Required CFRP thickness t_f	Provided CFRP thickness t_f	Minimum required anchorage length l_{df}	Provided anchorage length l_{df}
	Kips (KN)	Kips (KN)	in (mm)	in (mm)	in (mm)	in (mm)
DS2	334.9 (1489.7)	20.4 (90.74)	0.019 (0.48)	0.04 (1)	4.7 (119.4)	8 (203)
DS5	334.9 (1489.7)	81.6 (362.97)	0.312 (7.92)	0.315 (8)	13.1 (332.7)	15 (380)

Table B1- 2. Comparison of CFRP-repair design using different approaches

Damage state	Simple equation (EQ-3.8)		ACI 440 2R-08		% Difference in CFRP effective strain	% Difference in required CFRP thickness
	Effective strain in CFRP	Required CFRP thickness	Effective strain in CFRP	Required CFRP thickness		
		in (mm)		in (mm)		
DS2	0.0037	0.019 (0.48)	0.0042	0.018 (0.46)	11.9 %	4.2 %
DS5	0.0009	0.312 (7.92)	0.0009	0.304 (7.72)	0 %	2.5 %

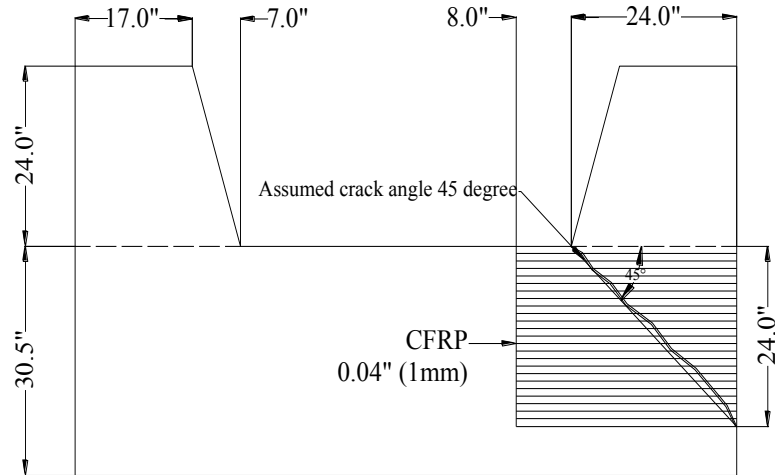


Figure B1- 1. Shear key repair design for DS2 (front view)

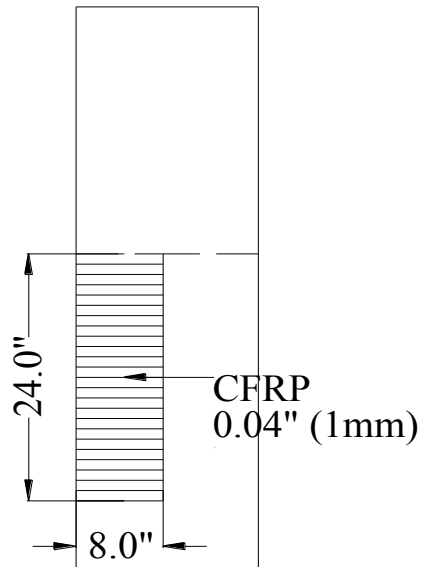


Figure B1- 2. Side view of repair for DS2

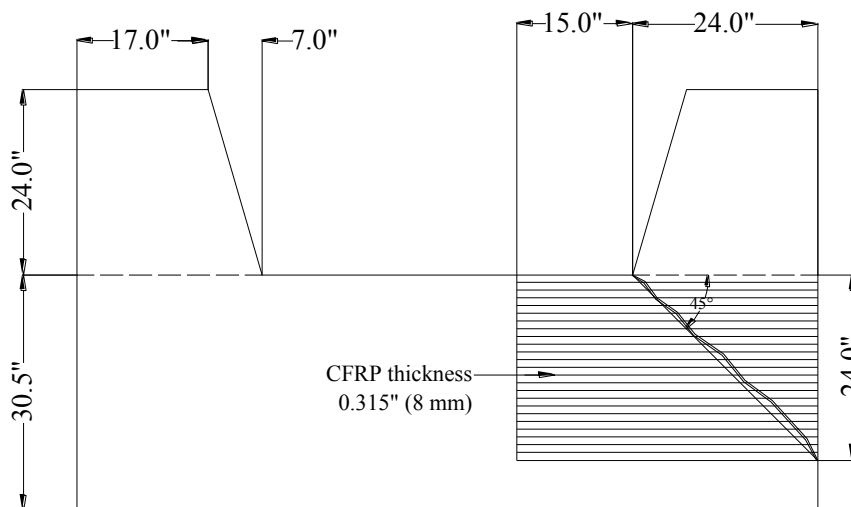


Figure B1- 3. Shear keys repair design for DS5 (front view)

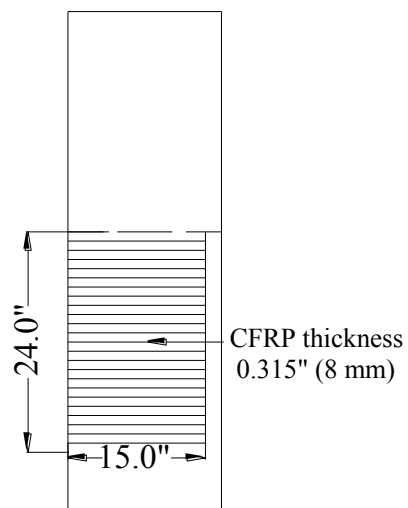


Figure B1- 4. Shear keys repair design for DS5 (side view)

B1-3 Repair of shear keys under DS6

The objective of repair for a shear key at DS6 is to restore the shear capacity and to change the mode of failure from diagonal shear failure of the abutment stem wall to sliding shear friction failure at the interface between the shear key and the stem wall. To

achieve sliding shear friction failure, a new detailing is recommended to isolate the shear key from the abutment stem wall.

To help clarify the example, test unit 4A (Figure 3-1) is used to identify different types of reinforcement in typical existing abutment and shear key connection region.

Figure B1- 5 and Figure B1- 6 represent a reinforcement layout of shear key test unit 4A.

For this example, shear key is designed for a capacity of 200 kips [890 kN]. The expected yield strength of steel is 68 ksi [302.5 MPa]. The following procedure is recommended to repair shear keys at DS6 (Figure B1- 7):

Step 1. Remove the concrete from the earthquake damaged shear key and expose the steel bars.

Step 2. Remove the existing shear key transverse and inclined reinforcement but keep the abutment stem wall vertical reinforcement (Figure B1- 8). Cut all the vertical reinforcement crossing the shear key-abutment stem wall interface above 45 degree failure plane (Figure B1- 8)

Step 3. Straighten the vertical reinforcement of abutment stem wall crossing the shear key-stem wall interface (Figure B1- 9) and then cut these bars at the shear key-stem wall interface level (Figure B1- 10). Remove all the reinforcement connecting the shear key to the abutment back-wall, if any.

Step 4. Required area and development length of shear key vertical reinforcement using Eq. 3-10 and 3-12 was determined as 1.63 in^2 [1052 mm^2] and 18 in [457 mm], respectively.

Step 5. Drill holes in the abutment stem wall and install the shear key vertical reinforcement determined in step 4 (4 No. 6 bars) near the center line of the shear key in the direction parallel to shear force (Figure B1- 11). Fill the drilled holes with epoxy prior to insertion of the bars.

Step 6. Provide minimum stirrups to provide confinement to the shear key. Area of the stirrups in the direction perpendicular and parallel to the flexural tensile reinforcement was calculated as 0.20 in^2 [129 mm^2] and 0.12 in^2 [77.4 mm^2], respectively.

Conservatively #3 stirrups at center to center spacing of 4.75 in [120.6 mm] in both directions were provided (Figure B1- 12 and Figure B1- 13). The actual stirrups area is 0.22 in^2 [144 mm^2].

Step 7. Provide a smooth construction joint at shear key-abutment stem wall interface to develop a weak plane so a shear friction coefficient of 0.4 can be used. For this example, the width (throat thickness) and depth of the shear key at construction joint is 7 and 24 in, respectively. The minimum 7 in [178 mm] throat thickness is recommended to have sufficient plastic moment capacity of the section so that, the shear key would not fail in flexure before sliding occurs.

Figure B1- 14, Figure B1- 15, and Figure B1- 17 show the elevation, cross section, and side view of the repaired shear key for DS6, respectively. Figure B1- 16 shows the side view of the shear key vertical reinforcement.

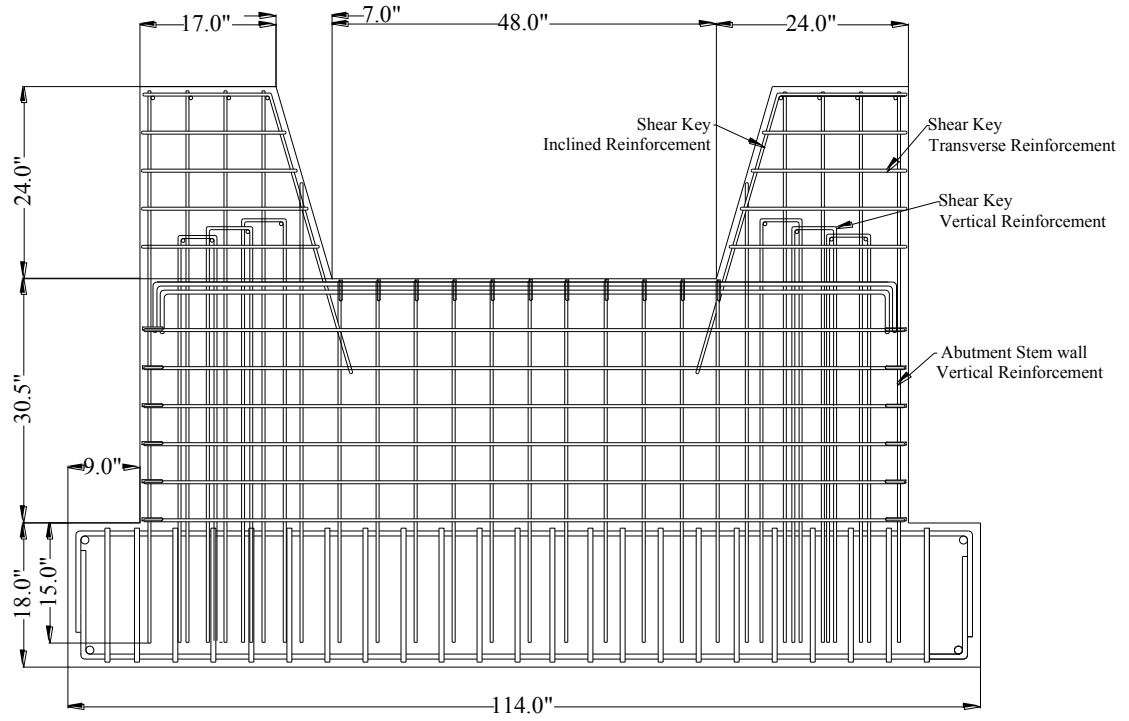


Figure B1- 5. Elevation view of reinforcement layout

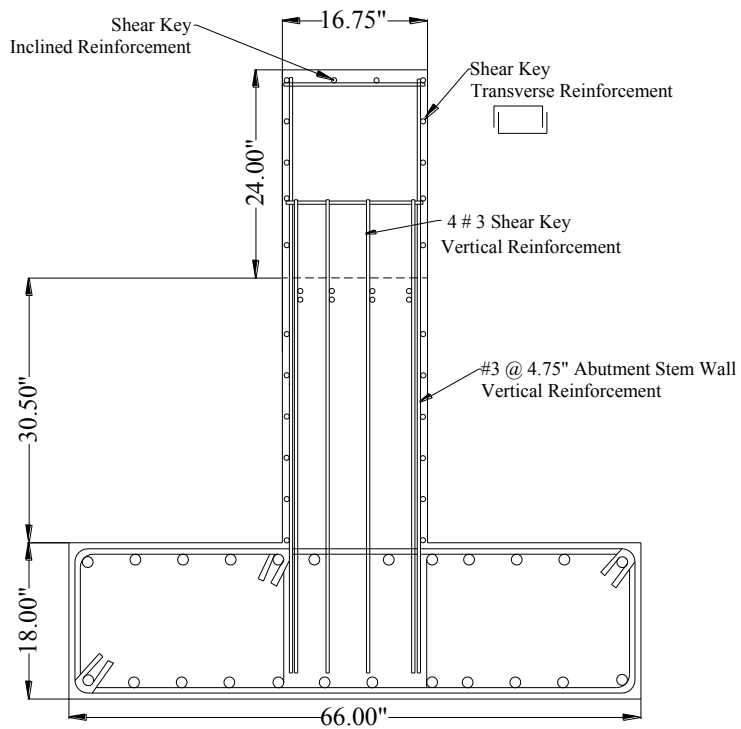


Figure B1- 6. Side view of shear key reinforcement layout

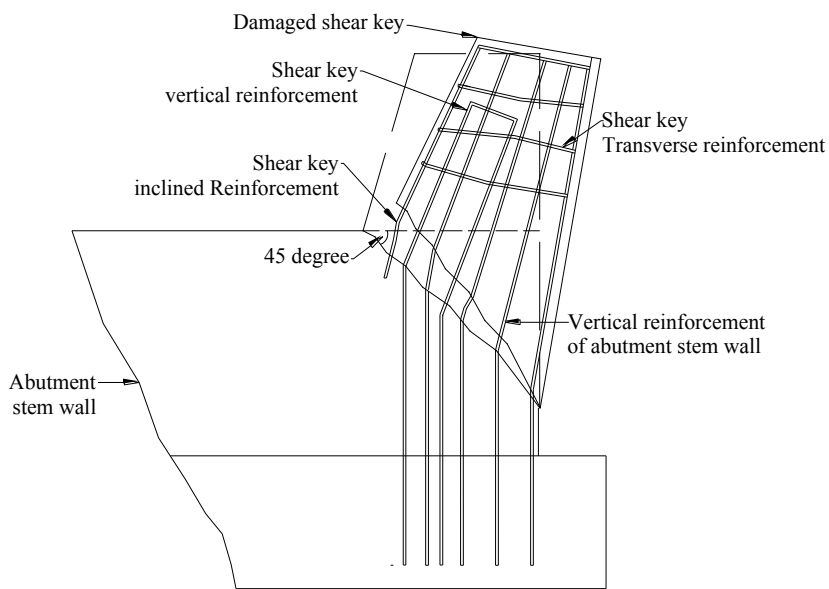


Figure B1- 7. Failure of shear key

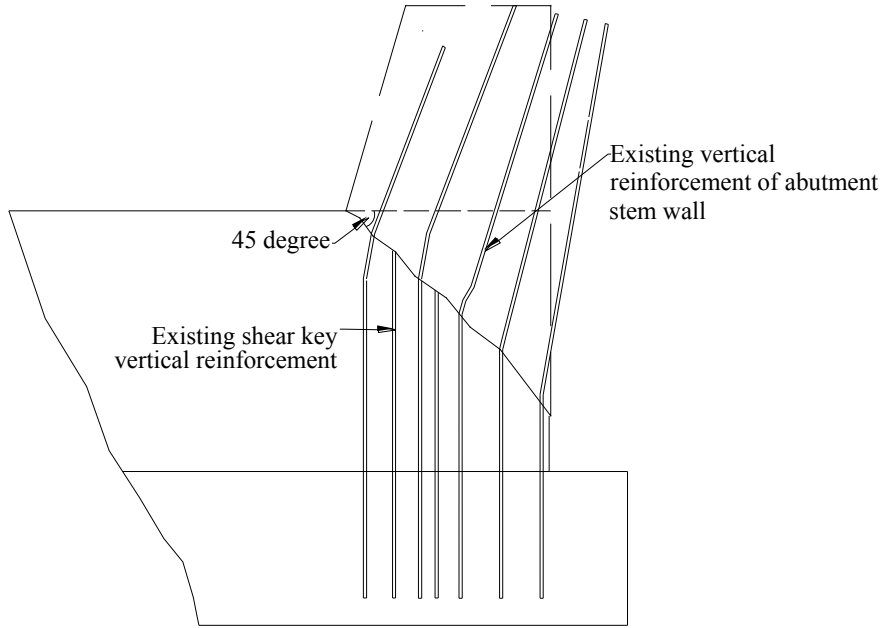


Figure B1- 8. Removal of shear key transverse and inclined reinforcement

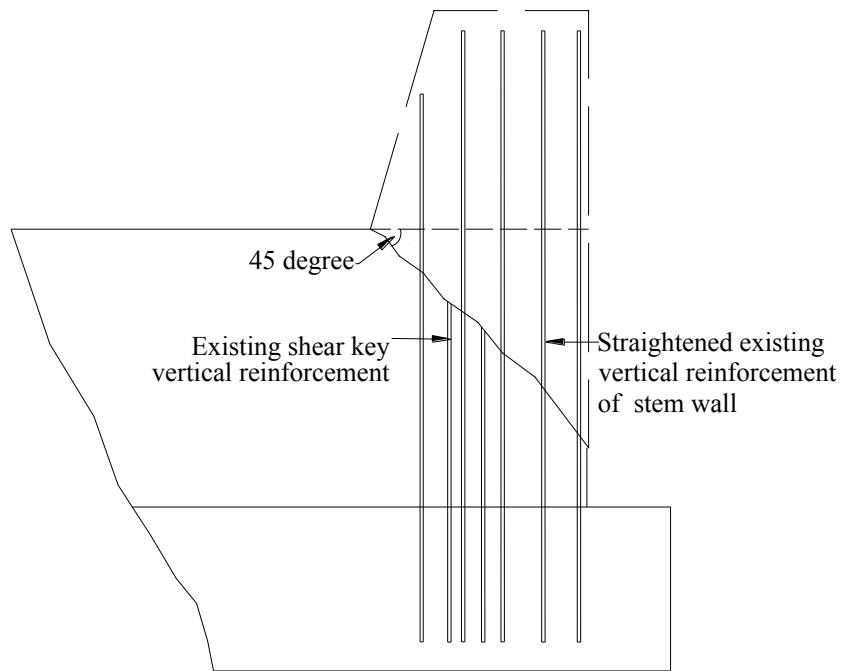


Figure B1- 9. Straightened existing stem wall vertical reinforcement

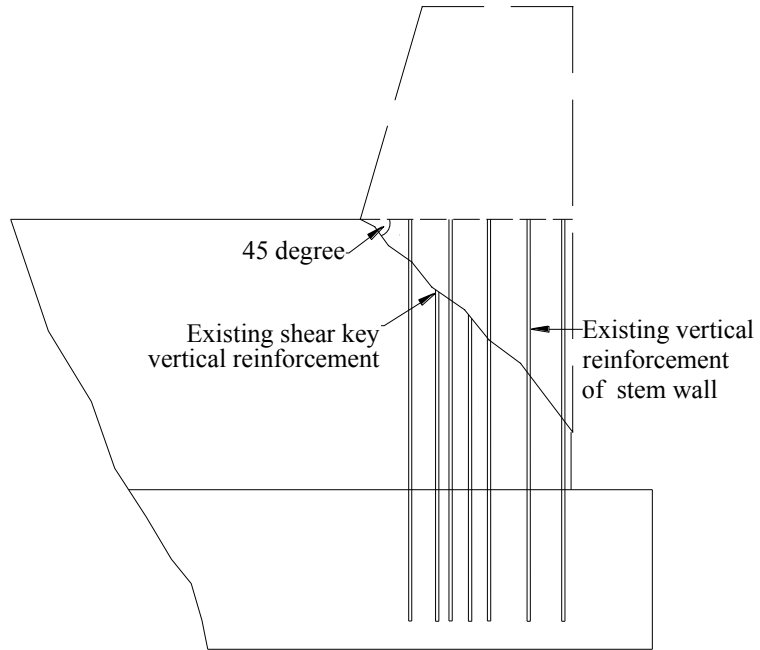


Figure B1- 10. Cut off existing stem wall vertical reinforcement and terminate at shear key-stem wall interface

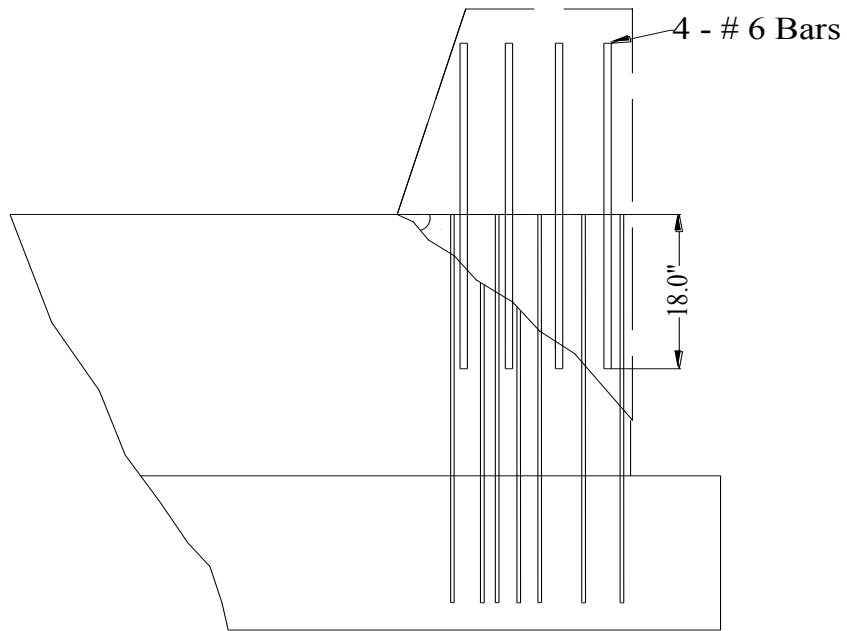


Figure B1- 11. Installation of new vertical bars

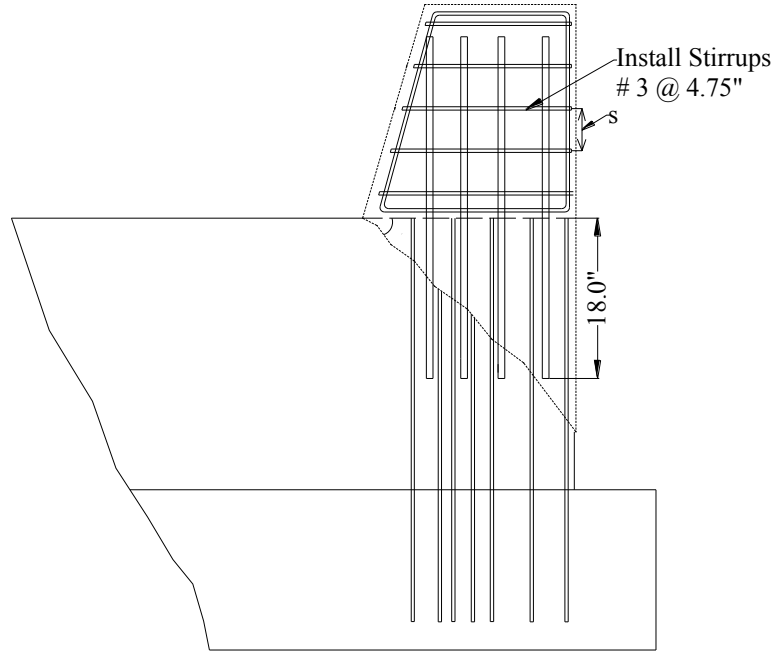


Figure B1- 12. Installation of stirrups (front view)

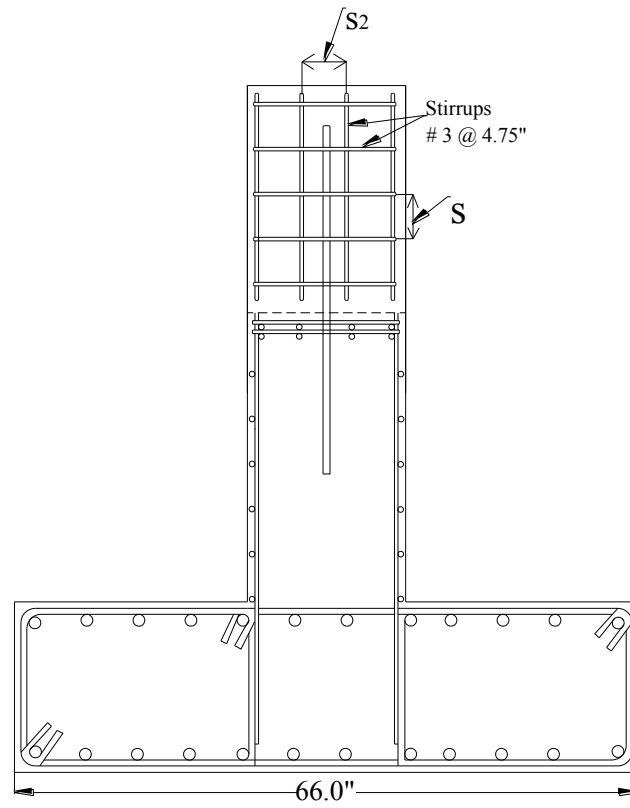


Figure B1- 13. Installation of stirrups (side view)

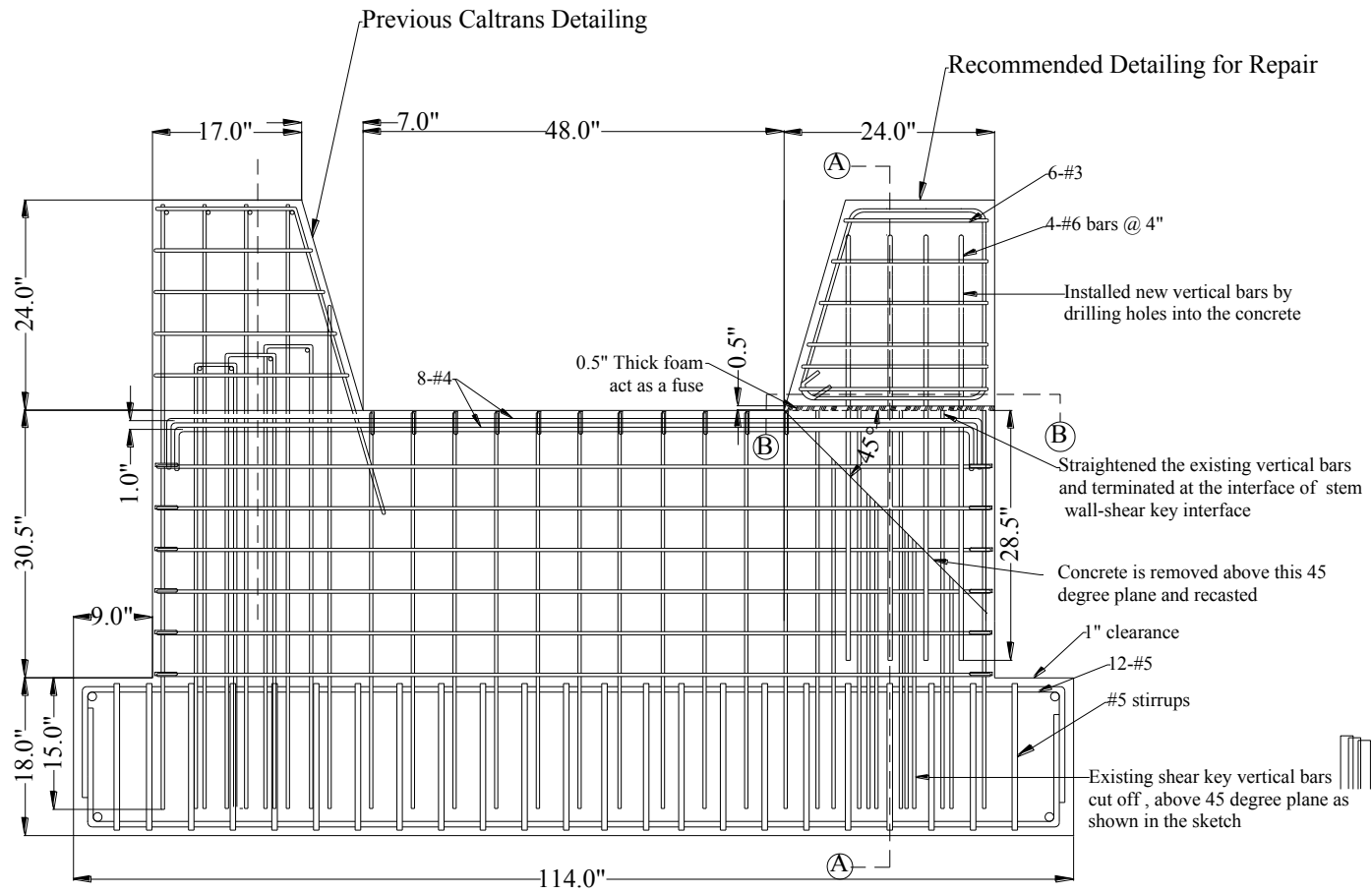


Figure B1- 14. Elevation view of a shear key repair for DS6

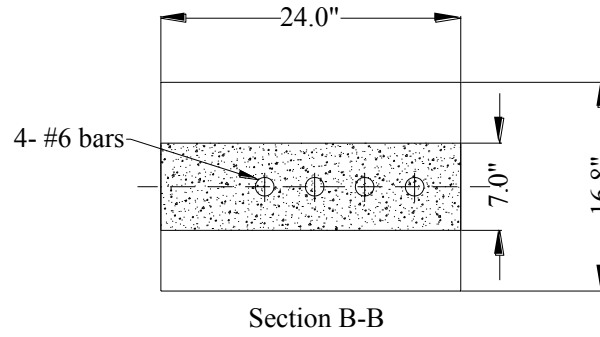


Figure B1- 15. Cross section of repaired shear key for DS6

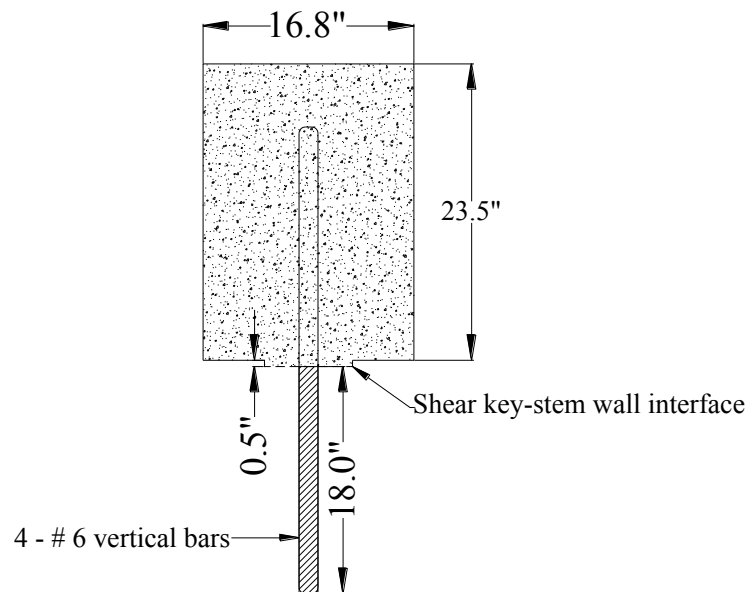


Figure B1- 16. Side view of shear key vertical reinforcement

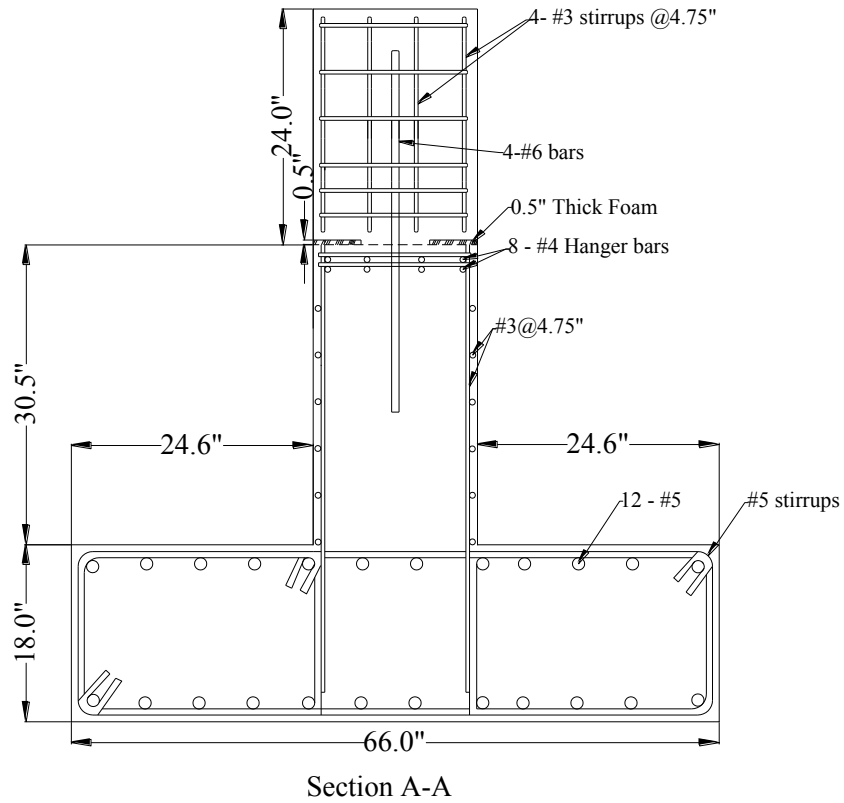


Figure B1- 17. Side view of shear key repair for DS6

Appendix B2. Girder Repair Design Examples

B2-1 Repair of P/S girders under DS2 and DS3

The repair of P/S girders under DS2 and DS3 is illustrated through an example in this section. The objective of the repair of P/S girders under DS2 and 3 is to restore section flexural capacity loss of 10%. The prototype P/S girder shown in Figure 4-5 and Figure 4-6. Prestressing strands detail were used as bench mark. The original moment capacity of the section is 4510 k-ft [6134 kN-m]. The moment capacity after 10% loss is equal to 4048 k-ft [5505 kN-m].

The material properties of unidirectional CFRP fabrics used are shown in Table 3-1. The required CFRP thickness and number of CFRP layers were calculated using the procedure recommended in section 4.6 of this report. The required CFRP thickness and area to restore 10% moment strength loss are 0.04 in. [1 mm] and 0.96 in² [619.4 mm²], respectively. The total capacity of the repaired P/S girder is 4555 k-ft [6195 kN-m] compared to the original girder capacity of 4510 k-ft [6134 kN-m]. Other parameters are compiled in Table B2- 1. Table B2- 1, shows the repaired P/S girder cross section under DS2 and 3.

B2-2 Repair of P/S girders under DS4

The objective of repair of P/S girders under DS4 is to restore flexural strength loss of 20% of prestressing steel. After 20% loss, the flexural capacity of the girder is equal to 3684 k-ft [5010 kN-m] compared to the original capacity of 4510 k-ft [6134 kN-m]. The repair method for DS4 is the same as that described in section 4.6.3 of this report.

The CFRP material properties used in repair of DS4 are the same as that used in DS2 and DS3. Unidirectional CFRP fibers are used in the longitudinal direction of the girder to repair P/S girders under DS4. The required CFRP thickness to make up 20% loss of flexural strength is 0.12 in. [3mm] (3 layers). The flexural strength provided with this design is 4318 k-ft [5873 kN-m] compared to the target strength of 4510 k-ft [6134 kN-m] which is 96% of the target capacity. To make up for the rest 4%, it is recommended to bend the CFRP around the girder soffit corners for at least half the bottom flange depth (U wrap). The flexural strength provided by this design is 4485 k-ft [6100 kN-m], which is approximately equal to the target strength of 4510 k-ft [6134 kN-m]. Other parameters are presented in Table B2- 1. Figure B2- 2 shows the P/S girder repair at DS4.

An attempt was made to determine the effectiveness of CFRP repair considering 25% loss of flexural strength rather than 20%. From the results presented in Table B2- 1, it was concluded that, once the loss in strand contribution to flexural strength is more than 20%, it is not possible to restore the original capacity of the girders. This is due to the fact that, in most cases CFRP repair is controlled by the debonding strain, which is inversely proportional to the CFRP thickness. Therefore, beyond certain limit of CFRP thickness, increase in flexural capacity is not significant. Due to this reason, in Table B2- 1, step no. 2, the area of CFRP (A_f) calculated for 25% loss in flexural strength is equal to that calculated for DS4. The flexural strength of the repaired girder with this design is 91.5% of the undamaged girder capacity and therefore, fails to completely restore the undamaged girder moment capacity.

Table B2- 1. CFRP repair design summary.

Step No.		10% loss	20% loss	25% loss
		DS2 & DS3	DS4	
1	f_{fu}^*	121	121	121
1	ε_{fu}^*	0.0085	0.0085	0.0085
1	C_E	0.85	0.85	0.85
1	f_{fu}	103	103	103
1	ε_{fu}	0.0072	0.0072	0.0072
2	cg strands	5.44	5.83	5.95
2	d_f	52.5	52.5	52.5
2	d_p	47.06	46.67	46.55
2	ε_{cu}	0.003	0.003	0.003
2	P_e	642	577	549
2	A_p	4.81	4.32	4.10
2	E_{ps}	28500	28500	28500
2	A_g	1272	1272	1272
2	E_f	11900	11900	11900
2	f'_c	5	5	5
2	E_c	4031	4031	4031
2	e	27.76	27.37	27.25
2	I	402400	402400	402400
2	r	17.8	17.8	17.8
2	ε_{pe}	0.0047	0.0047	0.0047
2	A_f	0.96	2.88	2.88
3	ε_{bi}	-0.00022	-0.00017	-0.00014
4	c	7.28	8.05	7.85
5	ε_{fd}	0.00650	0.00489	0.00489
5	ε_{fe} (cc)	0.01886	0.01673	0.01721
5	ε_{pi}	0.00512	0.00507	0.00505
5	ε_{fe} (psr)	0.03419	0.03461	0.03470
6	ε_{pnet} (cc)	0.01639	0.01439	0.01479
6	ε_{pnet} (FRP)	0.00553	0.00410	0.00411
6	ε_{ps} (cc)	0.02152	0.01947	0.01985
6	ε_{ps} (FRP)	0.01066	0.00918	0.00917
7	f_{ps}	241	236	236
7	f_{fe}	77	58	59
8	ε_c	0.00101	0.00086	0.00083
8	ε'_c	0.00211	0.00211	0.00211
8	β_1	0.70	0.69	0.69
8	α	0.58	0.51	0.50
9, 10	c check	7.28	8.06	7.87
11	M_{np}	4290	3722	3532
11	M_{nf}	312	700	701
11	Ψ_f	0.85	0.85	0.85
11	M_n	4555	4318	4128

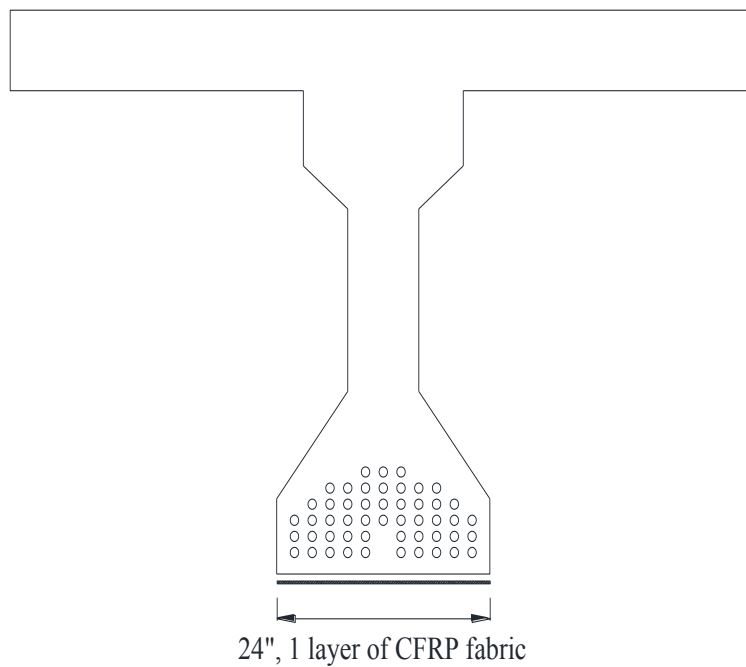


Figure B2- 1. P/S girder repair under DS2 and DS3

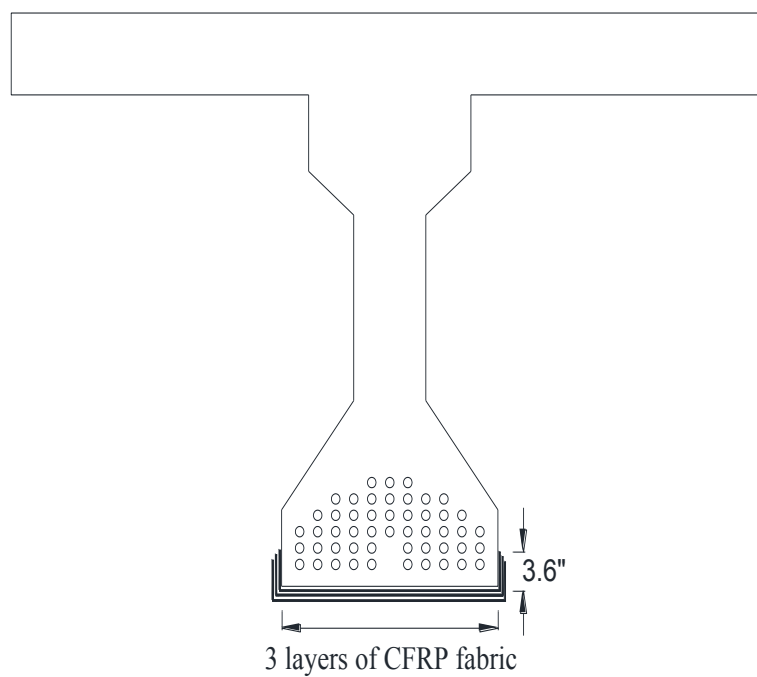


Figure B2- 2. P/S girder repair under DS4

Appendix B3. Repair of Bridge Abutments Walls

B3-1 Repair for DS3/4

The repair of abutment stem wall under DS3/DS4 is illustrated through an example in this section. The objective of the repair for abutments under DS3/DS4 is to restore shear strength loss of 50% of concrete component. The abutment shown in Figure 5-5 was used as bench mark with original shear capacity of 6109 kips [27174 kN]). In calculating A_{cv} , the entire l_w was conservatively used. If damage is localized, the designer may use a shorter length not to be less than $1.5 \times h_w$. The material properties of abutment stem wall are presented in Table 5-1.

The material properties of unidirectional CFRP fabrics used are shown in Table 3-1. The required CFRP thickness to restore strength loss is calculated using the proposed equation (Eq. 3-8). The concrete shear strength in the original abutment is 6109 kips [27174 kN]. The required CFRP thickness presented in Table B3- 1 for DS3 and DS4 are based on the assumed concrete shear strength loss of 50%, which is 3055 kips [13589 kN]. The required CFRP thickness was determined to be 0.24 in [6 mm] in each direction (horizontal and vertical). Six layers with a total thickness of 0.24 in [6 mm] are provided in each horizontal and vertical direction. Figure B3- 1 shows the repair of abutment stem wall under DS3/DS4.

B3-2 Repair for DS6

The objective of repair of stem wall under DS6 is to restore shear strength loss of 80%. The CFRP material used in repair of DS6 is the same as that used in DS3 and DS4.

CFRP fibers were used in the horizontal or vertical directions to repair abutments with DS6. The required CFRP thickness to restore shear strength loss at DS6 is determined by utilizing Eq. 5-2 and 3-8. In this example, the entire l_w was conservatively used to calculate A_{cv} . If damage is localized, the designer may use a shorter length not to be less than $1.5xh_w$. The required CFRP thickness presented in Table B3- 1 for DS6 are based on the assumed shear strength loss of 80%, which is 4887 kips [21738 kN]. The required CFRP thickness was determined to be 0.62 in [15.5 mm]. Sixteen layers with a total thickness of 0.64 in [16 mm] are provided in each horizontal and vertical direction. Figure B3- 2 shows the repair of abutment stem wall for DS6.

Table B3- 1. CFRP layer thickness for DS3, DS4, and DS6

Damage State	Shear capacity of undamaged stem wall V_c	CFRP Required Shear Strength $(V_f)_{Required}$	Required CFRP Thickness t_f , in Each Direction	Provided CFRP Thickness t_f , in Each Direction	Minimum Required Anchorage Length l_{df}	Provided Anchorage Length l_{df}
	Kips (KN)	Kips (KN)	in (mm)	in (mm)	in (mm)	in (mm)
DS3 and DS4	6109 (27174)	3594 (15987)	0.24 (6)	0.24 (6)	11.5 (292)	12 (305)
DS6	6109 (27174)	5750 (25577)	0.62 (15.5)	0.64 (16)	18.7 (475)	24 (610)

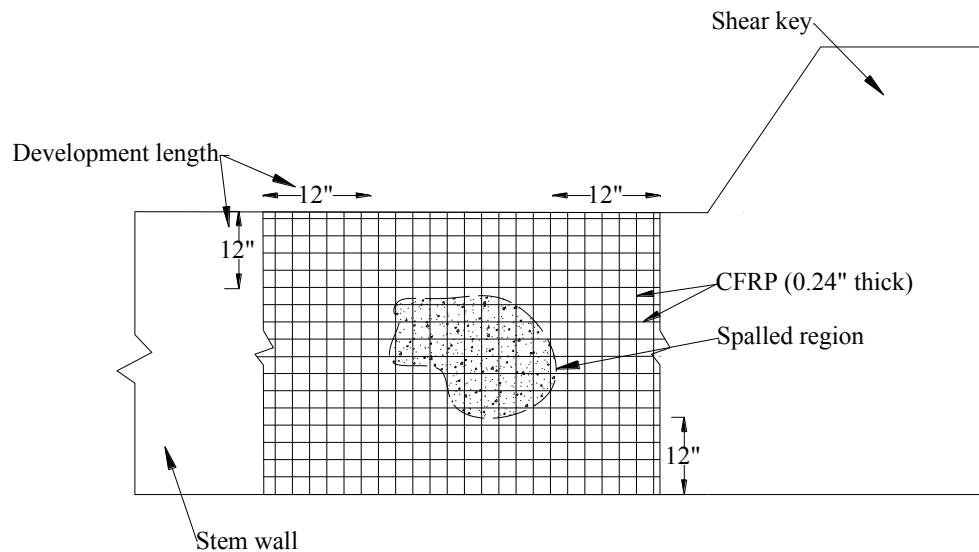


Figure B3- 1. Repair of abutment wall under DS3 and DS4

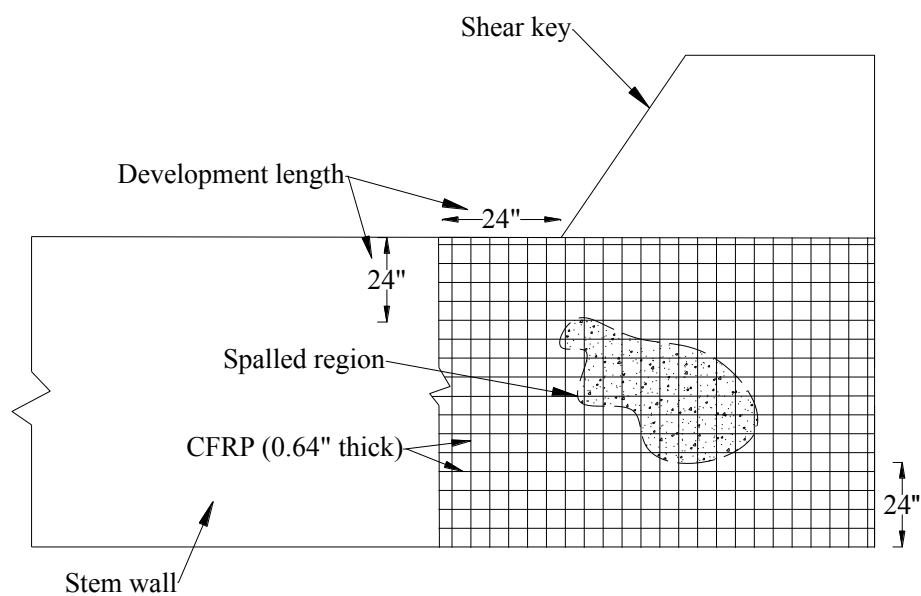


Figure B3- 2. Repair of abutment wall under DS6

Appendix B4. Repair Design Examples for Bridge Cap Beam-Column Joints

B4-1 Repair for DS2

The repair of RC bridge joints under DS2 is illustrated through an example in this section. The objective of the repair for joints under DS2 is to restore shear strength loss of 30%. The joints shown in Figure 6-6 to Figure 6-9 were used to illustrate the method. The original shear strength of T and knee joint was calculated as 1100 kips [4893 kN] and 733 [3261 kN], respectively. The expected compressive strength of concrete was assumed to be 5 ksi [34.5 Mpa].

The Unidirectional CFRP fabrics material properties presented in Table 3-1 were used. The required CFRP thickness to restore loss in the shear strength is calculated by utilizing the proposed equation (Eq. 3-8). The required CFRP thickness presented in Table B4- 1 for T-joints under DS2 is based on the assumed shear strength loss of 30%, which is 330 kips [1468 kN]. The required CFRP thickness was determined to be 0.11 in [2.8 mm] in each direction (horizontal and vertical) on each side of the cap beam. Three layers with a total thickness of 0.12 in [3 mm] are provided in each direction on each side of the T joint. Figure B4- 1 and Figure B4- 2 show the elevation and section view of T-joints repair under DS2, respectively. The same repair procedure used for T-joints was applied to determine the required CFRP thickness for knee joints under DS2. The required CFRP thickness presented in Table B4- 2 for knee joints under DS2 is based on the assumed shear strength loss of 30%, which is 220 kips [979 kN]. The U-wrap configuration was used for knee joints. The required CFRP thickness for knee joints under DS2 was determined to be 0.05 in [1.25 mm] in each direction. Two layers of U-

wrap with a total thickness of 0.08 in [2mm] are provided in each direction of the knee joint. Figure B4- 5, Figure B4- 6, and Figure B4- 7 show the elevation, side, and plan view of the repair for knee joints under DS2, respectively.

B4-2 Repair for DS3 and DS4

The objective of repair of joints under DS3 and DS4 was to restore shear strength loss of 60%. The CFRP material used in repair of DS3 and DS4 was the same as that used in DS2. Unidirectional CFRP fabrics were used with fibers in the horizontal or vertical directions to repair joints with DS3 and DS4. The required CFRP thickness to restore shear strength loss at DS3 and DS4 was determined by utilizing Eq. 3-8. The required CFRP thickness presented in Table B4- 1 for T-joints under DS3 and DS4 is based on the assumed shear strength loss of 60%, which is 660 kips [2936 kN]. The required CFRP thickness was determined to be 0.44 in [11 mm] in each direction (horizontal or vertical) on each side of the cap beam. Eleven layers with a total thickness of 0.44 in [11 mm] are provided in each direction. Figure B4- 3 and Figure B4- 4 show the elevation and section view of the repair of T-joints under DS3 and DS4, respectively. The same repair procedure used for T-joints was applied to determine the required CFRP thickness for knee joints under DS3 and DS4. The required CFRP thickness presented in Table B4- 2 for knee joints under DS3 and DS4 is based on the assumed shear strength loss of 60%, which is 440 kips [1957 kN]. The required CFRP thickness for knee joints under DS3 and DS4 was determined to be 0.20 in [5 mm] in each direction. Five layers of U-wrap with a total thickness of 0.20 in [5 mm] are installed in each direction. Figure

B4- 8, Figure B4- 9, and Figure B4- 10 show the elevation, side, and plan view of the repaired knee joints under DS3 and DS4, respectively.

Table B4- 1. CFRP layer thickness for T joints under DS2, DS3, and DS4

Damage State	Shear strength of undamaged joint V_{jn}	CFRP required shear strength $(V_f)_{Required}$	Required CFRP thickness t_f , in each direction	Provided CFRP thickness t_f , in each direction	Minimum required anchorage length l_{df}	Provided anchorage length l_{df}
	Kips (KN)	Kips (KN)	in (mm)	in (mm)	in (mm)	in (mm)
DS2	1100 (4893)	388 (1726)	0.11 (2.8)	0.12 (3)	8.6 (218)	12 (305)
DS3 and DS4	1100 (4893)	776 (3452)	0.44 (11)	0.44 (11)	16.4 (417)	18 (457)

Table B4- 2. CFRP layer thickness for knee joints under DS2, DS3, and DS4

Damage State	Shear strength of undamaged joint V_{jn}	CFRP required shear strength $(V_f)_{Required}$	Required CFRP thickness t_f , in each direction	Provided CFRP thickness t_f , in each direction	Minimum required anchorage length l_{df}	Provided anchorage length l_{df}
	Kips (KN)	Kips (KN)	in (mm)	in (mm)	in (mm)	in (mm)
DS2	733 (3261)	259 (1152)	0.05 (1.25)	0.08 (2)	7 (178)	12 (305)
DS3 and DS4	733 (3261)	517 (2300)	0.20 (5)	0.20 (5)	11.1 (282)	12 (305)

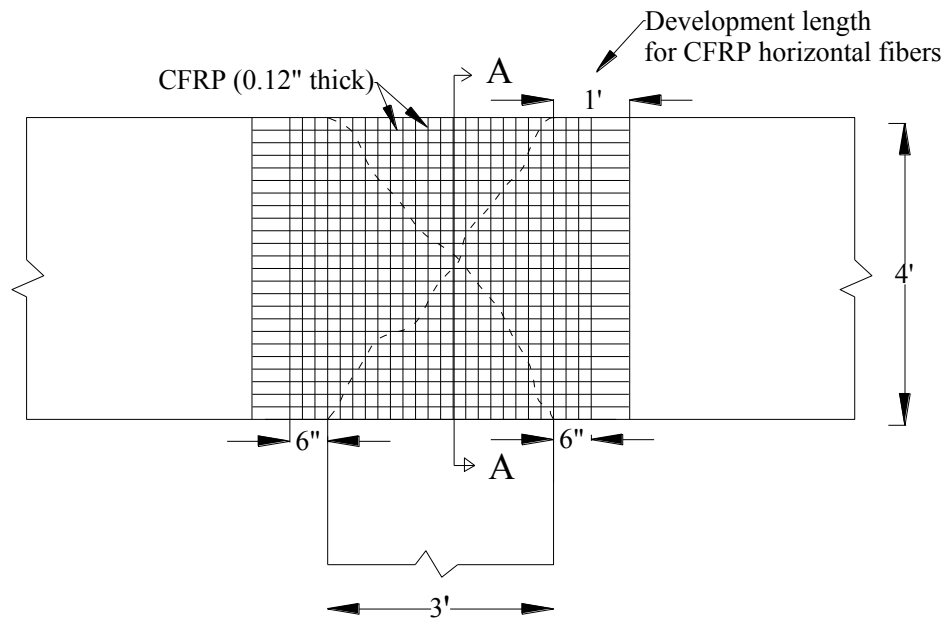


Figure B4- 1. Elevation view of T joints repair under DS2

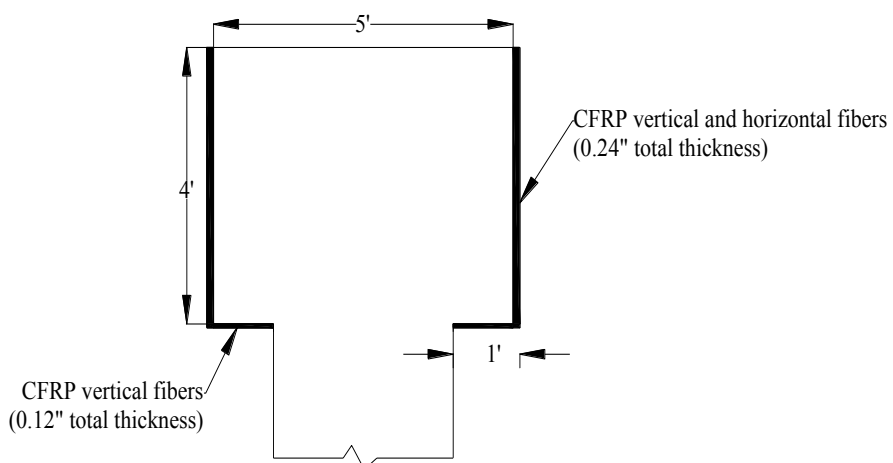


Figure B4- 2. Section A-A of T joints repair under DS2

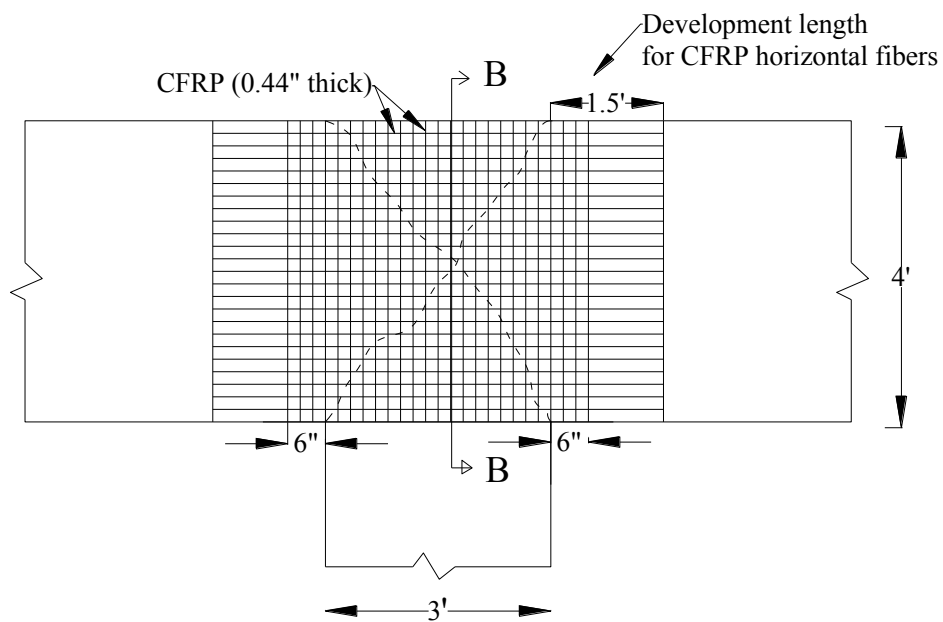


Figure B4- 3. Elevation view of T joints repair under DS3 and DS4

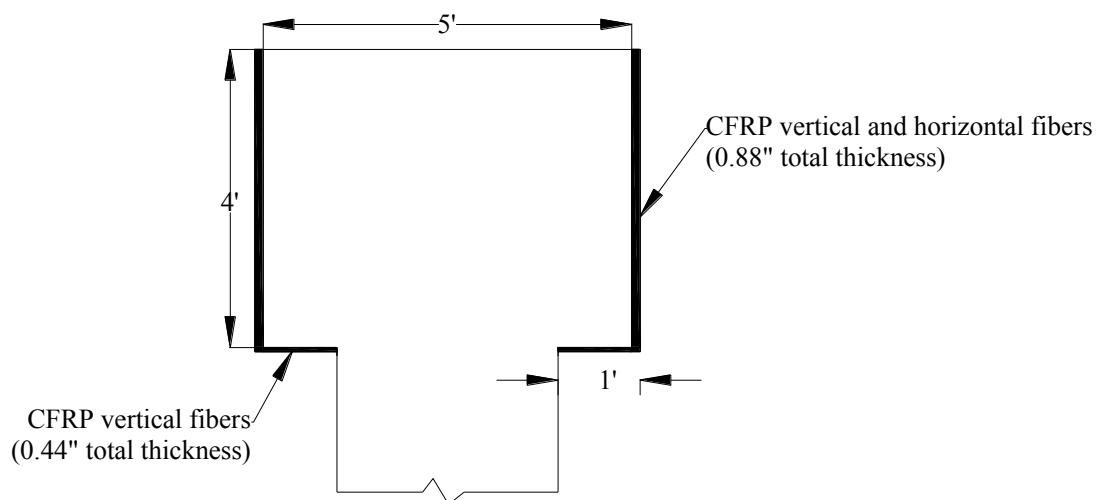


Figure B4- 4. Section B-B of T joints repair under DS3 and DS4

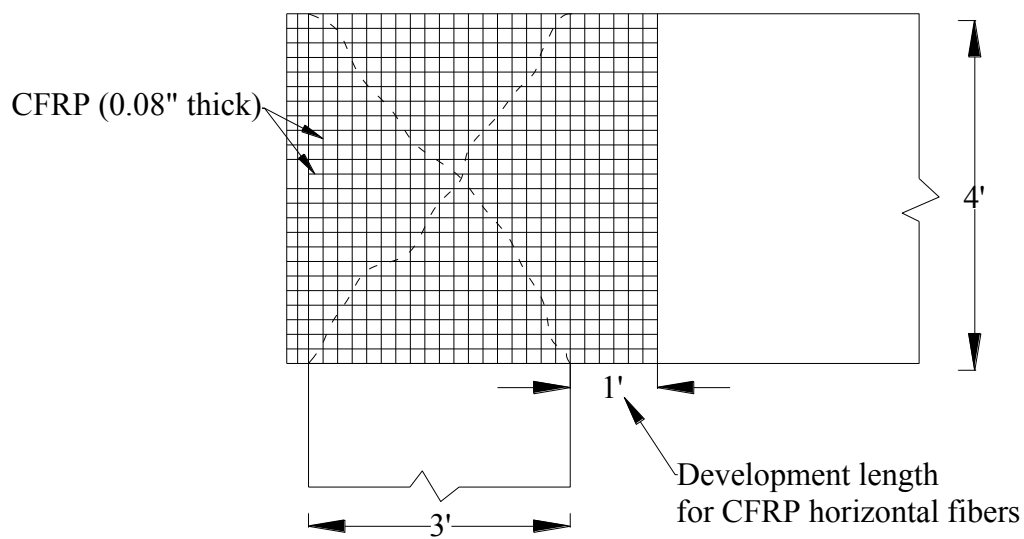


Figure B4- 5. Elevation view of knee joints repair under DS2

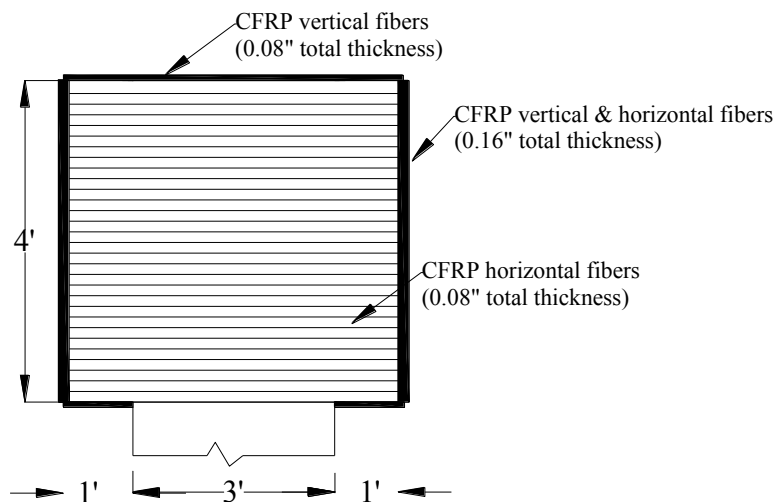


Figure B4- 6. Side view of knee joints repair under DS2

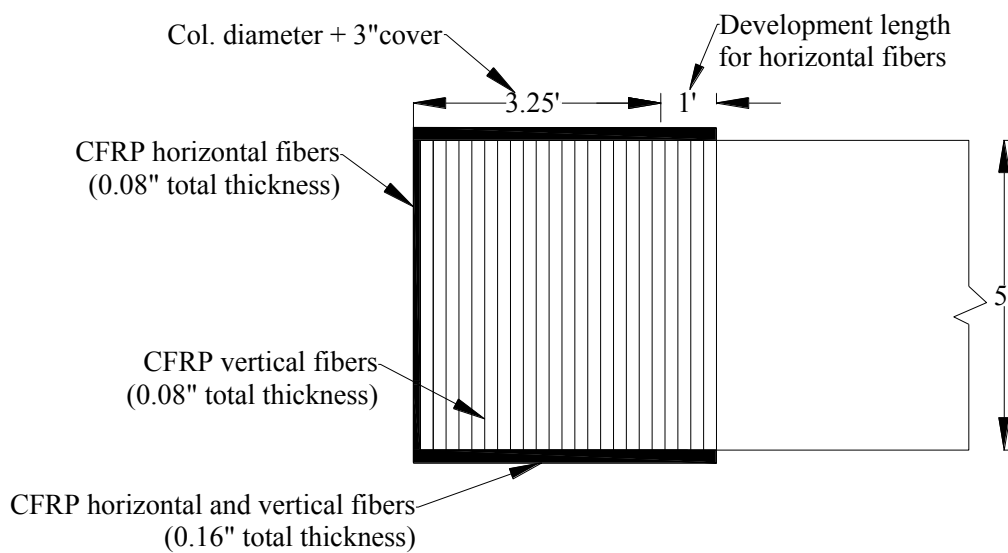


Figure B4- 7. Plan view of knee joints repair under DS2

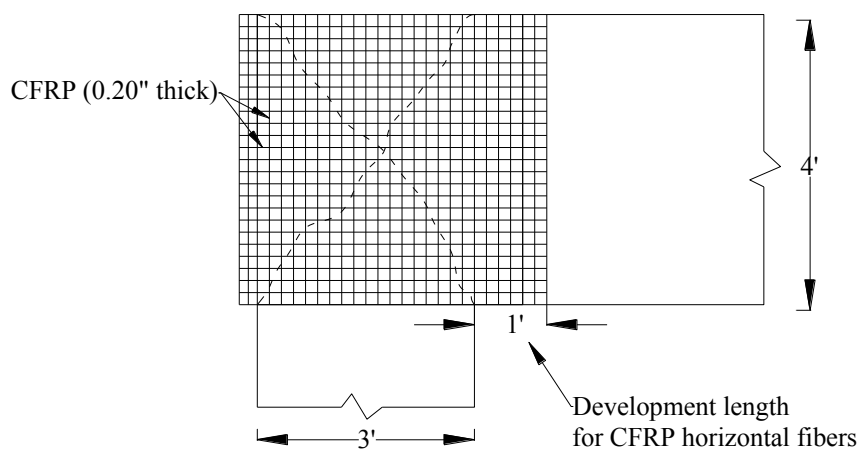


Figure B4- 8. Elevation view of knee joints repair under DS3 and DS4

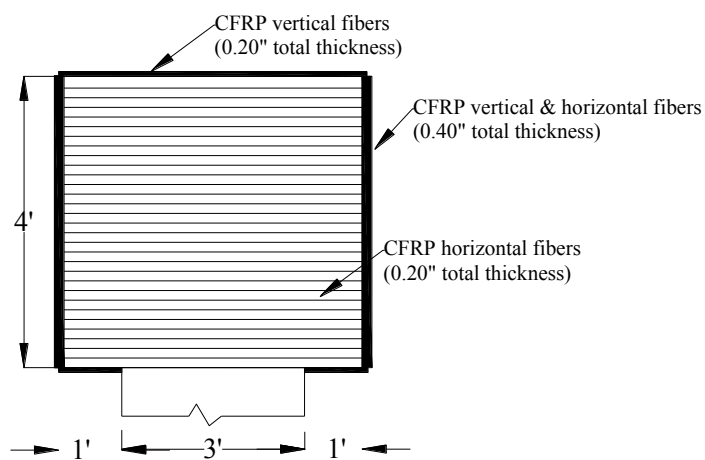


Figure B4- 9. Side view of knee joint repair under DS3 and DS4

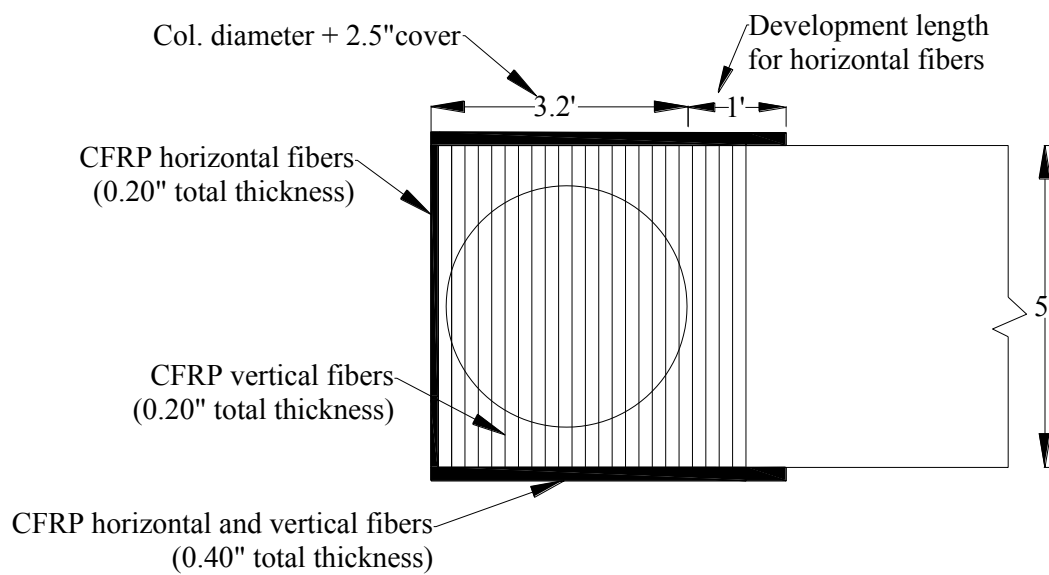


Figure B4- 10. Plan view of knee Joint repair under DS3 and DS4